

Year-Round Biodiesel Use Strategy in Diesel Engines in Canadian Adverse Cold Weather Conditions

By: Arvind Mangad

Supervised by Dr. Murari Mohon Roy, Department of Mechanical
Engineering

Co-supervised by Dr. Wilson Wang, Department of Mechanical
Engineering

February, 2017

A thesis submitted in partial fulfilment of the requirement of
the MSc degree in
Mechanical Engineering

Faculty of Engineering

Lakehead University

Thunder Bay, Ontario

Abstract

The effects of climate change that have been seen at an unprecedented scale over last decade or so, have sparked intensive efforts toward the identification and development of clean, environmentally compatible, and renewable fuels. Biofuels such as alcohol and biodiesel have been identified as alternatives for powering internal combustion engines. When using vegetable oil as a feedstock for the production of biodiesel, major issues that arise include its poor low temperature properties. In this study, an experimental analysis was conducted to test the feasibility of biodiesel in cold climates specifically in Thunder Bay region and to suggest an appropriate solution for the biodiesel usage throughout the year. Weather reports from last decade were studied to compare with the cloud points of biodiesel blends. Biodiesel was produced from canola oil from transesterification and fractionation processes. Summer diesel and winter diesel have been used as reference fuels. Five different fuel series were used. The first series was summer diesel-biodiesel with ten blends (SB10, SB20, SB30, SB40, SB50, SB60, SB70, SB80, SB90 and B100). The second series was winter diesel-biodiesel with ten blends (WB10, WB20, WB30, WB40, WB50, WB60, WB70, WB80, WB90 and B100). The third series was winter diesel-biodiesel with 2 volume percent of (cold flow additive) Wintron Synergy series (WB20S2, WB50S2 and B100S2). The fourth series was winter diesel-fractionated biodiesel (FB20, FB50 and FB100). The final was winter diesel-fractionated biodiesel with 2 volume percent of Wintron Synergy series (FB20S2, FB50S2 and FB100S2). Except for winter diesel-biodiesel with 2 vol% synergy, all the fuel blend series were tested on two separate diesel engines; a four-cylinder heavy-duty diesel engine at constant speed of 800 rpm for emissions at idling condition followed by a two-cylinder light-duty diesel engine to investigate effects of fuel blends on performance and emission, under low, medium and high loads, at variable engine speeds of 1000 rpm, 2100 rpm and 3000 rpm. Results showed that normal biodiesel and fractionated biodiesel with 2 vol% synergy showed significant improvement in the cloud point. FB40S2 has the lowest cloud point compared to other fuel blends measuring -48.5°C . The effect of fuel blends on engine performance in light duty engine was investigated. The emissions of carbon monoxide (CO), hydrocarbon (HC), oxides of nitrogen (NO_x) and smoke opacity from different fuel blends were measured and compared to summer and winter diesel fuels. In both the engines, fractionated biodiesel and synergy blends were found to be effective in reducing both CO and HC emissions. Smoke opacity emissions when compared from both the engines had a contrasting results. However, all biodiesel blends increased NO_x

emission. Results indicated that fractionated biodiesel with 2 vol% synergy had better engine performance, and lower emission compared with diesel fuel and normal biodiesel blends. Thus, fractionated biodiesel up to 80 vol% with 2 vol% synergy was found to be suitable for use in diesel engines in extreme winter conditions in Canada without the need for any engine modification.

Acknowledgments

I am grateful to Dr. Murari Mohon Roy, Associate Professor in Department of Mechanical engineering. He has been my guide and philosopher, and instilled in me a sense of fulfilment and strive hard to find relevant information and data related to my thesis.

My deep gratitude goes to Dr. Wilson Wang, Professor in Department of Mechanical engineering, for his kind supervision, generous advice and support during the study. It is a great honour to work under his supervision.

I would like to express my deep and sincere gratitude to Dr. Birbal Singh and Dr. Leila Pakzad for reviewing my thesis and their valuable suggestions.

I convey my deep gratitude to Mr. Joe Ripku and Ms. Debbie Puumala for all the maintenance throughout the experiment.

Finally, I extend my sincere thanks to my colleagues for the time and support they spared for me during my thesis work and studies at Lakehead University.

Table of Contents

Abstract.....	II
Acknowledgments.....	IV
List of Tables	VII
List of Figures.....	VIII
Nomenclature.....	XI
Chapter 1 Introduction	1
1.1 Overview.....	1
1.2 Biodiesel Properties:.....	3
1.2.1 Specific Gravity:.....	3
1.2.2 Flash Point	3
1.2.3 Viscosity	3
1.2.4 Cetane Number	3
1.2.5 Calorific Value (Heating Value).....	4
1.3 Cold Flow Properties (CFP) of Biodiesel.....	4
1.3.1 Cloud Point	4
1.3.2 Pour Point.....	4
1.3.3 Cold Filter Plugging Point.....	4
1.4 Fatty Acids	4
1.4.1 Techniques used to Improve CFPs	6
Chapter 2 Literature Review and Thesis Objective	9
2.1 Engine Performance.....	9
2.2 Engine Emissions.....	11
2.3 Review on Cold Flow Improving Additives.....	15
2.4 Review on Fractionation of Biodiesel.....	18
2.5 Thesis Objective.....	19
Chapter 3 Methodology	20
3.1 Biodiesel Production:.....	20
3.2 Urea Fractionation Process:	21
3.3 Measurement of Density:	24
3.4 Measurement of Viscosity:	25

3.5 Measurement of the Heating Value:	26
3.6 Thunder Bay Green Fleet Plan.....	29
3.7 Engine under Study:.....	29
3.8 Engine Test Procedure:	33
3.9 Calculation	34
Chapter 4 Results and Discussion.....	35
4.1 Cloud Points:.....	35
4.2 Alternative Fuels to be used for Each Month	36
4.3 Crystal Structure	37
4.4 Heavy-duty Diesel Engine:	38
4.4.1 Summer Diesel-Biodiesel series:	39
4.4.2 Winter Diesel-Biodiesel series:.....	41
4.4.3 Winter Diesel-Biodiesel-Wintron Synergy Additive Series:.....	44
4.4.4 Winter Diesel-Fractionated Biodiesel and 2% Wintron Synergy Additive Series:	46
4.5 Light-duty Diesel Engine:.....	49
4.5.1 Summer Diesel-Biodiesel Series:	49
4.5.2 Winter Diesel-Biodiesel Series:.....	59
4.5.3 Winter Diesel-Fractionated Biodiesel and 2% Wintron Synergy Additive Series:	69
Chapter 5 Conclusion.....	81
Appendices.....	84
References.....	93

List of Tables

Table 1.1: Fatty acid composition of canola oil.....	6
Table 3.1: Properties of canola biodiesel.....	21
Table 3.2: Fuel properties of summer diesel-biodiesel, summer diesel-biodiesel-synergy blends, winter diesel-biodiesel, winter diesel-fractionated biodiesel, winter diesel-fractionated biodiesel-synergy blends	28
Table 3.3: Engine specification for heavy-duty engine.	30
Table 3.4: Engine specifications for light-duty engine.....	31
Table 3.5: Gas analyzer specifications.....	34
Table 4.1: Comparison of various fuel blends to be used according to average lowest temperature of respective month.....	37

List of Figures

Figure 1.1: Cold flow mechanism of biodiesel	5
Figure 3.1: Urea crystals formed after 24 hours	22
Figure 3.2: Buchner funnel	22
Figure 3.3: Magnetic stirrer	23
Figure 3.4: Weighing scale	24
Figure 3.5: Viscometer.....	25
Figure 3.6: Calorimeter.....	26
Figure 3.7: Heavy-duty engine test setup	30
Figure 3.8: Schematic diagram of heavy-duty engine test setup	31
Figure 3.9: Light-duty engine test setup	32
Figure 3.10: Schematic diagram of the experimental test setup for the light-duty diesel engine. 32	
Figure 4.1: Variation of biodiesel content in diesel fuel with respect to cloud points	36
Figure 4.2: Crystal formation of B20 and B20S2 fuel blends at -10°C and -20°C	38
Figure 4.3: Engine fuel consumption.....	39
Figure 4.4: CO emissions at 800 rpm for different summer diesel-biodiesel fuel blends	39
Figure 4.5: HC emissions at 800 rpm for different summer diesel-biodiesel fuel blends	40
Figure 4.6: NOx emissions at 800 rpm for different summer diesel-biodiesel fuel blends	41
Figure 4.7: CO emissions at 800 rpm for different winter diesel-biodiesel fuel blends.....	42
Figure 4.8: HC emissions at 800 rpm for different winter diesel-biodiesel fuel blends.....	42
Figure 4.9: NOx emissions at 800 rpm for different winter diesel-biodiesel fuel blend	43
Figure 4.10: Smoke opacity emissions at 800 rpm for different winter diesel-biodiesel fuel blends	43
Figure 4.11: CO emissions at 800 rpm for different summer diesel-biodiesel-synergy fuel blends	44
Figure 4.12: HC emissions at 800 rpm for different summer diesel-biodiesel-synergy fuel blends	45
Figure 4.13: NOx emissions at 800 rpm for different summer diesel-biodiesel-synergy fuel blends	45
Figure 4.14: CO emissions at 800 rpm for different winter diesel-fractionated biodiesel fuel blends	46

Figure 4.15: HC emissions at 800 rpm for different winter diesel-fractionated biodiesel and 2% synergy additive blends.....	47
Figure 4.16: NOx emissions at 800 rpm for different winter diesel-fractionated biodiesel and 2% synergy additive blends.....	48
Figure 4.17: Smoke opacity emissions at 800 rpm for different winter diesel-fractionated biodiesel and 2% synergy additive blends	48
Figure 4.18: BSFC values for summer diesel-biodiesel under different loads at (a) 1000 rpm (b) 2100 rpm (c) 3000 rpm	50
Figure 4.19: BTE values for summer diesel-biodiesel under different loads at (a) 1000 rpm (b) 2100 rpm (c) 3000 rpm	51
Figure 4.20: CO emission for summer diesel-biodiesel blends under different engine loads at (a) 1000 rpm (b) 2100 rpm (c) 3000 rpm	53
Figure 4.21: HC emission for summer diesel-biodiesel blends under different engine loads at (a) 1000 rpm (b) 2100 rpm (c) 3000 rpm	55
Figure 4.22: NOx emission for summer diesel-biodiesel blends under different engine loads at (a) 1000 rpm (b) 2100 rpm (c) 3000 rpm	57
Figure 4.23: Smoke opacity emission for summer diesel-biodiesel blends under different engine loads at (a) 1000 rpm (b) 2100 rpm (c) 3000 rpm	59
Figure 4.24: BSFC values for winter diesel-biodiesel under different loads at (a) 1000 rpm (b) 2100 rpm (c) 3000 rpm	61
Figure 4.25: BTE values for winter diesel-biodiesel under different loads at (a) 1000 rpm (b) 2100 rpm (c) 3000 rpm	62
Figure 4.26: CO emission for winter diesel-biodiesel blends under different engine loads at (a) 1000 rpm (b) 2100 rpm (c) 3000 rpm	64
Figure 4.27: HC emission for winter diesel-biodiesel blends under different engine loads at (a) 1000 rpm (b) 2100 rpm (c) 3000 rpm	66
Figure 4.28: NOx emission for winter diesel-biodiesel blends under different engine loads at (a) 1000 rpm (b) 2100 rpm (c) 3000 rpm	67
Figure 4.29: Smoke opacity emission for winter diesel-biodiesel blends under different engine loads at (a) 1000 rpm (b) 2100 rpm (c) 3000 rpm	69

Figure 4.30: BSFC values for winter diesel-fractionated biodiesel under different loads at (a) 1000 rpm (b) 2100 rpm (c) 3000 rpm	71
Figure 4.31: BTE values for winter diesel-fractionated biodiesel under different loads at (a) 1000 rpm (b) 2100 rpm (c) 3000 rpm	72
Figure 4.32: CO emission for winter diesel-fractionated biodiesel blends under different engine loads at (a) 1000 rpm (b) 2100 rpm (c) 3000 rpm	74
Figure 4.33: HC emission for winter diesel-fractionated biodiesel blends under different engine loads at (a) 1000 rpm (b) 2100 rpm (c) 3000 rpm	76
Figure 4.34: NOx emission for winter diesel-fractionated biodiesel blends under different engine loads at (a) 1000 rpm (b) 2100 rpm (c) 3000 rpm	78
Figure 4.35: Smoke opacity emission for winter diesel-fractionated biodiesel blends under different engine loads at (a) 1000 rpm (b) 2100 rpm (c) 3000 rpm	80

Nomenclature

DI	Direct injection
CI	Compression ignition
SD100	Summer Diesel
WD100	Winter Diesel
B100	100% biodiesel
SB10	10% biodiesel / 90% summer diesel
SB20	20% biodiesel / 80% summer diesel
SB30	30% biodiesel / 70% summer diesel
SB40	40% biodiesel / 60% summer diesel
SB50	50% biodiesel / 50% summer diesel
SB60	60% biodiesel / 40% summer diesel
SB70	70% biodiesel / 30% summer diesel
SB80	80% biodiesel / 20% summer diesel
SB90	90% biodiesel / 10% summer diesel
WB10	10% biodiesel / 90% winter diesel
WB20	20% biodiesel / 80% winter diesel
WB30	30% biodiesel / 70% winter diesel
WB40	40% biodiesel / 60% winter diesel
WB50	50% biodiesel / 50% winter diesel
WB60	60% biodiesel / 40% winter diesel
WB70	70% biodiesel / 30% winter diesel
WB80	80% biodiesel / 20% winter diesel
WB90	90% biodiesel / 10% winter diesel
FB20	20% fractionated biodiesel / 80% winter diesel
FB50	50% fractionated biodiesel / 50% winter diesel
FB100	100% fractionated biodiesel
FB20S2	20% fractionated biodiesel / 80% winter diesel+ 2% synergy
FB50S2	50% fractionated biodiesel / 50% winter diesel+ 2% synergy
FB100S2	100% fractionated biodiesel + 2% synergy
WB20S2	20% biodiesel / 80% winter diesel+ 2% synergy
WB50S2	50% biodiesel / 50% winter diesel+ 2% synergy
B100S2	100% biodiesel + 2% synergy
BP	Brake power
BTE	Brake thermal efficiency
BSFC	Brake specific fuel consumption
FAME	Fatty acid methyl ester
CO	Carbon monoxide
HC	Hydrocarbons
PM	Particulate matter
NO	Nitric oxide
NO ₂	Nitrogen dioxide

NO _x	Oxides of nitrogen
CFPP	Cold filter plugging point
CFP	Cold Flow Property
ASTM	American Society of Testing and Materials
CP	Cloud point
PP	Pour point
EGR	Exhaust gas recirculation
BMEP	Brake mean effective pressure
\dot{m}_a	Fuel mass flow rate (g/h)
B_p	Engine power (kW)
HHV	Higher heating value of fuel (kJ/kg)

Chapter 1

Introduction

1.1 Overview

Due to the significant growth of world's population, energy consumption has rapidly increased over the last century. This unprecedented growth of population has caused unlimited demands on traditional fossil fuel resources and has thus caused fossil fuel depletion leading to energy crisis in different parts of the world. Since fossil fuels are derived from limited natural resources, there has been an increased demand for alternative resources of energy.

Whereas environmental pollution is becoming a big concern all over the world due to indiscriminate use of fossil fuel. Besides causing irreparable damage to natural environment, it is leading human civilization to a near catastrophe of ozone depletion and climate change as never seen before. World Meteorological Organisation (WMO) has revealed that in 2015, for the first time, carbon dioxide levels in the atmosphere were at 400 ppm on an average across the whole year [1]. They have predicted that the carbon dioxide concentration will not dip below the 400 ppm mark for many generations. This has given scientists, researchers and decision makers even stronger motivation to search for alternative sources of energy that are sustainable and more environment friendly. Countries like France, Germany, USA, China and India have made giant leap in generating power through clean energy sources. Generation of green energy through renewable sources like hydro, solar, wind, nuclear, geothermal and biomass is catching up fast in many developed and developing countries.

Renewable fuel made from biomass have the desired potential to substitute fossil fuels in stationary applications such as heat or electricity as well as automotive or transportation sector. It would solve several burning issues like rising prices of energy worldwide, the increased and compelling need for energy imports that deprive many developing economies of genuine developmental activities, the negative and disastrous environmental consequences of fossil fuel combustion and the threat to the security of national energy supply for many countries.

Biodiesel which is derived from biomass have been proposed as alternative in the market. The most widely used standard is ASTM D6751. Biodiesel has been defined as the mono alkyl esters of long chain fatty acids derived from renewable lipid feedstocks, such as vegetable oils and animal fats [2]. Biodiesel in particular has been proven to be one of the best and possible alternatives for

fossil fuel as it emits less pollutants. Many of the leading countries like France, Germany, USA, Brazil and India have been conducting biodiesel research extensively. Some of the developing countries are also constantly conducting similar research with a view to tide over the emerging situation. Diesel engines do not require much modifications when using biodiesel and many countries have already converted extensively to this fuel.

Biodiesel has proven to be good for diesel engines. It provide improved and healthy lubrication than fossil diesel and has near excellent solvent properties. Whereas fossil diesel leave polluting deposits in fuel lines and fuel tanks over time. When fuel filters clogged with polluting diesel sediments are replaced, the biodiesel dissolves any leftover sediment while generating no deposits of its own, resulting in cleaner reliable and more trouble free fuel handling systems. Biodiesel has a lower heating value and higher cetane number, viscosity and density than fossil diesel [3]. Therefore, due to different physicochemical properties of biodiesel, it has been found to affect the emissions in diesel engines [4].

One of the main challenges in using biodiesel in cold countries like Canada is its high cloud point. The accumulation of paraffin wax crystals take place when ambient temperature fall below the fuel's cloud point. These solid crystals causes start-up problems like filter clogging when ambient temperature of petroleum diesel drop to around -15°C [5]. The cloud point of biodiesel is around 0°C which limits its use to ambient temperature above freezing [6]. It has been proven that the presence of higher amount of saturated components increases the cloud point and pour point of the biodiesel [7]. To overcome this problem, several approaches have been proposed like blending with petroleum diesel, use of additives and chemical or physical modification of the oil feedstock. Additives specifically designed for neat diesel has been considered unsuccessful in biodiesel for improving the low temperature properties [8]. Therefore special attention should be made before choosing the desired additives for biodiesel. In our previous studies, biodiesel was treated with Wintron Synergy, XC30, XC40, heptane, ethanol and diethyl ether. In this study, fractionated biodiesel would be used specifically with Wintron Synergy to overcome the challenges of low cold flow properties of biodiesel.

1.2 Biodiesel Properties:

1.2.1 Specific Gravity:

It is the ratio of density of a substance compared to the density of a reference substance (mass of the same unit volume). Biodiesel is slightly heavier than conventional diesel fuel. For improved blending of fuels, biodiesel is added to diesel fuel. Blending of biodiesel with diesel helps in reducing the biodiesel fuel density promoting improved fuel atomization during the fuel injection taking place inside the combustion chamber.

1.2.2 Flash Point

It is the temperature at which the fuel becomes a mixture that will ignite when exposed to a spark or flame. The flash point of biodiesel should be at least 130⁰C. The flash point of biodiesel is higher than that of diesel fuel. Diesel fuel has flash point minimum of 52⁰C. Therefore, biodiesel is considered as a safer fuel than diesel due to its high flash point. However, the flashpoint can be reduced if the alcohol used in producing biodiesel is not removed properly, which in-turn affect the fuel pumps and also reducing the combustion quality.

1.2.3 Viscosity

It is an important property of any fuel as it is an indication of the ability of a material to flow. Biodiesel is more viscous than diesel fuel, which provides improved lubrication for the fuel pumps. Diesel fuel has low viscosity and does not provide sufficient lubrication for the fuel pumps. High viscosity could lead to poor combustion, affecting engine's power output and resulting in excessive exhaust smoke. ASTM D445 provides the method for obtaining the kinematic viscosity and calculation method to determine the dynamic viscosity [9]. The kinematic viscosity for biodiesel at 40⁰C is between 1.9 to 6 mm²/s.

1.2.4 Cetane Number

The cetane number can be defined as a measurement of the ignition performance of a diesel fuel obtained by comparing it to reference fuels in a standardized engine test. The cetane number of biodiesel is determined by ASTM D613. The cetane number of biodiesel depends on the feedstock used for its productions. The higher the cetane number, the better its ignition properties are. The cetane number affects various engine parameters like combustion, stability, drivability, white smoke, noise and emissions of CO and HC. Biodiesel has a higher cetane number than mineral diesel fuel, resulting in smoother combustion.

1.2.5 Calorific Value (Heating Value)

It is defined as the total quantity of heat liberated by the complete burning one unit of mass of fuel. The calorific value of a substance is the amount of energy released when the substance is completely burned to a final state and has released all of its energy. Biodiesel has a lower heating value as compared with diesel fuel.

1.3 Cold Flow Properties (CFP) of Biodiesel

1.3.1 Cloud Point

It is defined as the temperature at which a cloud of wax crystals first appear in a liquid when it is cooled under the conditions prescribed in ASTM D 2500 [10]. The cloud point depends upon the feedstock used. In cold climatic conditions, feedstock plays an important role in decision making, whether the fuel should be used or not. It is important because the fuel line might get clogged if the fuel's cloud point is high. This is due to the presence of saturated esters in biodiesel. Biodiesel has a higher cloud point than diesel fuel.

1.3.2 Pour Point

It is the lowest temperature at which a petroleum product will begin to flow. Usually, the pour point or Cold Filter Plugging Point (CFPP) is specified, since the pour point more accurately reflects the cold weather condition of fuel. But according to ASTM standards, the CFPP and the pour point are not specified due to the reason that the global climatic conditions vary significantly and therefore, the needs of biodiesel users vary accordingly [11]. Therefore in this study, cloud point would be used as the main cold flow property to compare the fuel blends.

1.3.3 Cold Filter Plugging Point

It is the lowest temperature at which fuel will still flow through a specific filter and it is usually lower than cloud point. In cold weather regions, high cold filter plugging point will clog up the diesel engine more easily. CFPP of biodiesel is an important factor in choosing the additives which will help the use of fuels at temperature below cloud point.

1.4 Fatty Acids

Vegetable oils are mixtures of triglycerides from various fatty acids. The composition of vegetable oils depends on the feedstock. Usually, fatty acid profile or fatty acid composition are used in terms to describe the specific nature of fatty acids occurring in fats and oils. Fatty acids that include long carbon chains affect cold flow properties. Fatty acids are composed of a carboxyl

group and a hydrocarbon chain. This chain can differ in length from 4 to 24 carbon atoms. There are three types of fatty acids that can be found in any oil or fats; saturated fatty acids, mono-unsaturated fatty acids and poly-unsaturated fatty acids. The most common fatty acids in edible oils and fats are those containing 18 carbons. It consists of palmitic acid, stearic acid, oleic acid, linoleic acid and linolenic acids. Saturated fatty acids in comparison to other, form crystals easily in cold temperatures. Vegetable oils having more saturation will produce biodiesel which has poor cold flow properties. Vegetable oils having more saturation will produce biodiesel which has poor cold flow properties. Canola oil contains low concentration of saturated fatty compounds and therefore it exhibit lower CP and PP. Due to its better cold flow properties compared to palm, rapeseed and tallow oils, canola oil can be recommended for cold flow operations [12]. From the Table 1.1, it can be figured that 18 carbon fatty acids account for about 95% of canola's total fatty acids [13]. Lipid numbers have been used to name the fatty acids which are in the form of X:Y, where X is the number of carbon atoms in the fatty acid and Y is the number of double bonds in the fatty acid. Figure 1.1 shows cold flow mechanism of biodiesel.

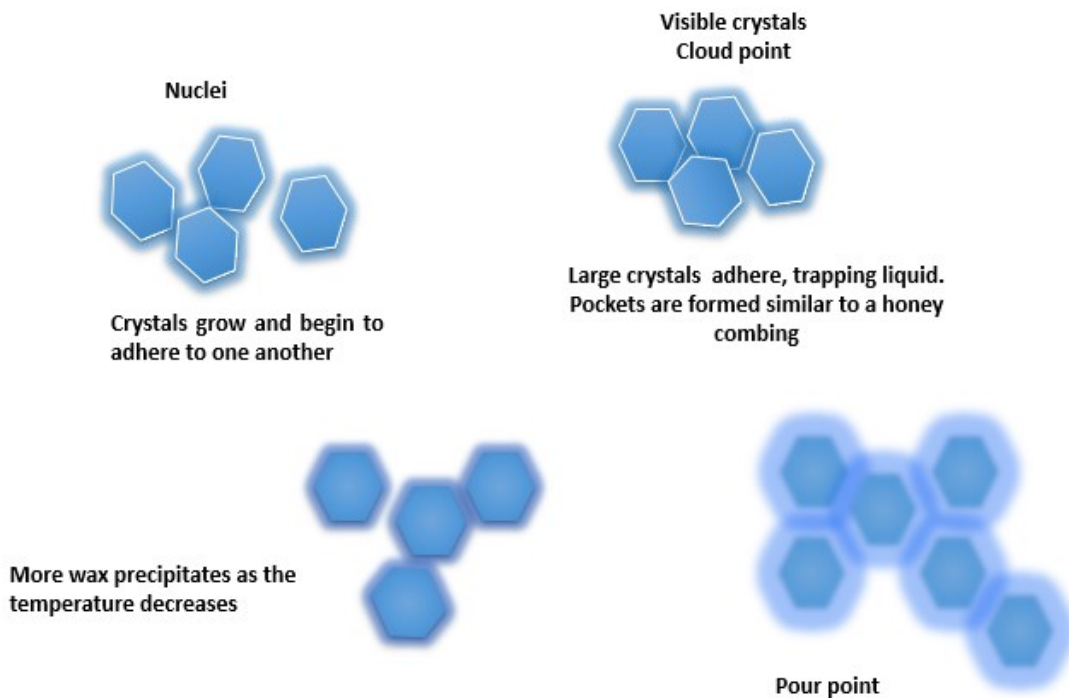


Figure 1.1: Cold flow mechanism of biodiesel

Table 1.1: Fatty acid composition of canola oil

Fatty Acid	Canola Oil
Palmitic (16:0)	4.2 %
Stearic (18:0)	2.2 %
Oleic (18:1)	62.8 %
Linoleic (18:2)	22 %
Linolenic (18:3)	6 %

1.4.1 Techniques used to Improve CFPs

To overcome these higher fatty acid concentration from the biodiesel fuel and to improve the cold flow properties of the biodiesel fuel, various processes and methods are used.

1. Biodiesel Blending

Blending of diesel with biodiesel is the most common biodiesel fuel blend. Splash and ratio are the two main techniques that can be used to create blends [14]. Splash blending is adding pure biodiesel into the tank and then adding the diesel. One of the main drawback in using this kind of method is that if the fuels have dissimilar density and viscosity, the blend would not be able to mix properly. Another disadvantage is that for the exact blend to be known, the fuel tank would have to be emptied before mixing. The second technique, which is known as ratio, consists of two fuels being blended before adding to the fuel tank. In this study, ratio-technique has been used for producing all fuel blends. Most biodiesel blends usually in use includes blends of B20 or lower in various applications. This is due to the reason that they have the perfect balance between cost, emissions and cold weather performance [15].

In this study, biodiesel would be blended with the two reference fuels i.e. summer-diesel and winter-diesel fuels. Fractionated (winterized) biodiesel and its blend with winter-diesel has also been blended to compare its cloud point with winter-diesel fuel. 2% of cold flow improver (Wintron Synergy) has been blended with winter diesel-biodiesel blends and fractionated biodiesel-winter diesel blends to enhance the cold flow properties of both biodiesel fuel series. Literature review on performance and emissions of blended biodiesel fuels would be discussed in the next chapter.

2. Winterisation of Biodiesel

Winterization includes the removal of saturated compounds accountable for the high values of CP, PP and CFPP. To overcome the disadvantage arising from low temperature properties of biodiesel, winterization technique could be applied [16]. It has been found that winterization of biodiesel could significantly reduce the cloud points (CP) and pour points (PP) of the biodiesel [17]. As mentioned earlier, in this process, the concentration of saturated fatty acid methyl esters from biodiesel is reduced. However, the various steps required in achieving a significant reduction in cloud point and the low yield translates into a higher production cost which affects the widespread use of winterized biodiesel process.

In this study, urea fractionation would be treated with pure biodiesel to improve its CFPs. There are limited studies available on fractionation of biodiesel in the literature. A review on winterized biodiesel would be discussed in the next chapter.

3. Additive

The best method for the cloud point problem is to mix biodiesel with an additive such as a pour-point depressant. These cold flow additives work by interacting with the crystals to reduce their crystal growth and to maintain the fluid flow. According to [18], most of the diesel cold flow additives have been proved insufficient for biodiesel's cloud point, however, there are some additives that are made specifically for biodiesel. Many additives lower the cold point by only few degrees, however, blending of biodiesel with diesel fuel and then adding additive would reduce cloud point significantly.

The cold flow improver chosen for this study is Wintron Synergy, which is a combination of polymethacrylate compounds in a solution of mineral oil [19]. Polymethacrylate (PMA) is an oxygenated compound with significant amount of oxygen in it [20]. From study [21], it has been found out that PMA is the best polymeric cold flow improver compared to other three improvers used in the same study. The important fuel properties of biodiesel did not worsen. It helped in the crystallization process of the crystals, by slowing down the crystal aggregation at low temperature. It improved the crystal behavior of the crystals by altering the shape of the crystals and preventing the formation of bigger crystals, which helped in improving the CFPs of biodiesel. PMAs have been present in lubricants for about 70 years now. It has been used as viscosity index improver, pour point depressants, dewaxing aids and dispersant improvers [22]. It helps in reducing the

viscosity of the fuel and improves the fuel flow in cold climatic conditions preventing the fuel line from clogging. It alters the low temperature crystallization process and disrupt the wax crystal size from becoming large enough to block the pores of the fuel filter. It is available for purchase in various quantities through Biofuelsystems.com. A 6.6-gallon drum costs \$293 and can be used for 2200 gallons of biodiesel at the suggested treatment rate of 0.3% [19]. According to the study done in [23], the added cost per gallon of biodiesel is only \$0.13 when Wintron Synergy was used as an additive.

Chapter 2

Literature Review and Thesis Objective

This chapter covers a summary of previous works on biodiesel. A brief literature on engine performance and emissions are mentioned, followed by a short review on cold flow improving additives and fractionation of biodiesel. Finally highlighting the objective of this study concludes the chapter.

A number of studies have been taken in literature for supporting the current results. Various authors have done work on improving the cold flow properties of biodiesel from edible oil sources. Many investigations show that the use of biodiesel can result in a substantial reduction in PM, CO and HC emissions. The cold flow properties of biodiesel such as high viscosity, cloud point (CP), pour point (PP), and cold filter plugging point (CFPP) causes gum formation and crystallization of fuel particles which can be enhanced by winterization (fractionation), blending and addition of cold flow improvers [24].

2.1 Engine Performance

The engine performance using biodiesel is dependent on many factors such as fuel injection and the fuel properties like oxygen content, lower heating value, and higher viscosity of biodiesel. The factors helps in influencing the spray formation and combustion of fuel. BSFC is the ratio between mass fuel consumption and brake power. Brake Specific Fuel Consumption for a particular fuel is inversely proportional to thermal efficiency. Verma et al. [25] found out that Brake Specific Fuel Consumption (BSFC) of biodiesel produced from cotton seed oil decreased as the load on the engine increased. It was also found that as the percentage of biodiesel in blend increase, BSFC also tend to increase. Roy et al. [26] investigated the effect of canola biodiesel on a two cylinder, four stroke DI diesel engine for performance under different load conditions. It was found that there was not any significant effect on BSFC up to 10 % of biodiesel blends. The BSFC of pure biodiesel increased to about 5% at low load condition and 9% at high load. The study concluded that biodiesel has higher fuel conversion efficiency than that of diesel fuel. Similar study [27] also revealed that there was no effect of BSFC up to 5% blend of biodiesel or canola oil in diesel fuel but there was 1.1% to 2.3% increase of BSFC on use of 20% blends at different speeds.

Due to lower calorific value of biodiesel, BSFC for higher biodiesel blends is higher than diesel fuel [28]. It is interesting to note that the BSFC is the actual mass of the consumed fuel to produce 1kW, however a large amount of fuel is consumed to produce the same amount of 1kW using biodiesel which would cause a tremendous increase in the BSFC [29]. Ozener et al. [30] studied the performance characteristic of conventional diesel fuel and biodiesel produced from soybean oil and its blends. Compared to diesel fuel, the average brake torque decreased with increasing biodiesel concentration over the entire speed range under full load condition. The study concluded that the average BSFC values at all engine speeds for B100, B50, B20 and B10 blends were 9%, 7 %, 4% and 2% higher than the BSFC values compared to diesel fuel. Liaquat et al. [31] studied the effect of coconut biodiesel blended fuels on the engine performance. The tests were carried at full load with biodiesel blends (B5, B15) and diesel fuel with variable speeds of 1500 to 2400 rpm at an interval of 100 rpm. The experiments revealed that the engine torque and brake power for biodiesel blends were lower compared to diesel fuel because of its lower heating value. The BSFC values for biodiesel blends were found to be increased due to higher densities as compared with conventional diesel fuel. In another study, Liaquat et al. [32] employed biodiesel-diesel blend (B20) produced from palm oil on a single cylinder, four stroke diesel engine during an endurance test which was carried out for 250 h at 2000 rpm and 10 Nm load. The test results showed that the B20 blend had higher BSFC compared to diesel fuel. The average percentage increase in BSFC was 3.88% during endurance testing for B20 compared with diesel fuel. The increased fuel consumption for B20 blend was due to higher oxygen content which resulted in lower heating value.

Habibullah et al. [33] investigated the performance evaluation of coconut, palm and their blends with diesel on a single cylinder, four stroke, direct injection diesel engine under a full load and varying speed conditions. The average BSFCs for PB30, CB30 and PB15CB15 were 8.58%, 9.03% and 8.55% higher than that of diesel fuel respectively. This was due to biodiesel's low heating value as it contains higher oxygen concentration in the fuel. On the other hand, BTE values for PB30, CB30 and PB15CB15 were approximately lower by 5.03%, 3.84% and 3.97% respectively than diesel fuel. The results indicated that the reduction in lower BTE is due to higher viscosity, density and low heating value of biodiesel than diesel fuel. Fattah et al. [34] studied the performance and emission characteristics of a diesel engine with coconut and jatropha biodiesel-diesel blends (B20) using antioxidants. The BSFC values for the B20 blends were higher by 4.76-

5.02% compared with diesel fuel and addition of antioxidants lowered the BSFC by 0.55-0.79% depending upon the feedstock. The use of antioxidant showed significant reduction in NO_x emission.

Dwivedi et al. [35] experimented diesel engine using biodiesel from pongamia oil under different load conditions. The results show that as the load increases, the fuel consumption for different blends of biodiesel decreases. This could be due to incomplete combustion of fuel at lower loads due to low cylinder gas temperature and lean fuel air mixture. At higher loads, increased wall temperature helps in reducing ignition delay which improves the combustion process and reduces the fuel consumption. In another study done by Dwivedi et al. [36] using jatropha biodiesel blends on engine performance showed BSFCs for B10 was 4% lower than diesel fuel and B20 showed similar to diesel. However, B30, B40 and B50 showed 3.4%, 5.7% and 7.5% higher than diesel fuel. The reason for similar BSFC values for B20 with diesel was due to the presence of inherent oxygen in the fuel dominating over lower calorific value for improved combustion.

2.2 Engine Emissions

In general, pure biodiesel and biodiesel blends reduces PM, HC, partially burned or unburned HC, CO₂, aromatics, PAHs and CO emissions. However, there is usually a slight increase of NO_x emissions compared to diesel fuels [37]. Armas et al. [38] tested biodiesel on a 4 cylinder, 4-stroke, turbocharged, intercooled diesel engine. The oxygenated biofuel was extracted from animal fats. The results showed lower HC, CO and PM emissions. In case of NO_x emissions, a slight decrease was achieved using biodiesel as an alternate fuel. Singh et al. [39] investigated the emissions from a diesel engine fueled with biodiesel and hydroprocessed renewable diesel (HRD). Both were produced from same feedstock i.e. Jatropha curcas oil by different processes. Using the European stationary cycle, an idle condition was experimented as one of the thirteen modes. Biodiesel was able to reduce PM, CO and HC more effectively, although HRD reduced NO_x by 29% and BSFC compared with conventional diesel fuel. An et al. [40] studied the effects of emission from diesel engine with biodiesel produced from waste cooking oils under multiple idling conditions at 800 and 1200 rpm. The tests revealed that higher HC and NO_x emissions were emitted at idle conditions but not at high rpm conditions, stating that low engine speed has significant effect on emissions when using biodiesel. Another experiments conducted by An et al. [41] on a common rail fuel injection diesel engine using ultra low sulfur diesel engine, biodiesel and their blends

concluded that partial load and idle conditions have major influence on BTE, BSFC and CO emissions.

Cheik et al. [42] conducted experiments using biodiesel blends on a naturally aspirated, direct injection diesel engine under different loads at 2500 rpm. The results revealed that the variation of engine speed and load had a great influence on engine emissions. Increasing the engine speed lead to increase in HC emissions. However, with increase in engine load lead to higher emissions of CO and PM. Due to higher amount of oxygen content in biodiesel blends, NO_x emissions increased slightly. Rahman et al. [43] used Jatropha biodiesel and their blends (B10 and B20) along with diesel fuel on an in-line four cylinder CI engine at different engine speed and load conditions. The results concluded that with higher amount of blend percentages, CO and HC emissions decreased. However, as blend percentages increased to NO_x emissions increased significantly. The experiment also revealed that compared to pure diesel fuel, fuel consumption increased for biodiesel-diesel blends with increasing amount of blend percentage. Yanh et al. [44] performed experiments on a common-rail fuel injection diesel engine using diesel fuel, biodiesel and their blends (B10, B20 and B50) under various loads. They noticed that engine load had an impact on CO emissions. It was found that at higher engine loads, CO emissions increases with decreasing biodiesel blend ratio and increasing engine speeds. Another tests conducted on a Euro IV diesel engine by Yanh et al. [45] with biodiesel produced from waste cooking oil and its blends at four different engine speeds and under three different loads. The study revealed that low engine speed has a significant effect on the formation of CO, HC and NO_x emissions.

Habibullah et al. [46] studied the effects of 20% palm biodiesel or coconut biodiesel blend, their combination (5%-15%) and diesel fuel on performance and emissions of a single cylinder, four stroke direct injection diesel engine under full load conditions at varying speeds from 1400- 2400 rpm. The experiments found that the coconut biodiesel blends showed lower break power of about 1.72% due to low heating value, and increased the NO_x emissions by 4.49% due to high oxygen content of coconut. It was concluded that the addition of palm biodiesel (5-15 vol. %) could significantly improve the low BP output and high NO_x emissions in coconut biodiesel-diesel blends. The CO and HC emissions from all the biodiesel blends decreased from 3.36% to 7.01% and 13.54% to 23.79% respectively compared with diesel fuel. An investigation [47] was done on performance and emissions of a four stoke, turbocharged, direct injection, four cylinder, and high-pressure common rail diesel engine with coconut biodiesel (B10, B20, B30 and B50) under

different loading conditions. The BSFC was found higher at all loading conditions due to lower calorific value. Carbon monoxide emissions decreased and NO_x emissions increased with increase in biodiesel concentration in the blend and engine load. At all load conditions, smoke emissions were found to be lower with coconut biodiesel blends as compared with conventional diesel fuel. At B50 and 0.86 MPa, the smoke opacity was reduced to 52.4%. The reduction in smoke emissions was due to lower carbon and high fuel borne oxygen content in biodiesel which helped in more complete combustion and limited the formation of smoke.

Rahman et al. [48] explored the blend properties of moringa oleifera biodiesel (5 and 10 vol. %) and compared with palm biodiesel and diesel fuel. The performance evaluation of all the fuel blends were done on a multi-cylinder diesel engine at various engine speeds and under full load condition, however the emission measurements were done under full load and half load condition. The study exhibited lower brake power for biodiesel blends (PB5, MB5, PB10 and MB10) with 1.38%, 2.27%, 3.16% and 4.22% reduction compared with diesel fuel. BSFC was found higher with 0.69%, 2.56%, 2.02% and 5.13% increase for PB5, MB5, PB10 and MB10 respectively, compared with diesel. Moringa oleifera biodiesel blends were found to produce lower CO and HC emissions compared with diesel fuels, Therefore, the study emphasised that these blends could be replaced with diesel fuel to lower exhaust emissions into the environment. Rahman et al. [49] did another test on the effect of jatropha curcas and moringa oleifera biodiesel blends on the performance of a four cylinder diesel engine and emission at full load condition at different engine speed. The study depicts that the brake powers of MB10 and JB10 were 4% and 5% lower than those of diesel fuel. Compared with diesel fuel, MB10 and JB10 decreased the HC emissions by 12% and 16% respectively, CO emissions by 11% and 14% respectively and increased the NO_x emission by 9% and 10% respectively, and CO₂ emissions by 5% and 7% respectively.

Zhu et al. [50] investigated the performance and emissions of a 4 cylinder direct injection diesel engine fueled with diesel and biodiesel fuels blended with 5%, 10% and 15% by volume of methanol and ethanol. The BSFC was found to increase with higher amount of alcohols in the fuel due to its lower heat values. CO and HC emissions increased and NO_x emissions decreased with the percentage of methanol and ethanol in the blended fuel. Moreover, Methanol blends proved more effective than ethanol in decreasing PM and NO_x emissions due to the higher latent heat of evaporation of methanol. Yilmaz et al. [51] studied the effects of emissions on a two cylinder, 4-cycle, DI diesel engine generator with biodiesel-ethanol-diesel blends. Ethanol concentrations

were varied at 3%, 5%, 15% and 25% in biodiesel-diesel blends. Engine tests were conducted from no load to high load. Main factors which affected the emission reduction was due to better cooling effects and oxygen content of alcohols. The experiments showed that the blends increased the CO emissions compared to diesel at low load conditions, however, there was no significant change in CO emissions at high loads based on fuel types or blends. Ethanol blended fuels reduced NO emissions for all concentrations. HC emissions were found to depend on both ethanol concentrations and operating conditions. With increasing amount of ethanol blends, HC emissions were found to increase up to 50% load. Nevertheless, above 50% load, ethanol decreased HC emissions for all concentration.

In study [52], 2.5%, 5% and 7.5% by volume of ethanol was blended with neat biodiesel from animal fat to test on a single cylinder, naturally aspirated, water cooled DI diesel engine at different load and constant speed of 1500 rpm. Ethanol addition was found to reduce CO, HC and smoke emissions when compared to neat biodiesel and the reduction was higher at higher load conditions. It was found that the HC reduction was achieved with higher amount of ethanol additives in the biodiesel blends. However, NO_x emissions increased tremendously with increase in ethanol addition at higher loads. In [53], Biodiesel with ethanol additive was tested on supercharged DI diesel engine at an engine speed of 1500 rpm with loads from 20% to 100%. NO_x emissions were found to increase with loads, although blending with ethanol helped reducing NO_x emissions. It was found that CO and HC increase with addition of ethanol at all load conditions. But these increases were reduced when the engine was supercharged. Two engines were used to test the fuel emissions in [54]. Ethanol-biodiesel blends were tested on a multi cylinder, turbocharged, common rail injection system and an exhaust gas recirculation system (EGR), and a single cylinder, direct injection, four stroke diesel engine running in low temperature condition. Three test conditions were tested: 1500 rpm at 3 bar Brake Mean Effective Pressure (BMEP); 2500 rpm and 6 bar of BMEP; and 4000 rpm at full load. It was noticed that higher NO_x and smoke, and lower CO and HC were obtained at higher load and higher speed condition (2500 rpm, 6 bar) than lower load, lower speed condition (1500 rpm, 3 bar) for all the fuel blends. However, ethanol blended fuel showed lower NO_x but higher CO and HC emissions than diesel fuel. Due to the weak sooting tendency of ethanol blends allowed higher EGR rates in reduction of NO_x emissions. Ethanol blends allowed for increase in operating range of low temperature condition mode in single cylinder diesel engine due to lower smoke emissions.

Zhang et al. [55] investigated the particulate emission characteristics of a single cylinder, direct injection diesel engine fueled with blends of butanol and pentanol in biodiesel at 10% and 20% by volume. The engine was operated at a constant engine speed of 3000 rpm and at three engine load of 25%, 50% and 75%. Organic carbon and water soluble organic carbon decreased significantly with loads whereas elemental carbon increased with loads. Both the alcohol blends were able to effectively reduce particulate mass, elemental carbon emissions and polycyclic aromatic hydrocarbons at all loads. Park et al. [56] studied the effect of biodiesel in bioethanol blended diesel fuel. The test engine was operated at an engine speed of 1200 rpm and at an injection pressure of 120 MPa. The biodiesel blending effect resulted in reduction of HC, CO and soot emissions at early injection timing. Rakopoulos [57] experimented HSDI diesel engine using blends of diesel fuel with ethanol, butanol and diethyl ether at different volume percentages for emission analysis. He found out that with increasing percentages of all the biofuels in the blends, significant reduction of smoke opacity was achieved mainly higher for butanol blends, reduction of NO_x emissions mainly higher for diethyl ether blends and reduction of CO emissions compared with diesel fuel. A study done by Lanjekar et al. [58] found out that coconut and palm kernel oils having high content of lauric acid produce lower amount of NO_x emissions, better oxidative stability and improved cold flow properties.

2.3 Review on Cold Flow Improving Additives

Biodiesel cold flow properties are usually depend on fatty acid methyl esters. [59]. Diesel has good cold flow and better oxidative stability than biodiesel due to no amount of saturated and unsaturated fatty acid methyl ester compounds [60]. In many literatures, it has been proved that biodiesel cold flow properties were improved when blended with conventional diesel fuel [61]. Various cold flow improver additives are available in the market which are used for winterization of biodiesel as well as to improve the emissions [62]. A study by Verma et al. [63] on the experimental analysis of palm biodiesel found out that CP and PP of palm biodiesel improved significantly by blending with diesel fuel, while blending with kerosene it showed remarkable enhancement. Bhale et al. [64] studied the effect of ethanol, kerosene and additives on cold flow properties of biodiesel. The study concluded biodiesel-ethanol blend as a sustainable alternative fuel for improved cold flow behavior and reducing CO, NO_x and smoke emissions without effecting the engine performance.

Altaie et al. [65] investigated the effect of methyl oleate and palm oil biodiesel blends on cold flow and fuel properties. It was found out that increasing the methyl oleate volume concentration in biodiesel blends enhanced its cloud points and cold filter plugging points. The test results show that 50% of methyl oleate decreased the cloud point and the cold filter plugging point up to 70.38% and 91.69% respectively. It was noticed that cetane number of the blends were reduced by 5% when blended with 50% methyl oleate and there was no substantial change in viscosity, density, gross and net heating results of all the blends with respect to palm oil biodiesel. A study [66] was done on ethyl acetoacetate as a diluent for improving the low temperature properties of biodiesel produced from waste cooking oil. It concluded that 20% by volume of diluent in biodiesel decreased both pour point and CFPP by 4°C. It also revealed that the acid value was decreased considerably using ethyl acetoacetate in the blends. In another test done by Cao et al. [67] to improve the cold flow properties of biodiesel, ethylene vinyl acetate copolymer was used as a cold flow improver. The results showed that EVAC minimized the crystallization rate of wax crystals in biodiesel blends. Therefore, it was able to reduce the cloud point, CFPP and pour point of B20 from -4°C, -5°C and -8°C to -12°C, -16°C and -18°C respectively when 0.04 percentage volume of EVAC was mixed.

Tests [68] were done on two branched chain fatty acid methyl esters mixed with biodiesel produced from canola, palm and soybean oil to decrease their cloud points and pour points. It was found that with increased amount of BC-FAME usually between 17 and 39 mass percentage helped in improving the CP and PP of the biodiesel blends without increasing the viscosity under the specified limits of ASTM standards. An investigation [69] was done to find out the cloud point improving additives using the thermodynamic model. It was revealed that the molar mass of the additive had an important role in improving the cloud point of the biodiesel fuel produced from cooking oils. The additives which were selected on the basis of their molar mass are tert-butyl alcohol, 2-butanol, cineol, 2-decanol, 2-decanone and oleyl alcohol. They proved in reducing the cloud point values with the maximum reduction obtained by using 10 weight percentage in the biodiesel blends. A study [21] was done on the effects of polymeric cold flow improvers on flow properties of biodiesel produced from waste cooking oil. Results showed that polymethyl acrylate (PMA) was the best cold flow improver without affecting other fuel properties of biodiesel. However, it was interesting to observe that the viscosity index of biodiesel was also improved with the use of PMA at low temperature conditions. It also helped in hindering the crystal aggregation

and reducing the formation of bigger crystals at low temperature. Mixing of 0.04% of PMA with biodiesel from waste cooking oil reduced its PP and CFPP by 8^oC and 6^oC respectively. Similar results [70] were obtained when olefin-ester copolymers (OECF) was used at 0.03% with soybean biodiesel. It prevented the formation wax crystals from growing. The cold flow improver was able to considerably decrease the pour point, CFPP and viscosity of biodiesel at low temperature conditions and therefore enhancing the cold flow properties of biodiesel. Katiyar et al. [71] studied the effect of poly (lactic acid)-oligomer (OLLA) as an additive on cold flow properties of soybean biodiesel. It reduced the cloud point, pour point, flash point and fire point by 6^oC, 2^oC, 31^oC and 20^oC respectively. The additive exhibited resistance to the evolution of crystal growth which helped in reducing the dynamic viscosity at lower temperature. The engine performance analysis showed no significant change on BSFC and brake thermal efficiency. On the other hand, CO and HC were decreased with addition of OLLA in B20 blends.

In an experiment [72], three different cold flow improvers; ethyl acetoacetate (EAA), iso-decyl methacrylate (EHMA) and iso-octyl methacrylate (IOMA) were mixed in different proportions. The best results on cold flow properties were found when 2.5 volume percentage of EAA and 10 volume percentage of IOMA were blended together in B50. The CFPP and PP of B50 were reduced by 11^oC and 12^oC. Moreover, it also helped in improving the biodiesel properties such as decreasing density, viscosity, flash point, acid value and increasing the oxidation stability of the fuel. A study [73] showed 2-Butyl esters of palm oil as the best cold flow improvers. It reduced the cloud point and pour point up to 6^oC when 5% of the additive was blended with biodiesel. The experimental analysis proved that the additive helps in decreasing the crystal size and had no significant influence on the fuel properties of palm biodiesel. Joshi et al. [74] tested ethyl levulinate as a diluent for biodiesel with high saturated fatty acid content, produced from cottonseed oil and poultry fats. Reduction in cloud point, pour point and CFPP up to 5^oC, 4^oC and 3^oC were noticed with 20 volume percentage of diluent in biodiesel blend. Other biodiesel fuel properties like oxidative stability, viscosity and flash point were improved. Chastek [75] experimented different solvent and polymeric additives to improve the cold flow properties of canola biodiesel. He found that 1% of poly (lauryl methacrylate) significantly improved the CFPP and PP by 20^oC and 30^oC, respectively.

Joshi et al. [76] studied the effects of cold flow properties of poultry fat methyl esters (PFME) when blended with short-chain alcohols such as ethanol, isopropanol and butanol. Results showed moderate improvement in low temperature conditions of PFME with increasing alcohol blend ratio. However, decrease in kinematic viscosity of PFME was observed with alcohol content. Study concluded that butanol-PFME blends showed slight superior cold flow properties than the other alcohol-biodiesel blends. A study [77] was done on butanol to replace methanol as an additive in fuels to improve the low temperature properties. The comparative studies of the cold flow properties of fuel mixtures containing diesel fuel, rapeseed oil methyl or butyl esters and butanol showed that in cold climatic conditions, it is possible to use fuel blends containing up to 14% rapeseed methyl esters and up to 18% rapeseed butyl esters. In [78], a mixture of 0.2% additive, 79.8% biodiesel and 20% kerosene reduced the pour point of B100 by 27°C.

2.4 Review on Fractionation of Biodiesel

Improved cold flow properties are formed with higher percentage composition of unsaturated, branched and short chain fatty esters. Winterization helps in reducing the saturated esters and hence improves the cold flow [79]. Winterization is a physical process which includes fractionating the oil to reduce its high melting components. There are various fractionation processes. The normal fractionation process consist of two stages. The crystallization stage consists of selective nucleation and crystal growth under a highly controlled cooling rate combined with mild agitation. Once well-defined crystals with a narrow distribution of specific sizes and characteristics are formed, the resulting mixture is moved to the second stage for separation into solid and liquid particles, usually by filtration or centrifugation [80]. The two oil fractionation process which are used widely are: dry fractionation through batch crystallization of the oil by controlled cooling and subsequent continuous filtration process and solvent fractionation through continuous crystallization of the oil in a solvent followed by separation of the liquid and the solid fraction through a continues filtration process [81]. To overcome the problem of lower yield with no significant reduction in pour point, researchers have come up with an idea of winterizing methyl esters with various solvents. Methanol, acetone, chloroform and hexane have been explored as diluting solvents [82]. Methanol offers the benefit that winterization may be easily incorporated into the industrial biodiesel production facilities due to its easy availability in the market. The saturated methyl esters showed a higher immiscibility in methanol than the higher molecular linear

alcohols in study [83]. Methanol has also been used as a reagent in transesterification process which may boost the winterization of biodiesel in industrial biodiesel production facilities.

In study [84], winterization of beef tallow biodiesel was done by fractional crystallization to reduce the saturated fatty acid content in it. The results showed reduction in cloud point from 21⁰C to 17.4⁰C, pour point from 10.8⁰C to 3.5⁰C, density from 899 kg/m³ to 861 kg/m³ and kinematic viscosity from 5.5 mm²/s to 5.32 mm²/s. Wang et al. [85] conducted experiments on improving the cold flow properties of biodiesel produced from waste cooking oil by two different processes namely surfactants and detergent fractionation. From the surfactant tests, the highest reduction in CFPP was achieved from -10⁰C to -16⁰C by addition of 0.02 wt% polyglycerol ester. In addition, detergent fractionation showed lowest CFPP of -17⁰C from waste cooking oil biodiesel with a yield of 73%. In [86], supercritical CO₂ extraction and fractionation were tested to recover the *Jatropha curcas* oil from biodiesel production. The highest amount of free fatty acids (26.3 wt.%) were extracted in the first fraction and then the pressure was increased to achieve higher amount of oil removal with very low amount of free fatty acids in the later stages.

2.5 Thesis Objective

As discussed in the aforementioned literature review, although there have been a number of studies on performance and emissions of biodiesel fuel, still the main problem limiting the application of biodiesel is its poor low temperature properties have been neglected. The objective of this study is to test the year-round biodiesel use strategy in diesel engines in Canadian adverse cold weather conditions specifically in Thunder Bay region. In this study, different blends of biodiesel and fractionated biodiesel will be tested to compare the emissions with two different diesel fuels used as a reference fuels. Furthermore, chemical additive (Wintron Synergy) is used to lower the cloud point of the blends. In this study, tests will be done on two separate engines; a heavy-duty diesel engine at low idling condition and a light-duty two cylinder diesel engine with varying engine loads at different engine speeds to compare the performance and emissions with diesel fuel. On the other hand, there are limited studies on fractionated biodiesel being treated as a blending fuel for improving low temperature properties of biodiesel for cold climatic conditions.

Chapter 3

Methodology

3.1 Biodiesel Production:

The method of producing biodiesel is started by mixing up the two components: sodium hydroxide which acts as the catalyst and methanol. These are added in the proportion of 200 ml methanol and 3.5 gm of catalyst. They both are taken in the air tight container and mixed up properly until the catalyst is properly dissolved in it. Methanol and sodium hydroxide pellets were all provided through Lakehead's Chemical Engineering Lab. Another component which is taken canola oil. Due to canola oil's high yield despite often short growing season in Canada's moderate temperature climate, it is considered as the main feed for the production of biodiesel in Canada. Canola oil was purchased from a local supermarket as the feedstock for this study. It is heated up to 65°C. After heating it up, the mixture of methanol and catalyst is added in blender. Then this solution is left to blend at high speed for at least 50 minutes, so that these should mix up properly. The speed of the blender should be high enough to mix it. During blending, the process is monitored at equal interval to check the temperature because the boiling point of the methanol is around 65°C. So, the temperature of the mixture should be below that point.

When the single-phase solution is ready, it is poured in 2 litre bottle, and kept for a single day. After 24 hours, 2 major products are formed: glycerin, which is known as the by-product of the biodiesel and the other one is the biodiesel itself. Due to its higher density, glycerin is settled at bottom of the bottle and biodiesel is separated by pouring it into new bottle carefully. Next process, starts by putting warm water in the biodiesel to purify it. It is washed twice for the better quality. The main purpose of washing it is, to get rid of the residues and any kind of soaps if present. The quantity of water added in both cases is nearly 50% of the biodiesel we have. After adding water, shake it properly for almost 5 minutes and keep it for almost day in both cases. After first time washing, there will be 2 products like biodiesel and fatty acids. Acids have higher density so they will be at bottom and again biodiesel is separated by pouring it carefully. For the second time, there will be 2 different liquids. One will be biodiesel with less density and the other will be water and very few marks of fatty acids. They again are separated. After this separation, biodiesel is finally ready. This final product is heated up to 70°C to make it purer and hence the final product is ready to use. Colour of biodiesel is usually reddish yellow. Biodiesel production quality was tested according to ASTM 6751 standards, which can be found in Table 3.1

Table 3.1: Properties of canola biodiesel

Test Name	Test Method	ASTM limit	Results
Free Glycerin (mass%)	ASTM D6584	Max. 0.02	0
Total Glycerin (mass%)	ASTM D6584	Max. 0.24	0.112
Flash Point, Closed Cup ($^{\circ}\text{C}$)	ASTM D93	Min. 130	169
Water & Sediment (vol.%)	ASTM D2709	Max. 0.505	0
TAN (mg KOH/g)	ASTM D664	Max. 0.5	0.14
Simulated Distillation, 50% recovery ($^{\circ}\text{C}$)	ASTM D2887	N/A	359.8
Cetane Index	ASTM D976 (2 variables formula)	N/A	50
Copper Corrosion, 3h @ 50°C (rating)	ASTM D130	Max. 3a	1a

3.2 Urea Fractionation Process:

This method is used to fractionate biodiesel into its saturated and unsaturated components. Urea has been proved to form an adduct with saturated biodiesel. Urea in the presence of suitable amount of guest molecule would form hexagonal channels allowing for guest addition. Crystalline solids would precipitate out of the urea-methanol-biodiesel mixture (usually containing the urea-saturated biodiesel adducts) when the solution is kept for a day at room temperature. A portion that is high in unsaturated fatty acid esters would have a much lower cloud point than the portion high in saturates [87]. The production of fractionated biodiesel has been described in the following steps:

1. 44gm urea is added to 150 ml methanol.
2. Mix it properly until most of the urea is dissolved in solution.
3. Add 50 ml of biodiesel and mix solution with heat up to 60°C to form single liquid phase.
4. Turn off heater and stir the solution to cool down up to 24°C .
5. Keep the solution for 24 hours and crystals would appear as shown in Figure 3.1



Figure 3.1: Urea crystals formed after 24 hours

6. Connect the Buchner funnel to Aspirator using tubing and filter the mixture to separate urea crystals as shown in Figure 3.2



Figure 3.2: Buchner funnel

7. The filtered solution is heated up to 70°C to derive off most of the methanol, leaving two liquid phase solution.
8. Turn on the stirrer (Figure 3.3) to cool the solution up to 24°C .



Figure 3.3: Magnetic stirrer

9. Place the solution for 24 hours.
10. Filter the solution and heat it up to 150°C to decompose urea [87].

3.3 Measurement of Density:

$$\text{Density} = \frac{\text{Mass}}{\text{Volume}}$$

Steps as follow:

1. Small beaker of scale 100 ml is taken and is weighed (me) on weighing scale (Figure 3.4). Taken beaker is empty.

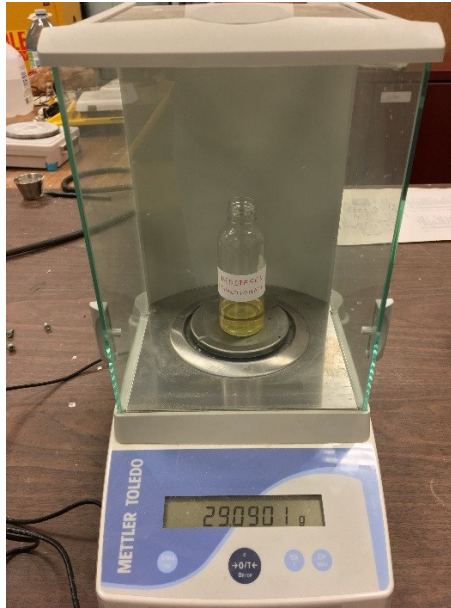


Figure 3.4: Weighing scale

2. Then 100 ml of biodiesel (v) is added in the beaker and weighed again (mf) which will tell you the weight of the biodiesel along with the beaker.
3. Subtracting the weight of empty beaker from the beaker having biodiesel will tell you the exact weight of the biodiesel itself.
4. $m_b = (m_f) - (m_e)$
5. Now using the formula of density which is mentioned above to find out the density of the biodiesel.

3.4 Measurement of Viscosity:

For measuring the viscosity, specific viscosity meter is used which is called Ostwald viscometer (Figure 3.5). The general temperature at which viscosity is measured is at 40°C, complying with ASTM D445 [46].



Figure 3.5: Viscometer

Below are the steps to measure:

1. The water inside the water tank is heated up to 40°C using water tank fixed heater and using external heater as well.
2. The heater should be placed constant at 40°C, so that the temperature should be kept constant all over the process.
3. Viscosity meter is placed inside the water tank using the clip to keep it fix for the test.
4. About 80% of the viscometer should be kept in water for getting the best result, i.e. keeping the both ends out.
5. Viscometer has 2 red marks marked, fill the solution till the first mark and then it is pumped to make the solution reach little ahead of the second red mark.
6. Pump is removed at once when it crosses the second park and wait until it reaches the second red point.
7. When the solution reaches the second point, at once turn on the stopwatch and wait until it reaches the first red mark again.
8. Turn off the stopwatch when it reaches the mark, and note the time.

9. Then an appropriate formula is used for calculating viscosity with the help of the noted time.

3.5 Measurement of the Heating Value:

Heating value of the liquid is the calorific value of that respective solution. It is measured with the help of the calorimeter. According to the standards set by ASTM for measuring heating value, the procedure is discussed below:



Figure 3.6: Calorimeter

1. Calorimeter (Figure 3.6) is turned on to heat up the water in the jacket up to 30°C, using heater, which is already a part of calorimeter.
2. Measure 2000 ml of distilled water in bucket and place it in the calorimeter.
3. Sample is taken whose heating value is needed to be calculated, it should be weighed around 0.6 gm in a weighing machine.
4. Next step is to take the wire of 10 cm.
5. Sample is placed in the head and the fuse wire is attached to the stings of the bomb head which is dipped completely into the fuel sample taken. But the wire should not touch the sides of the container in which fuel is taken.
6. Put few drops (2-5) of distilled water in the bomb.
7. The head is put into the cylindrical bomb, which is closed tight enough.
8. Oxygen gas is put into the bomb with enough pressure for 30 seconds. Later, the nozzle on the top of the bomb is closed and the pressure of 160 psi is made inside the bomb.
9. Using tong, place the bomb inside the bucket, which is already been placed inside the calorimeter and attach the ignition wires to the bomb head.

10. After removing the tong, the top of the calorimeter is closed manually.
11. Two thermocouples are used, to measure the temperature of the jacket and the bucket.
12. Temperature of both the parts are made to be equal, to make it an adiabatic process.
13. Make the temperature of the jacket and bucket in between 25-27°C.
14. Press the ignition button for 5 secs to ignite the wire.
15. Let the process go on for at least 9 minutes.
16. Note the temperature at every single minute, and turn off the power after 9 minutes.
17. Lift the thermocouple and the top of the calorimeter to take out the bomb and the bucket, by disconnecting the igniting wires with the help of tong.
18. Open the bomb, by opening the nozzle of the bomb to remove all the oxygen carefully, take out the wire from it.
19. Calculate the length of wire remaining and later, calculate the wire burnt.
20. See the temperature difference as well.
21. Heating value formula is used to calculate it.

Table 3.2 summarises the density, viscosity, CP and heating value of summer diesel-biodiesel blends, winter diesel-biodiesel blends, winter diesel-biodiesel-synergy blends, winter diesel-fractionated biodiesel blends and winter diesel-fractionated biodiesel-synergy fuel blends. All the tests except CP were performed at Lakehead University. Fuel samples were sent to a Canadian laboratory to examine the CP. The cloud point was measured according to ASTM D5773 standard. A viscometer was employed to quantify the viscosity of the sample fuels in a water bath at a constant temperature of 40°C. A bomb calorimeter was used to measure the heating value of all the fuel blends.

Table 3.2: Fuel properties of summer diesel-biodiesel, summer diesel-biodiesel-synergy blends, winter diesel-biodiesel, winter diesel-fractionated biodiesel, winter diesel-fractionated biodiesel-synergy blends

Fuels	Cloud Point ($^{\circ}\text{C}$)	Heating Value (kJ/Kg)	Density (kg/m 3)	Viscosity (cSt @ 40 $^{\circ}\text{C}$)
SD100	-26	44768	832	1.92
SB10	-17.4	44320	837	2.16
SB20	-16	43871	842	2.4
SB30	-14.6	43436	846	2.63
SB40	-12.7	42984	851	2.98
SB50	-10.4	42537	856	3.2
SB60	-8.2	42073	861	3.42
SB70	-7.4	41642	866	3.71
SB80	-5.1	41195	870	3.91
SB90	-3.5	40748	875	4.12
B100	-2.6	40296	880	4.32
WD100	-41	45574	830	1.96
WB10	-34	45046	835	2.18
WB20	-28	44519	840	2.46
WB30	-23.5	43107	845	2.67
WB40	-19.7	43476	850	3.02
WB50	-16	42953	855	3.22
WB60	-14	42419	860	3.44
WB70	-11.4	41883	865	3.72
WB80	-9	41357	870	3.91
WB90	-6.2	40832	875	4.14
WB20S2	-34.8	44534	824	2.65
WB50S2	-21	42966	857	3.51
B100S2	-7.9	40354	912	5.16
FB20	-36.6	44486	843	2.45
FB50	-35.6	42855	863	3.29
FB100	-31.7	40136	895	4.41
FB20S2	-47.5	43887	850	2.67
FB50S2	-48.2	42265	870	3.51
FB100S2	-37.7	39564	901	5.19

3.6 Thunder Bay Green Fleet Plan

The objective of the plan is to reduce greenhouse gas emissions from Government operated city buses and vehicles. This Green Fleet Implementation Plan makes a contribution to the Governments of Ontario and Canada's commitment to the reduction of harmful vehicle emissions. This strategic plan has established the framework to reduce the emissions by 2016; the annual corporate fleet emissions by up to 21.5% from 2005 baseline levels and contribute towards its goal of reducing GHG emissions as noted in the Community Environmental Action Plan. Benefits can be measured in terms of social, economic and environmental benefits, such as improved energy efficiency, reduced traffic on city roads, cleaner air and reduced GHG emissions contributing to a better quality of life, and reducing health care costs in the long term. From 2009 to 2016 inclusive, the plan is expected to reduce emissions from internal combustion engines by 9774 tonnes overall combined. A phased implementation of biodiesel fuel was required in all fleet areas starting with B5 blends biodiesel in 2009 and 2010, and increasing the blend by 5% every two years thereafter to 2016 reaching a blend rate of B20. Biodiesel blend fuel has the ability of reducing the fleet CO₂ emissions by 5770 tonnes from 2009 to 2016. Biodiesel blend fuel testing shows an increase of 3 to 5% over the normal consumption.

Under this plan, biodiesel usage is only valid in summer season due to biodiesel's high cloud point which will deter its use in winter season. However, comparing to this study, it is proved that fractionated biodiesel could be used even in cold weather conditions. This study might help the government to revive their current plan and increase the average biodiesel usage currently being used under the plan. This study may also help in addition of fractionated biodiesel under this plan which will be used in winter months that will assist in achieving the goal of reducing harmful combustion engine emissions while improving local air quality. The study will also help in focusing on reduction in consumption of non-renewable energy and wasteful use of energy. According to the U.S National Board of Biodiesel, Colorado's Aspen Resorts, The City of Keene, New Hampshire; Harvard University and Yellowstone national Park, all uses B20 fuel blend year round [88].

3.7 Engine under Study:

Two different engines are being tested in this study. A heavy-duty (Figure 3.7) Cummins engine is a 4-cylinder turbocharged diesel engine with a high pressure common rail injection system. This kind of engine is mainly used in agriculture, mining and construction. It consists of a cooled EGR

system and a diesel oxidation catalyst (DOC)/diesel particulate filter (DPF). A dual tank fuel system was installed for switching between various fuel blends. Figure 3.8 shows a schematic diagram of the experimental test setup.

Table 3.3: Engine specification for heavy-duty engine.

Engine Make and Model	Cummins QSB 4.5 T4I
Engine Type	Inline 4-Cylinder
Number of Cylinders	Four
Bore * Stroke	102mm * 138mm
Swept Volume	4.5 l
Compressions Ratio	17.3:1
Rated Power	97KW @ 2300 RPM



Figure 3.7: Heavy-duty engine test setup

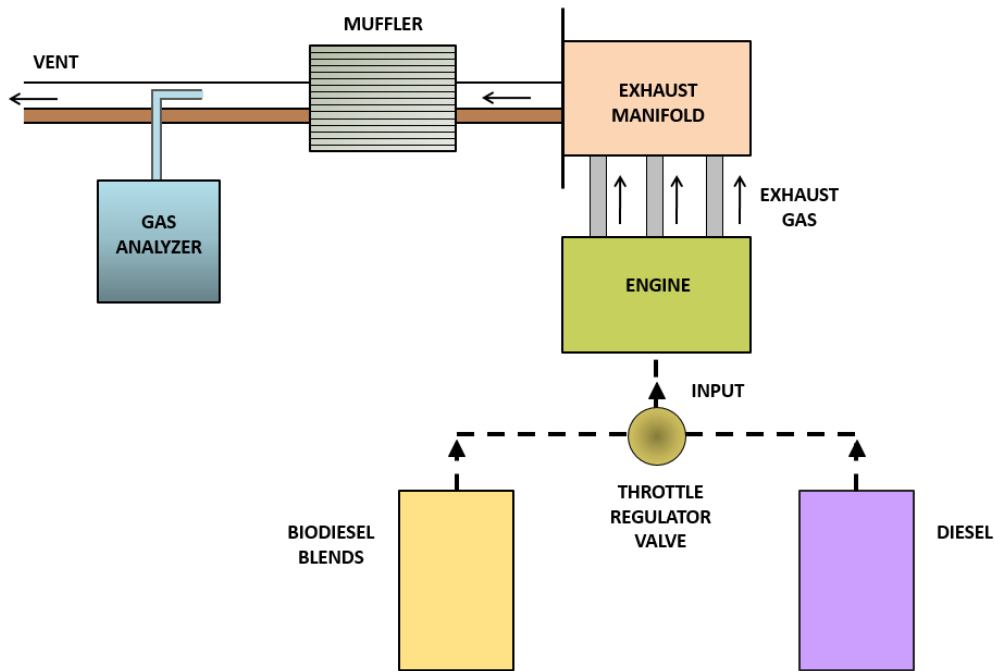


Figure 3.8: Schematic diagram of heavy-duty engine test setup

A light-duty diesel engine (Figure 3.9) have also being used at variable engine load and speed. Hatz 2G 40 is an air-cooled 2-cylinder four stroke diesel engine. This engine is rated for Tier 4 regulations. Figure 3.10 shows the schematic diagram of the experimental test setup for the light-duty engine.

Table 3.4: Engine specifications for light-duty engine

Engine Make and Model	Hatz 2G40/2G40H
Engine Type	Four stroke
Number of Cylinders	Two
Bore/Stroke	92mm/75mm
Displacement	997 cm ³
Rated power	17 kW @ 3000 rpm



Figure 3.9: Light-duty engine test setup

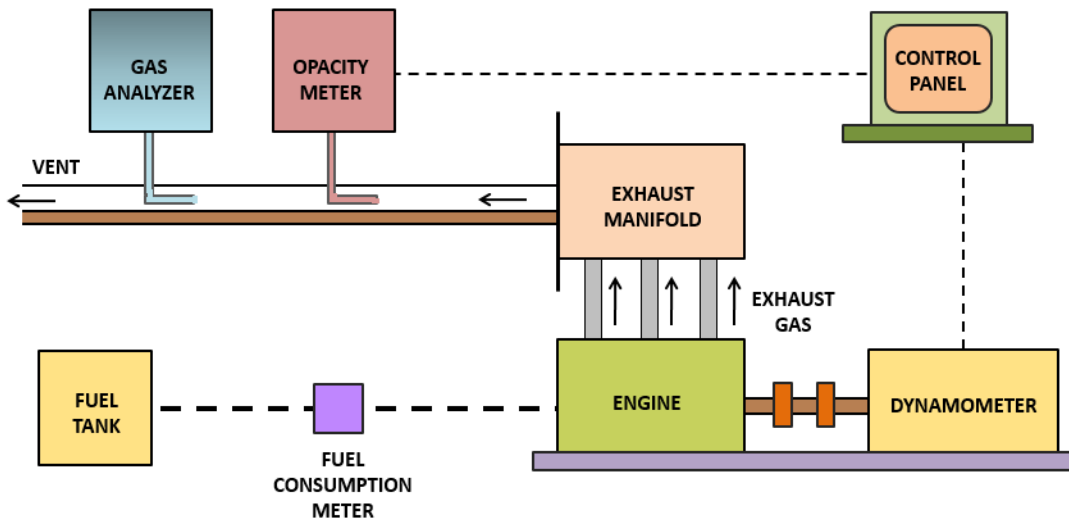


Figure 3.10: Schematic diagram of the experimental test setup for the light-duty diesel engine

3.8 Engine Test Procedure:

The tests were done to examine the performance and emissions of various summer and winter diesel fuel blends. The first series consisted of summer diesel blends which has been blended with normal biodiesel at different volume percentages (10-100 vol%). The second series consisted of winter diesel blends which has been blended with normal biodiesel at different volume percentages (10-100 vol%). The third series comprised of 2 volume percent of Wintron Synergy in winter diesel-biodiesel fuel blends (20 vol%, 50 vol% and 100 vol%). The fourth series comprised of fractionated biodiesel blends in which winter diesel was blended with fractionated biodiesel at three different volume percentages (20 vol%, 50 vol% and 100 vol%). Finally, winter diesel-fractionated biodiesel was treated with 2 vol% Wintron Synergy with 20 vol%, 50 vol% and 100 vol% of fractionated biodiesel.

Two types of engine were used. A heavy-duty engine was tested at idling condition at 800 rpm. Various emissions were examined from five different fuel series. The tests were conducted over 30 minutes under no load condition from a cold start. The regulated emissions were measured at different time intervals of 2, 4, 6, 8, 10, 15, 20 and 30 minutes after starting the engine.

A light-duty diesel engine was tested over 90 minutes under low, medium and high loads. At the beginning of each test, engine was run for warm-up for approximately 5 minutes. The engine was run at three different engine speeds (1000, 2100 and 3000 rpm). CO, HC, NO_x and smoke opacity emissions were measured at a specific engine load and speed at an interval of one minute. A multi-gas analyzer (NOVA Model 7466 PK) was used to measure regulated emissions. A separate CO analyzer (DWYER 1205A) was applied to measure the CO emissions. A smoke opacity meter has also been used in this study. Specifications on measurement devices are summarized in Table 3.5. At least three different experimental tests of the same kind were done to calculate the average data as shown in the results graphically with \pm standard error of average value. Similar conditions are maintained for all the tests for better comparison of the results.

Table 3.5: Gas analyzer specifications

Method of Detection	Species	Measured Unit	Range	Resolution	Accuracy
NovaGas 7466K					
ElectroChemical/ Infrared detector	CO	%	0-10%	0.10%	±1%
Infrared Detector	CO ₂	%	0-20%	0.10%	±1%
Electro Chemical	NO	ppm	0-2000 ppm	1 ppm	±2%
Electro Chemical	NO ₂	ppm	0-800 ppm	1 ppm	±2%
Electro Chemical	O ₂	%	0-25%	0.10%	±1%
Infrared Detector	HC	ppm x 10	0-20000 ppm	10 ppm	±1%
Dwyer 1205A					
Electro Chemical	CO	ppm	0-2000	1 ppm	±5%
ExTech EA10	Temp	0.1 °C	(-)200°C to 1360°C	0.1°C	±0.3%
Smart 2000	Opacity	%	0-100%	0.1%	±5%
	Soot Density	mg/m ³	0-10 mg/m ³	0.00001	±5%

3.9 Calculation

BSFC: It is calculated from fuel consumption data which is measured manually, and engine power from various engine load and speed data. The following formula is used to calculate brake thermal fuel consumption.

$$BSFC = \frac{\dot{m}_a}{B_p} \left(\frac{g}{kWh} \right) \quad (1)$$

BTE: It is calculated from engine power data at particular engine speed and load with the help of fuel consumption data and higher heating value of the fuel blend used. The following formula is used to calculate brake thermal efficiency.

$$BTE = \frac{3600}{BSFC * HHV} \text{ , } (\%) \quad (2)$$

Chapter 4

Results and Discussion

In this study, different series of fuels would be used in light-duty and heavy-duty engine; namely, summer diesel-biodiesel series (SB10, SB20, SB30, SB40, SB50, SB60, SB70, SB80, SB90, B100), winter diesel-biodiesel series (WB10, WB20, WB30, WB40, WB50, WB60, WB70, WB80, WB90, B100), winter diesel-biodiesel + 2% Wintron Synergy series (WB20S2, WB50S2, B100S2), winter diesel-fractionated biodiesel series (FB20, FB50, FB100) and winter diesel-fractionated biodiesel + 2% Wintron Synergy series (FB20S2, FB50S2, FB100S2). Comparison of cloud points from different fuel blends are discussed. Month-wise fuel blend usage have been discussed. Crystal structure of normal biodiesel blend and synergy blend have been studied. Fuel consumption and emissions for the heavy-duty diesel engine is then summarized. Discussion and comparison of performance and emissions in light-duty diesel engine for all the fuel blends is summarized later in this sections.

4.1 Cloud Points:

Figure 4.1 shows the variation of biodiesel content in diesel fuel with respect to cloud points. Summer diesel has a CP of -26°C and winter diesel has a much lower CP of -41°C . Pure biodiesel (100 vol%) has a cloud point of -2.6°C . From the figure, it can be seen that with addition of higher percentage of biodiesel in diesel fuel, higher amount of CP was obtained which was due to the deteriorating effect of higher CP of normal biodiesel. With blending of 2 vol% Wintron Synergy in normal biodiesel blends improved the cloud points measuring -34.8°C with WB20S2. Furthermore, fractionation of biodiesel proved as a good method for improving the cloud point of biodiesel. The lowest CP attained by fractionated biodiesel series is -36.8°C with FB40. Base fractionated biodiesel (FB100) measured a CP of -31.7°C . With 2% addition of cold flow improver, Wintron Synergy improved the CP even more. FB10S2 and FB100S2 measured CP of -47.5°C and -37.7°C respectively. The lowest CP achieved among all the fuel series is -48.5°C with FB40S2.

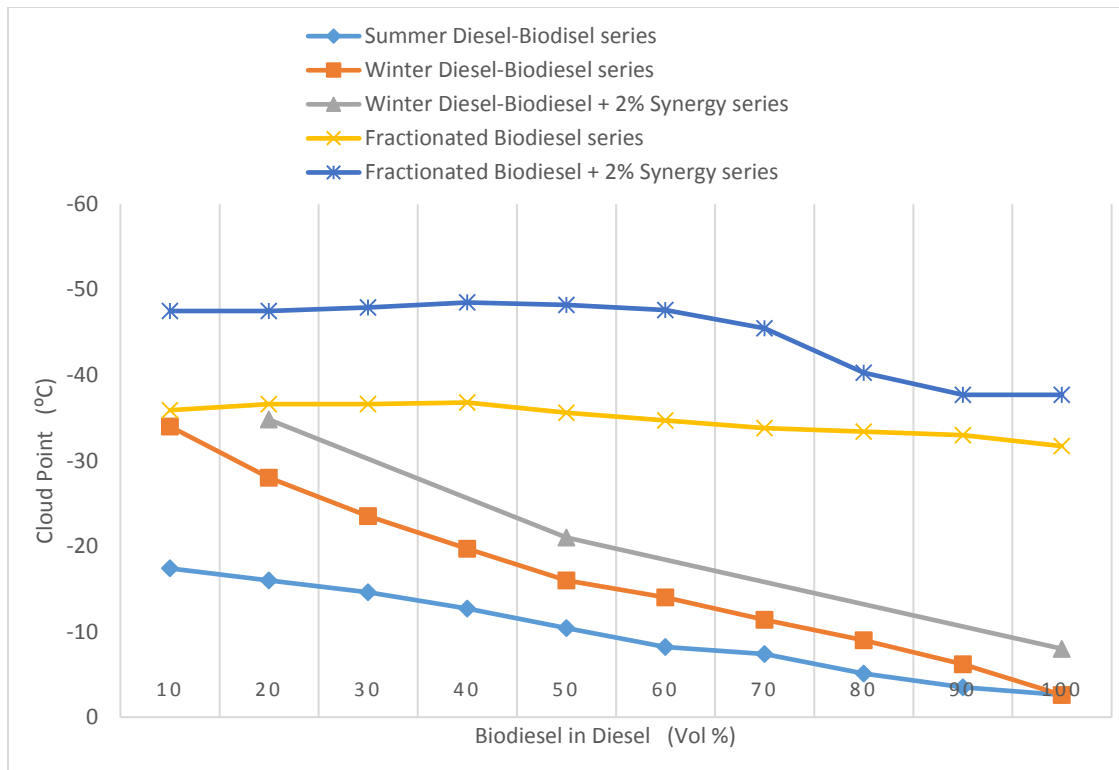


Figure 4.1: Variation of biodiesel content in diesel fuel with respect to cloud points

4.2 Alternative Fuels to be used for Each Month

The objective of this study was to test the feasibility of biodiesel in cold climatic regions such as Thunder Bay which is located in the north-western part of Ontario, Canada. This region experiences extreme cold weather conditions in winter season. The northern part of the province has longer and colder winters than southern Ontario. Table 4.1 shows the fuel blend usage based on the average lowest temperature of each month. Ten years (2005-2015) weather report of Thunder Bay was studied to figure out the average lowest temperature of each month [89]. In the summer months (July and August), when the minimum temperature is above the cloud point of normal biodiesel, the preference would be to use pure biodiesel (100 vol%) in diesel engines. For rest of the summer months, this study would recommend using summer diesel-biodiesel fuel blend series. In the month of June, biodiesel ranging from 10 vol% to 80 vol% blended in summer diesel could be used; or pure biodiesel with 2 vol% synergy could be used. For the months of May and September when the minimum temperature is -6.5°C and -5.3°C respectively measuring above the cloud point of SB70 (-7.4°C), therefore it would be suitable to use biodiesel up to 70 vol% in summer diesel. Pure biodiesel could also be used with 2 vol% of synergy to maximize the biodiesel usage. In October, fuel blends SB10 to SB50 could be used. In the beginning of winter season and

ending of the season, winter diesel-biodiesel fuel series could be used. WB10 fuel blend or 2 vol% of synergy blended up to WB20 blend could be used or any of the fractionated biodiesel fuel blends could also be used in November. Biodiesel up to 40 vol% in winter diesel can be proposed to be used in the month of April. In March, when the average minimum temperature is around -33.7°C, it would be better to use fractionated biodiesel + 2% synergy blends or fractionated biodiesel fuel blends up to 60 volume percent without any effect on filter clogging. Fuel blends ranging from FB10S2 to FB80S2 are recommended to be used in the months of December, January and February. Using fractionated biodiesel blends with synergy won't be economical to be used in rest of the months.

Table 4.1: Comparison of various fuel blends to be used according to average lowest temperature of respective month

Months	Lowest temp (°C)	Summer diesel-Biodiesel blends	Winter diesel-biodiesel blends	Winter diesel-biodiesel + 2% synergy blends	Fractionated Biodiesel blends	Fractionated biodiesel + 2% Synergy		
JAN	-39.5					FB10S2-FB80S2		
FEB	-37.4					FB10S2-FB80S2		
MAR	-33.7					WB10S2-WB20S2	FB10-FB60	FB10S2-FB100S2
APR	-19.3					WB10-WB40	WB10S2-WB50S2	
MAY	-6.5	SB10-SB70	WB10-WB80	WB10S2-B100S2	FB10-FB100			
JUN	-3.9	SB10-SB80	WB10-WB90					
JUL	2.9	B100	WB10-B100					
AUG	0.4							
SEP	-5.3	SB10-SB70	WB10-WB90	WB10S2-WB80S2				
OCT	-9.1	SB10-SB50	WB10-WB70					
NOV	-29.7		WB10	WB10S2-WB20S2		FB10S2-FB80S2		
DEC	-39.6							

4.3 Crystal Structure

Figure 4.2 represents four pictures taken at 500x magnification by a polarizing microscope of two fuel blends. Figure 4.2 (a) and (b) indicated the crystal formation of B20 at -10°C and -20°C respectively, whereas Figure 4.2 (c) and (d) showed the crystal formation of B20S2 at -10°C and -20°C respectively. Crystal formations in B20S2 (Figure 4.2 (c) and (d)) seemed smaller than those compared with B20 (Figure 4.2 (a) and (b)) crystal formations. Figure 4.2 (b) shows a long thin

crystal structure in the top right corner. These structures were hardly seen in B20S2 images, showing that Wintron Synergy can change the shape of crystal formation. Synergy prevents the size and formation of crystal structures. Smaller crystal structures in synergy blends will advance CFPP, due to decreased plugging of fuel lines.

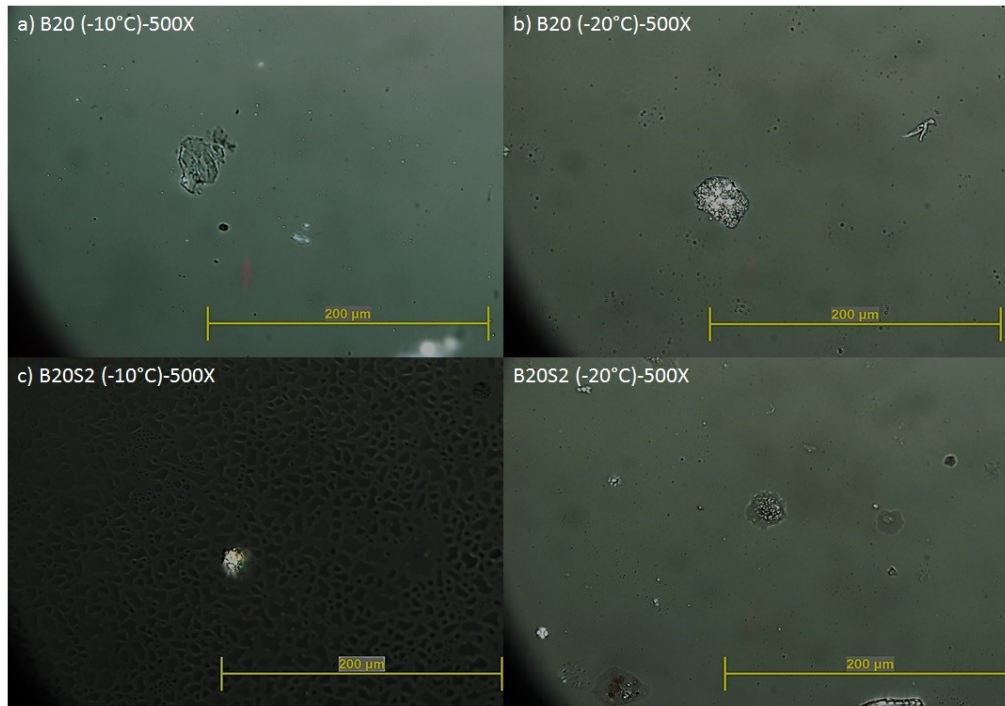


Figure 4.2: Crystal formation of B20 and B20S2 fuel blends at -10°C and -20°C

4.4 Heavy-duty Diesel Engine:

Fuel Consumption:

Figure 4.3 shows the fuel consumption for the neat diesel, SB10, SB20, SB30, SB40, SB50, SB60, SB70, SB80, SB90 and B100 fuel blends. Measurement of the fuel amount was before and after the each engine test. It was observed that the fuel consumption by weight increased gradually with increase in biodiesel content in diesel fuel. This is due to increase in density with biodiesel and decrease in heating value. The lower heating value will be compromised with better combustion efficiency due to higher oxygen content in biodiesel. It was noticed that winter diesel-biodiesel blends and fractionated biodiesel blends showed similar fuel consumption as compared with summer diesel-biodiesel blends. Also, addition of (2% by weight) Wintron Synergy in fractionated biodiesel did not have clear effect on fuel consumption.

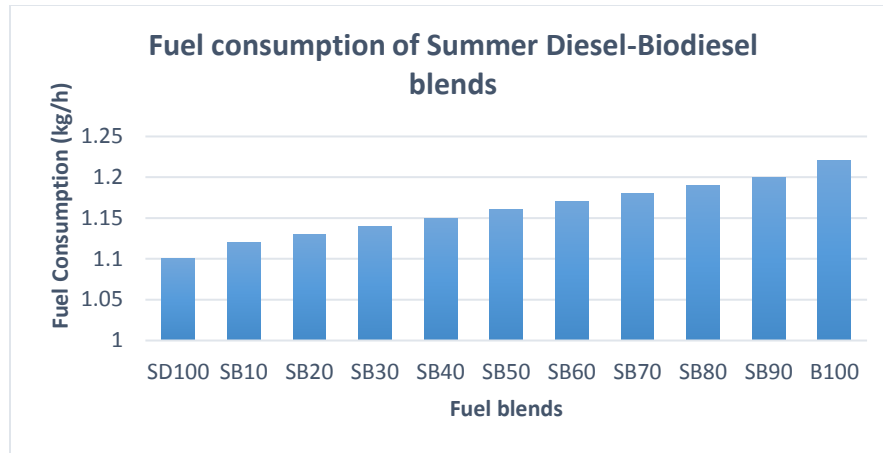


Figure 4.3: Engine fuel consumption

4.4.1 Summer Diesel-Biodiesel series:

Emissions:

a) CO Emissions

Figure 4.4 shows the CO emissions at different engine speeds for different summer diesel-biodiesel fuel blends at all idle conditions. The average CO emissions throughout the experiments from different blends were compared with pure summer diesel. At 800 rpm, summer diesel produced the highest amount of CO emissions (172 ppm) which decreased gradually with increasing percentage of biodiesel in diesel fuel. SB90 and B100 showed significant reductions of CO emissions up to 24% and 30% respectively compared with summer diesel fuel. The reduction in CO emissions is due to biodiesel's higher oxygen content which improves the combustion with oxygen enrichment of the fuel which in turn enhances CO oxidation.

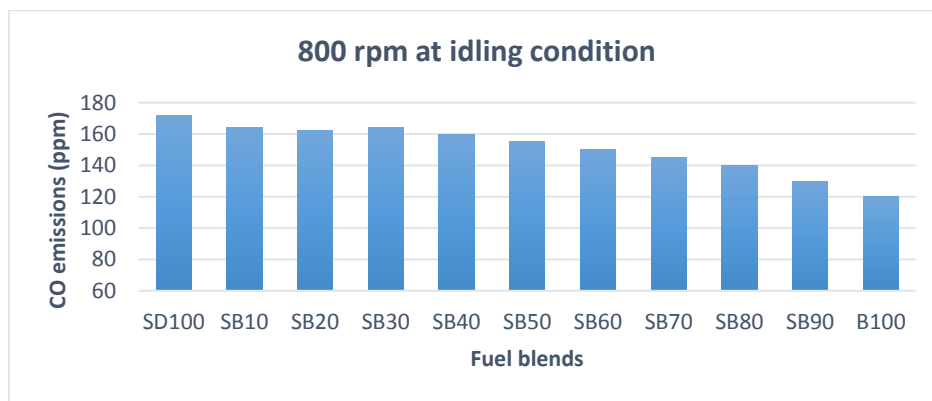


Figure 4.4: CO emissions at 800 rpm for different summer diesel-biodiesel fuel blends

b) HC Emissions

Figure 4.5 illustrates the average HC emissions for 800 rpm. HC followed similar trend compared with CO emissions. All summer diesel-biodiesel blends reduced HC emissions when compared with neat summer diesel. Pure biodiesel emitted 25 ppm (38% lower) of HC emissions compared with 40 ppm of HC emissions with pure summer diesel. Generally higher oxygen content of biodiesel could lead to more efficient combustion and therefore could reduce HC emissions.

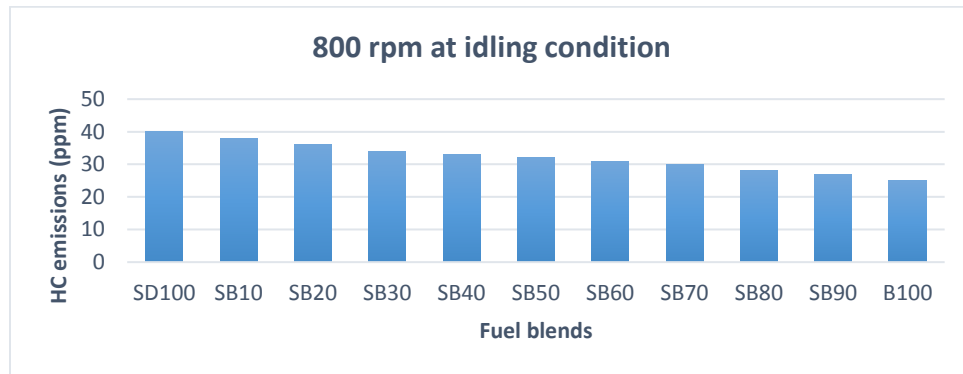


Figure 4.5: HC emissions at 800 rpm for different summer diesel-biodiesel fuel blends

c) NOx Emissions

Figure 4.6 illustrates the NOx emissions for all idle conditions. NO and NO₂ emissions were combined to form the average NOx emissions in Figure 4.6. At 800 rpm, NOx emissions for pure biodiesel increased slightly measuring almost 370 ppm as compared with pure summer diesel fuel (350 ppm). Higher oxygen content in biodiesel and higher cetane number result in higher combustion temperature compared to diesel fuel which increase the NOx emissions. Although idle conditions usually exhibit lower combustion temperature. Higher NOx emissions can also be associated with local phenomena in the combustion chamber. Biodiesel fuel properties like higher viscosity could lead to poor spray characteristics resulting in longer ignition delay causing higher NOx emissions.

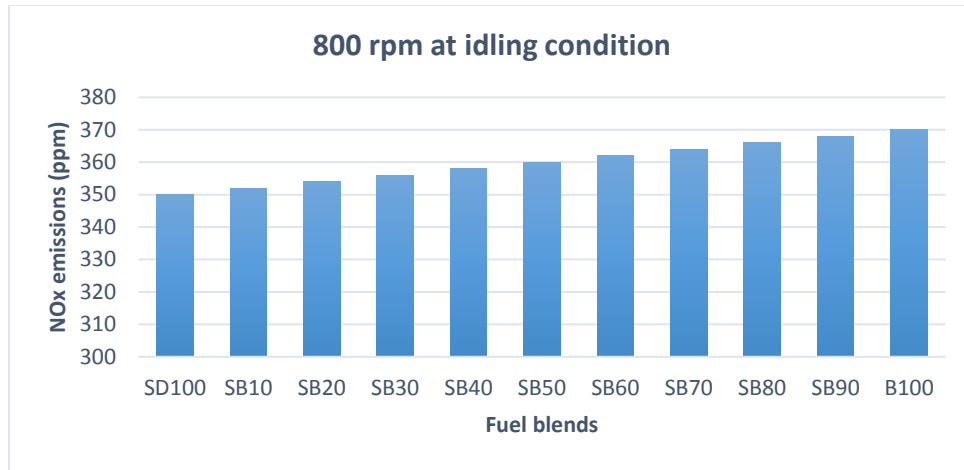


Figure 4.6: NOx emissions at 800 rpm for different summer diesel-biodiesel fuel blends

4.4.2 Winter Diesel-Biodiesel series:

1. Emissions:

a) CO Emissions

CO is mainly formed during the combustion of air-fuel mixture where insufficient oxygen oxidizes the fuel and can be formed in two ways. As an excessively lean air-fuel mixture, CO can be formed from the incomplete propagation of flame through mixture and fuel pyrolysis with partial oxidation. Excessively rich air-fuel mixtures do not properly mix with adequate measures of air, but even if they do, the time to oxidize is insufficient. Figure 4.7 show CO emissions of different fuel blends for winter diesel-biodiesel series. The average peak readings of CO emissions over testing period from different blends were compared to those of pure (winter) diesel. At low idle condition, CO emissions of WB20, WB50 and B100 decreased by 2%, 12% and 27%, respectively compared to winter diesel CO emissions. This is thought to be due to higher oxygen concentration in the air-fuel mixture, which can improve combustion and enhance further CO oxidation.

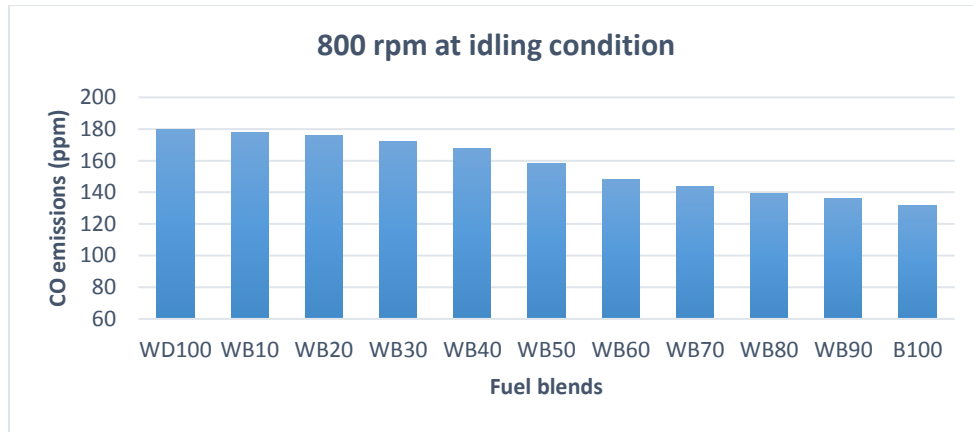


Figure 4.7: CO emissions at 800 rpm for different winter diesel-biodiesel fuel blends

b) HC Emissions

Figure 4.8 represent the average HC emissions for winter diesel-biodiesel series blends. At 800 rpm, WB10, WB20, WB30, WB40, WB50, WB60, WB70, WB80, WB90 and B100 produced less HC emissions than diesel. Pure biodiesel reduced HC emissions to 40% compared with conventional (winter) diesel fuel. This can be attributed to the higher oxygen content of biodiesel blends allowing for a complete combustion.

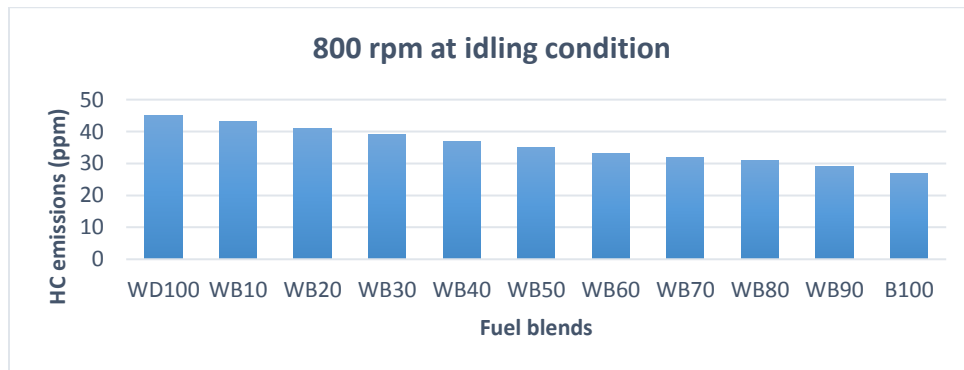


Figure 4.8: HC emissions at 800 rpm for different winter diesel-biodiesel fuel blends

c) NOx Emissions

Figure 4.9 illustrate the average NOx emissions from different blends of winter diesel-biodiesel series at a constant engine speed of 800 rpm. Average NOx emissions over testing period were compared to neat diesel NOx emission values. All the winter diesel-biodiesel blends from WB10 to B100 emitted slightly higher NOx emissions than winter diesel. Pure biodiesel showed the highest emission among all other fuel blends with 372 ppm (6% higher). Biodiesel is an oxygenated fuel containing almost 11% of oxygen by weight. High oxygen content of biodiesel

promotes high combustion efficiency which leads to high reaction temperature and NOx formation.

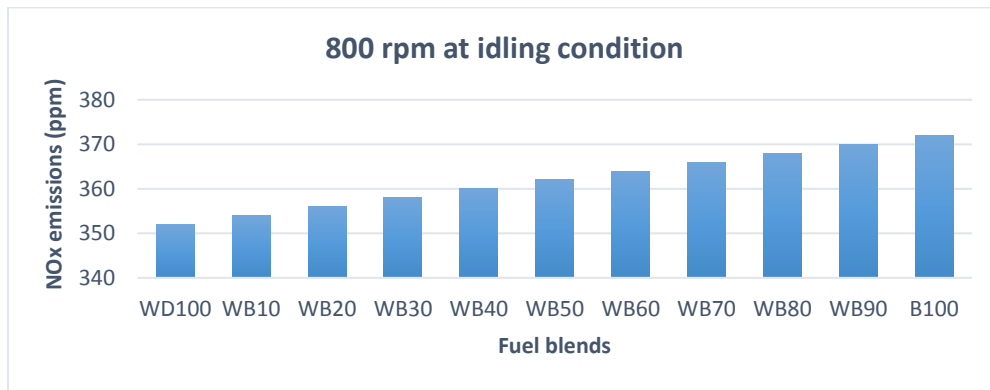


Figure 4.9: NOx emissions at 800 rpm for different winter diesel-biodiesel fuel blend

d) Smoke Opacity Emissions

Figure 4.10 demonstrates the average smoke opacity emissions at an idle condition for winter diesel-biodiesel blends series at constant speed of 800 rpm. Addition of biodiesel in winter diesel showed significant reduction in smoke opacity. Pure biodiesel showed the highest reduction in smoke opacity measurement with up to 96% reduction as compared with winter diesel fuel. Generally biodiesel combustion produces lesser soot than conventional diesel because of fuel bound oxygen, reduced aromatic content, absence of sulphur and unsaturated fatty acid contents. However, it was interesting to note that winter diesel produced only 0.38% of smoke emission which could be due to Diesel Particulate Filter (DPF) installed inside the engine exhaust which helps in trapping the smoke and prevents from higher smoke emissions.

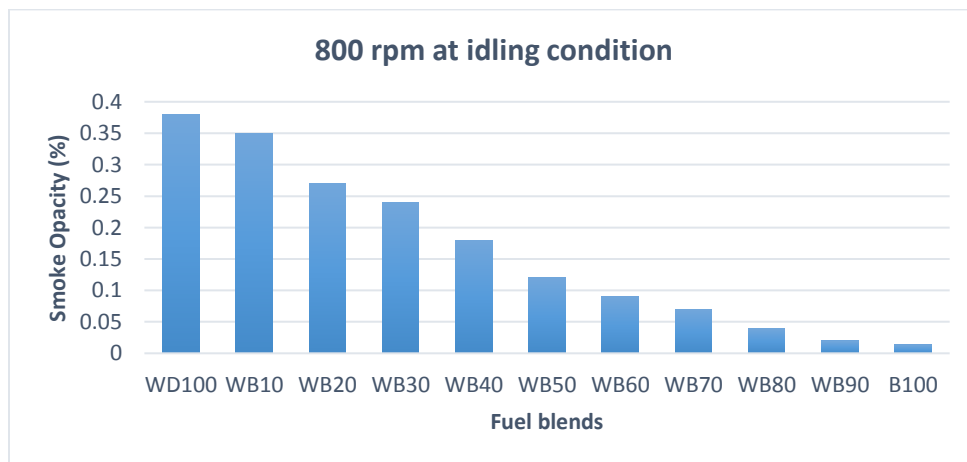


Figure 4.10: Smoke opacity emissions at 800 rpm for different winter diesel-biodiesel fuel blends

4.4.3 Winter Diesel-Biodiesel-Wintron Synergy Additive Series:

Emissions

a) CO Emissions

Figure 4.11 represents the CO emissions at 800 rpm for various fuel blends. The average CO emissions over the testing period from different blends were compared to those of conventional diesel. It can be observed from Figure 4.11 that higher biodiesel content causes higher reduction in CO emissions. CO reduced by 5%, 14% and 60% with WB20, WB50 and B100 respectively. With addition of Wintron Synergy in B20 and B50 blends, lower amount of CO emissions were generated. Similar to biodiesel, the addition of synergy caused increase in oxygen content of the fuel blend which provided efficient combustion. However, when synergy was added to normal biodiesel, the effects of synergy were weakened due to already high oxygen content of biodiesel. CO reduced by 22% for WB20S2, 33% for WB50S2 and 9% for B100S2 when compared with WB20, WB50 and B100 respectively.

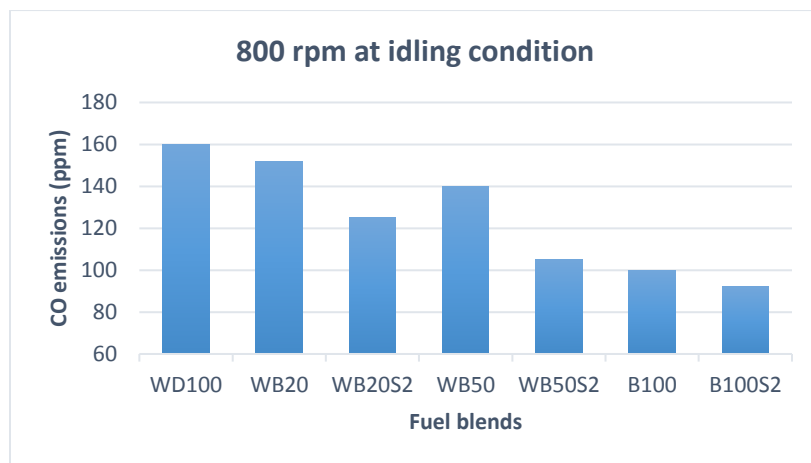


Figure 4.11: CO emissions at 800 rpm for different summer diesel-biodiesel-synergy fuel blends

b) HC Emissions

Figure 4.12 illustrates the average HC emissions at 800 rpm. All the fuel blends decreased HC emissions when compared to diesel fuel. It was found that higher biodiesel and synergy content would reduce HC emissions due to higher oxygen content proving a more complete combustion profile. HC emissions emitted from WB20S2, WB50S2 and B100S2 were 27 ppm, 20 ppm and 14 ppm respectively.

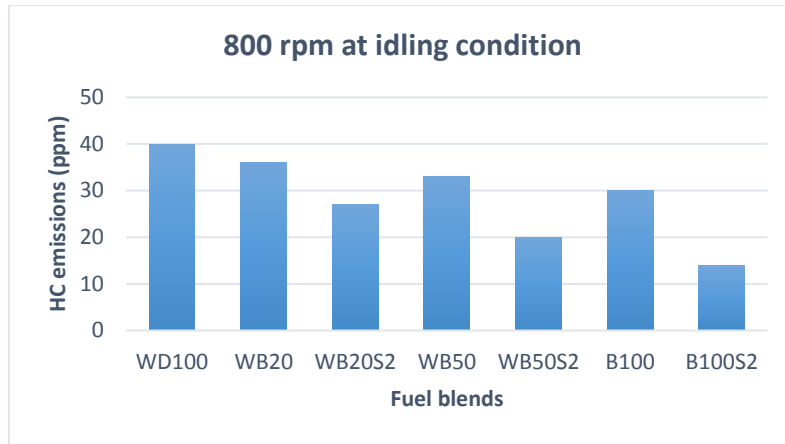


Figure 4.12: HC emissions at 800 rpm for different summer diesel-biodiesel-synergy fuel blends

c) NO_x Emissions

Figure 4.13 demonstrates the NO_x emissions for idle condition at 800 rpm. NO and NO₂ emissions were combined to form average NO_x emissions in Figure 4.13. B20 produced slightly higher amount of NO_x emissions as compared to diesel fuel. With addition of Wintron Synergy in normal biodiesel blends, NO_x emissions increased drastically generating higher amount of NO_x emissions measuring almost 335 ppm and 340 ppm of NO_x with WB50S2 and B100S2 respectively due to higher content of oxygen in synergy.

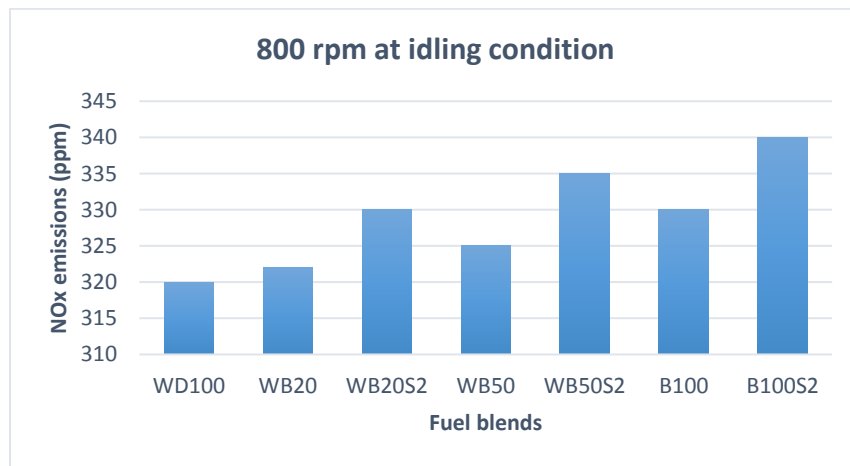


Figure 4.13: NO_x emissions at 800 rpm for different summer diesel-biodiesel-synergy fuel blends

4.4.4 Winter Diesel-Fractionated Biodiesel and 2% Wintron Synergy Additive Series:

1. Emissions:

a) CO Emissions

Figure 4.14 shows CO emissions at 800 rpm for various fuels. Winter diesel produces the maximum CO (180 ppm), which decreases drastically with addition of fractionated biodiesel blends and becomes the lowest (85 ppm) for FB100 in the fractionated biodiesel series. However, CO emissions with fractionated biodiesel-synergy series follows similar trend as compared to fractionated biodiesel series and decreases significantly as compared with winter diesel fuel. The lowest CO emissions was achieved by FB100S2 (approximately 56 % lower) in all the fuel series. It was noticed that higher the fractionated biodiesel percentage in winter diesel-fractionated biodiesel blends, the lower the CO emissions. This could be due to higher oxygen concentration in the air-fuel mixture, which can improve combustion and enhance further CO oxidation. Similarly, 2% Wintron Synergy addition into the fractionated biodiesel blends improved the oxygen concentration because it has been found out that Wintron Synergy contains oxygen compounds in its chemical structure and therefore improves combustion.

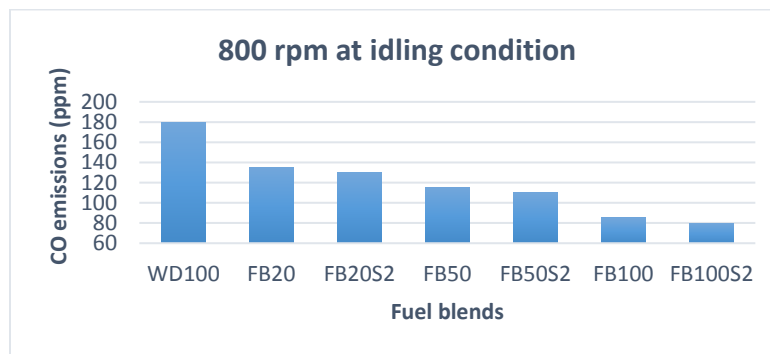


Figure 4.14: CO emissions at 800 rpm for different winter diesel-fractionated biodiesel fuel blends

b) HC Emissions

The catalysts usually reduces the HC emissions from the diesel engines in the exhaust system. However, engine efficiency is reduced due to the unburned HC release, which prevents the potential chemical energy from the fuel burnt inside the engine from being liberated. Unburned HC are produced in several forms, namely, drops of fuel, vapor and products of fuel after thermal degradation. Figure 4.15 shows the variation of HC emissions with different fuel blends of fractionated biodiesel and 2% synergy additive blends with winter diesel. The biodiesel blends with additives showed lower HC emissions than diesel because Wintron Synergy contain oxygen

that can improve oxidation and reduce HC emissions. The average HC reduction for pure fractionated biodiesel was found to be 62% compared with winter diesel fuel because of high oxygen content and high CN can contribute to a complete combustion.

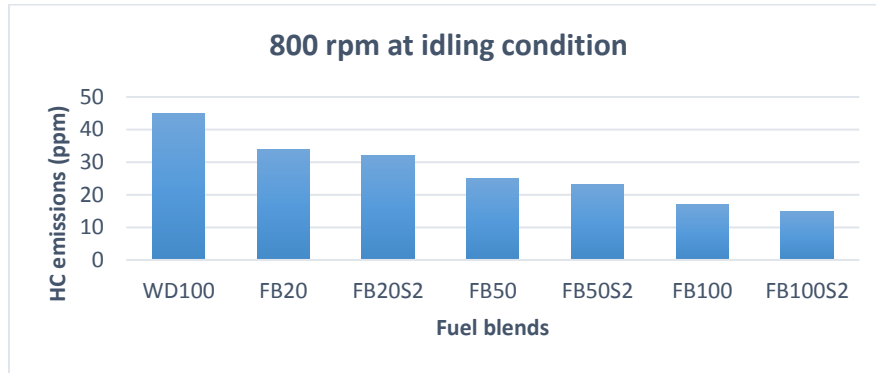


Figure 4.15: HC emissions at 800 rpm for different winter diesel-fractionated biodiesel and 2% synergy additive blends

c) NO_x Emissions

The formation of oxides of nitrogen strongly depends on burning gas temperature, nitrogen and oxygen contents and peak flame temperature. Figure 4.16 shows the change in NO_x emissions at constant speed of 800 rpm. Average values of NO and NO₂ were combined to form average NO_x emissions. It is clear from the figure that increasing the amount of fractionated biodiesel in fractionated biodiesel-diesel and 2% synergy additive blends increases the NO_x emissions. At 800 rpm, FB20 produced slightly higher amount of NO_x emissions as compared with diesel fuel. It was noticed that blending with 2% synergy addition increased the NO_x emission. This is due to higher oxygen content in synergy. NO_x emissions increased when synergy was added to FB50. FB100 followed the similar trend when Wintron Synergy (2%) was added into the blend. Therefore, high NO_x emissions were obtained with higher percentage of fractionated biodiesel and synergy blends mainly due to oxygen content. NO_x emissions increasing can be attributed to local phenomena in the combustion chamber. Due to higher viscosity of biodiesel and synergy additive, poor spray characteristics may lead to longer ignition delay causing higher NO_x emissions.

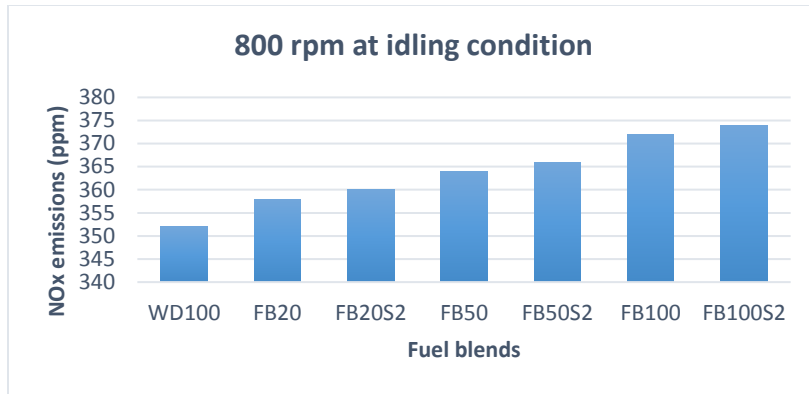


Figure 4.16: NOx emissions at 800 rpm for different winter diesel-fractionated biodiesel and 2% synergy additive blends

d) Smoke Opacity Emissions

Smoke opacity is normally produced from the incomplete combustion of hydrocarbon fuel and the composition of this parameter strongly depends on the type of fuel, engine operating conditions and carbon residues. Figure 4.17 shows decrease of smoke opacity at 800 rpm for all the tested samples of fractionated biodiesel blends. The results showed that the average smoke opacity (%) was 89% for FB100 and 95% for FB100S2 which were lower than those of diesel fuel. Higher oxygen and low sulfur content in biodiesel fuels were responsible for reducing smoke. The oxygen content in biodiesel and synergy fuel blends helps improve combustion, resulting in lower smoke opacity. Removal of saturated fatty acid methyl esters during fractionation process proved advantageous in reducing smoke significantly.

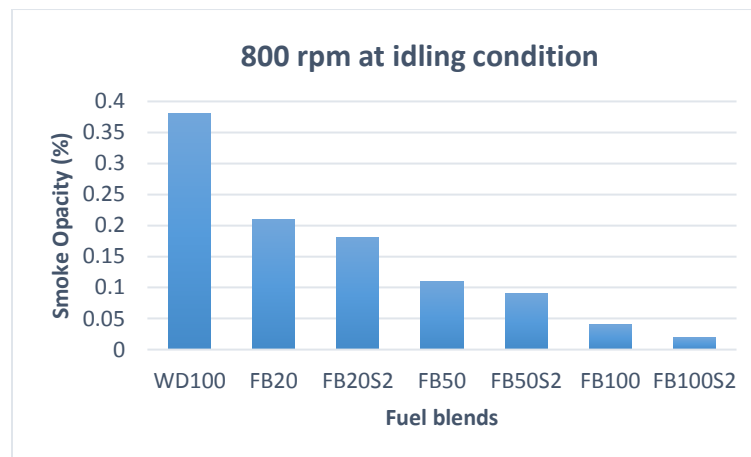


Figure 4.17: Smoke opacity emissions at 800 rpm for different winter diesel-fractionated biodiesel and 2% synergy additive blends

4.5 Light-duty Diesel Engine:

4.5.1 Summer Diesel-Biodiesel Series:

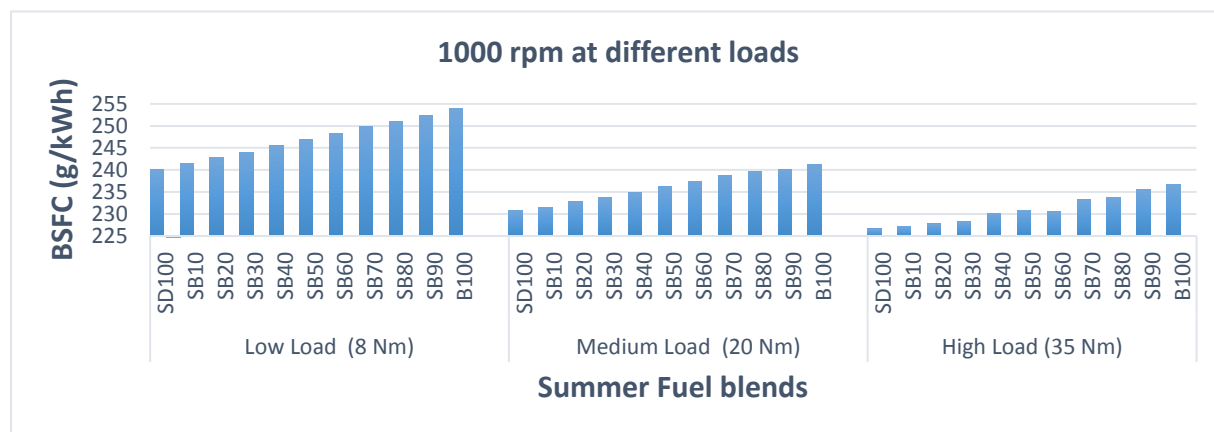
1. Engine Performance:

a) BSFC

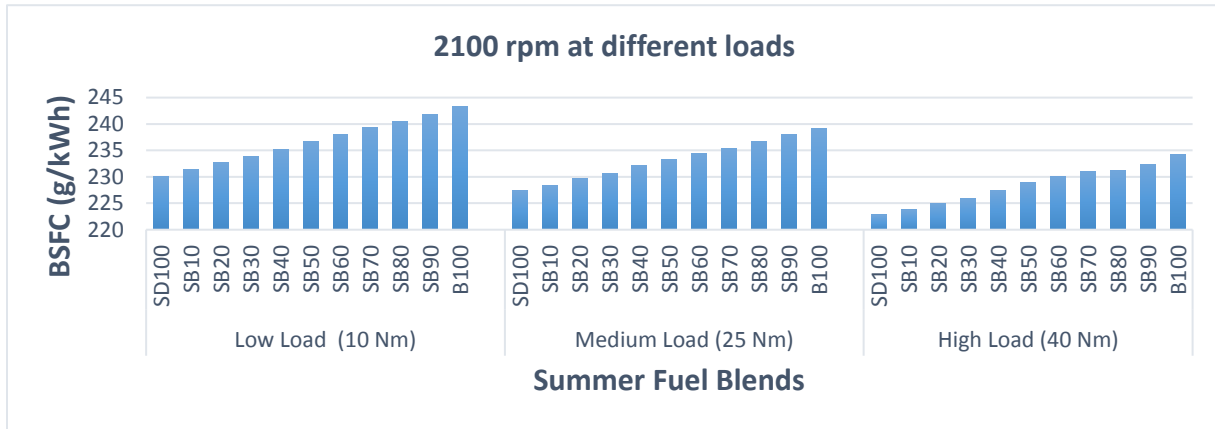
Figure 4.18 shows the change in BSFC with engine load and speed for various blends of summer diesel-biodiesel fuel samples. BSFC refers to consumption of fuel per unit power and in a unit time. The BSFC of diesel engine depends on the relationship among volumetric fuel injection system, fuel density, viscosity and lower heating value [90]. Figure 4.18 shows that the BSFC of the tested fuel samples increased with increase in biodiesel content due to higher density, viscosity and lower heating value of biodiesel. BSFC of the tested samples decreased with increase in engine load. This is due to the better reactivity of oxygen at higher average temperature of the combustion chamber leading to more complete combustion.

From the Figure 4.18 (a), (b) and (c), it can be noticed that BSFC of summer diesel-biodiesel blends decreased as the engine speed was increased to 2100 rpm, as increasing the atomisation and air-fuel equivalence ratio reduces air-fuel mixing. At higher speed, the frictional loss increases and volumetric efficiency decreases compared to lower speed and therefore BSFC increases. The BSFC of diesel fuel was found to be lower than biodiesel blends because biodiesel contain lower heating value and higher density, which influence the atomization ratio by slowing down air-fuel mixing [91]. The BSFC of pure biodiesel increases to approximately 5.5% at low load condition and increases to about 4.26% and 4.8% at high load operation at 1000 rpm and 3000 rpm respectively.

(a)



(b)



(c)

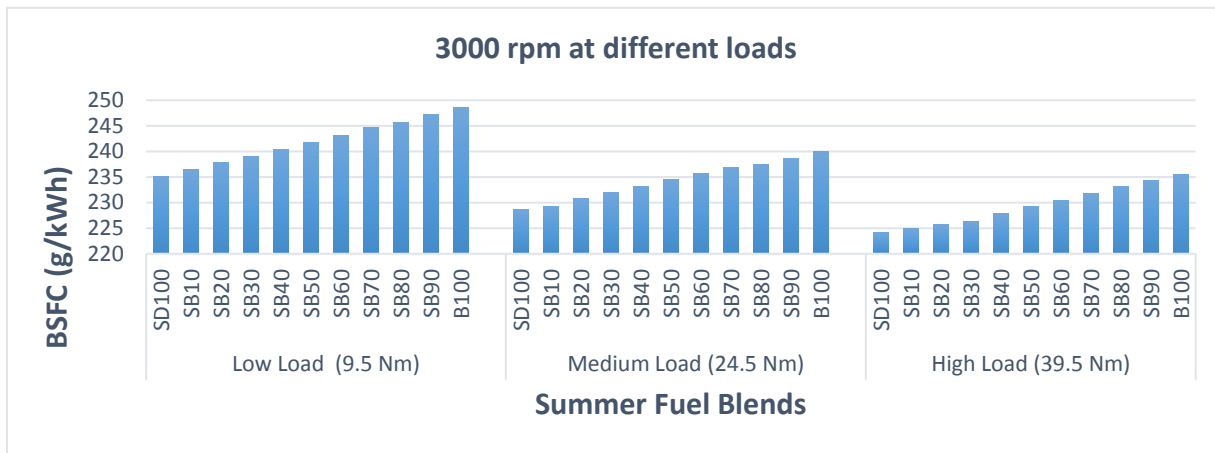


Figure 4.18: BSFC values for summer diesel-biodiesel under different loads at (a) 1000 rpm (b) 2100 rpm (c) 3000 rpm

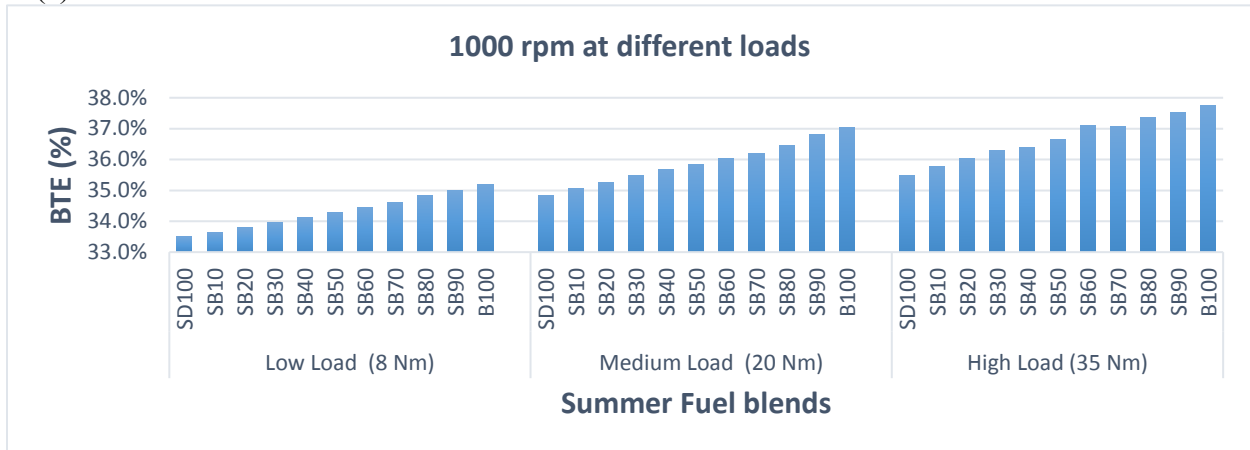
b) BTE

Brake thermal efficiency is a parameter that determines the transformation of heat energy to useful work. This parameter is obtained by dividing the effective power from the engine to the amount of energy given to the engine. Even though biodiesel blends have higher BSFC, the efficiency of the blends is also higher than diesel fuel because of better combustion due to higher oxygen content in the blends. The results indicate that biodiesel blends are better than diesel at all load conditions, and inherent oxygen of biodiesel can enhance the combustion process. It is observed from the Figure 4.19 that there is an increase of BTE for all fuel blends with increasing loads. This is due to the reason of increase of average combustion temperature at higher loads.

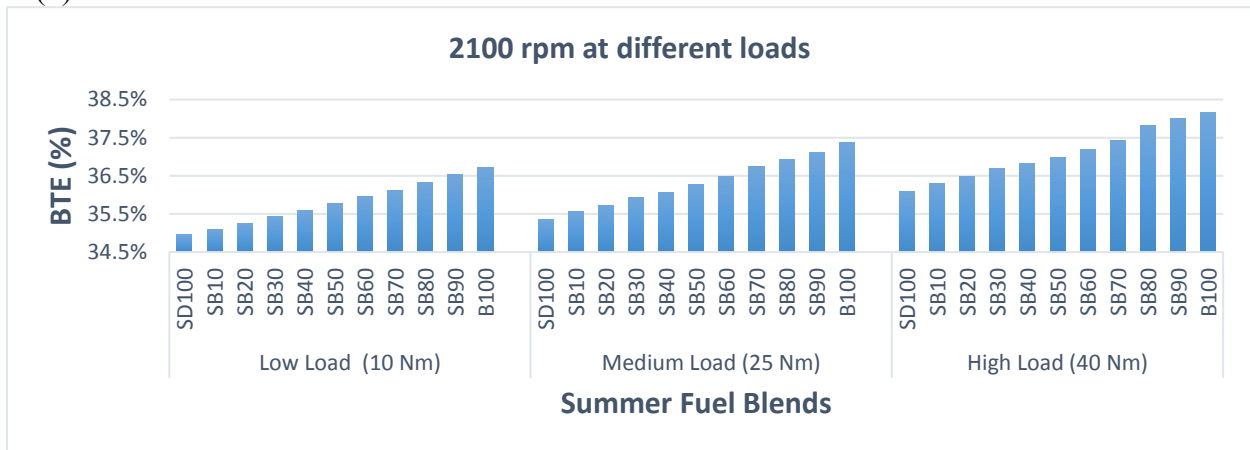
With increasing amount of engine speed, BTE increased up to 2100 rpm. This could be due to better atomization and better fuel-air mixing leading to increase in BTE. At 3000 rpm, BTE

reduced slightly due to poor spray characteristic. On an average, pure biodiesel show about 4.8% higher efficiency at low load condition, about 5.7% under medium load, and about 5.4% under high load operation at 1000 rpm, 2100 rpm and 3000 rpm respectively.

(a)



(b)



(c)

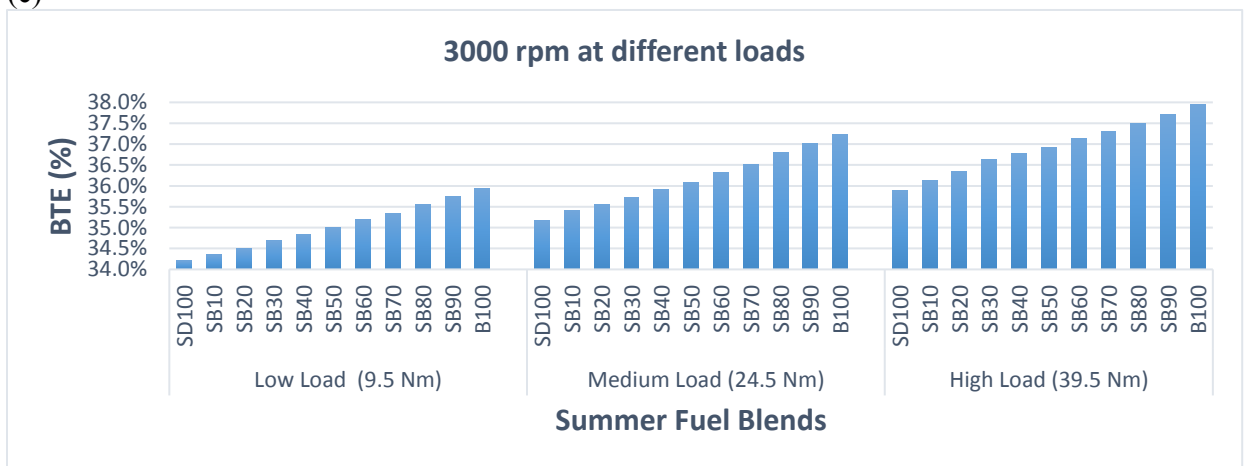


Figure 4.19: BTE values for summer diesel-biodiesel under different loads at (a) 1000 rpm (b) 2100 rpm (c) 3000 rpm

2. Emissions:

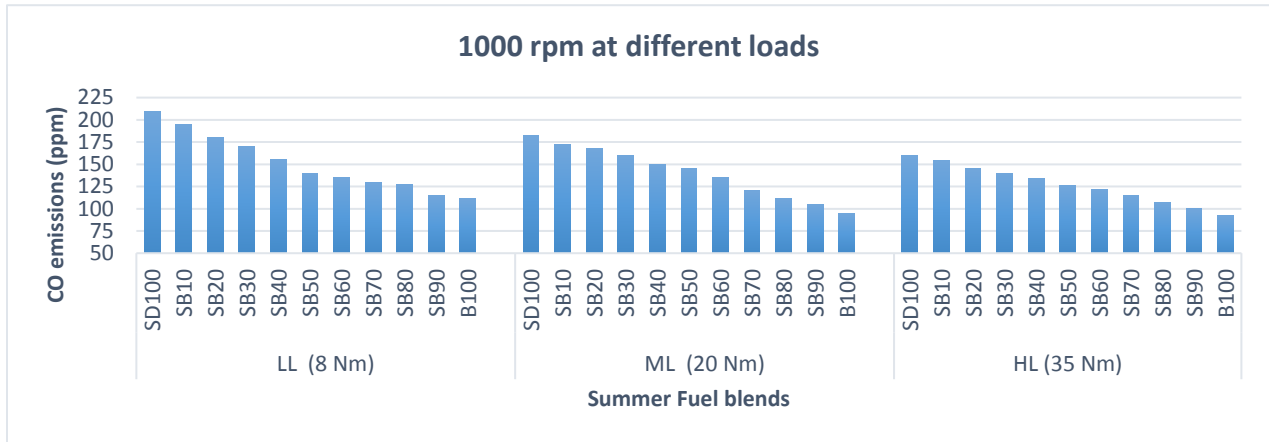
a) CO Emissions

Figure 4.20 (a), (b), (c) illustrates the CO emissions at different engine loads and speeds for various fuel blends. Average CO emissions over the testing period from different blends were compared to those of conventional diesel fuel. It was found that higher biodiesel content causes higher reductions in CO emissions. This was due to higher oxygen content in the biodiesel compared to diesel fuel which results in more efficient combustion and lower carbon to hydrogen ratio in biodiesel compared to diesel fuel.

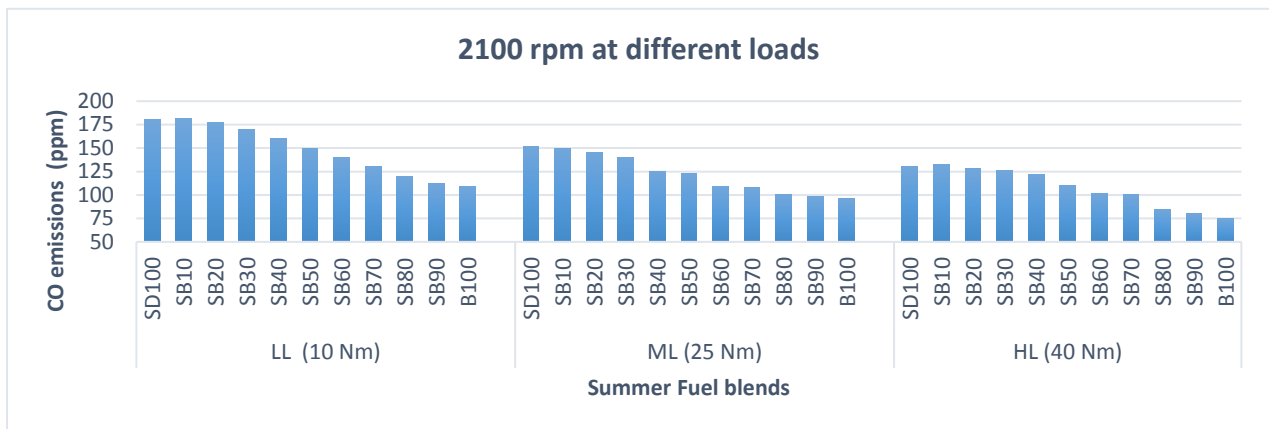
In addition, engine load was proved to have a big effect on CO emissions. The results showed decrease of CO emissions with higher engine loads. This could be due to the fact that air-fuel ratio is too lean for complete combustion at low load conditions leading to higher CO emissions than at high loads. It was also observed that all the blends showed lower CO emission than diesel fuel all over the engine speed range and decreased with increasing engine speed. Changes in CO emission depend on the fuel/air equivalence ratio inside the cylinder. When this ratio is high, the amount of CO increases. However, the fuel/air equivalence ratio increases with engine speed, which results in increased gas temperature in the engine cylinder. This increases the conversion rates of CO to CO₂ resulting in low CO emission at high engine speeds.

In Figure 4.20 (a), at 1000 rpm, summer diesel produced the maximum amount of CO emission (209 ppm) at low load compared to other summer diesel fuel blends at all load and speed conditions. Figure 4.20 (b) and (c), followed similar trend of CO emission compared to Figure 4.20 (a). At 3000 rpm, normal biodiesel produced lowest CO emission (90 ppm) at high load compared to other summer diesel fuel blends. B100 reduced CO emission by almost 28% lower on an average compared with summer diesel at high load condition. The significant lower CO emission of B100 compared with that of diesel can be attributed to the higher fuel-bound oxygen.

(a)



(b)



(c)

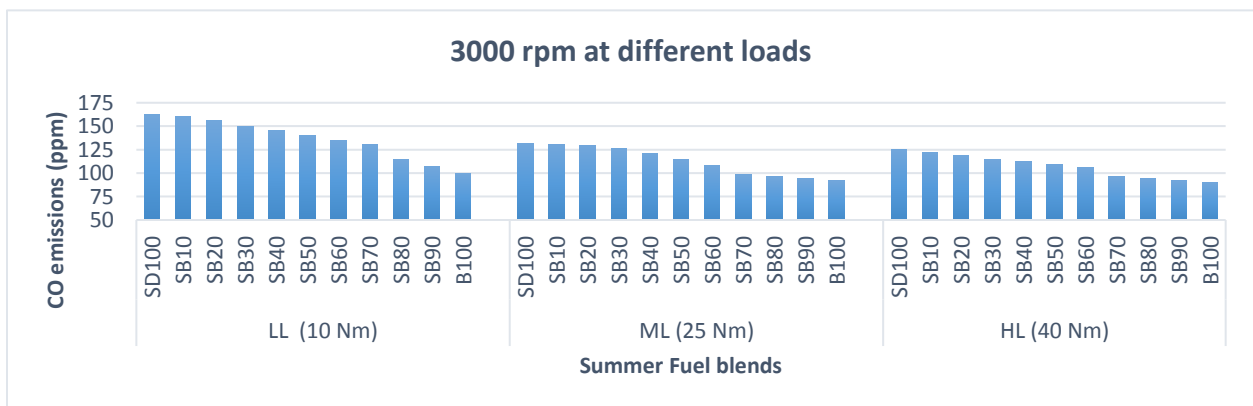
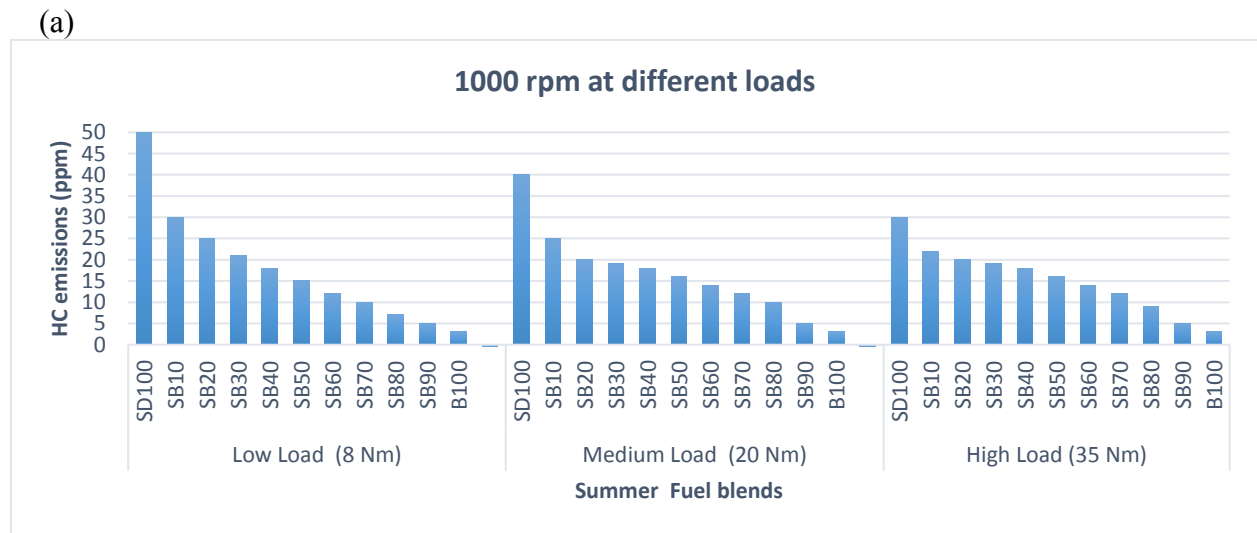


Figure 4.20: CO emission for summer diesel-biodiesel blends under different engine loads at (a) 1000 rpm (b) 2100 rpm (c) 3000 rpm

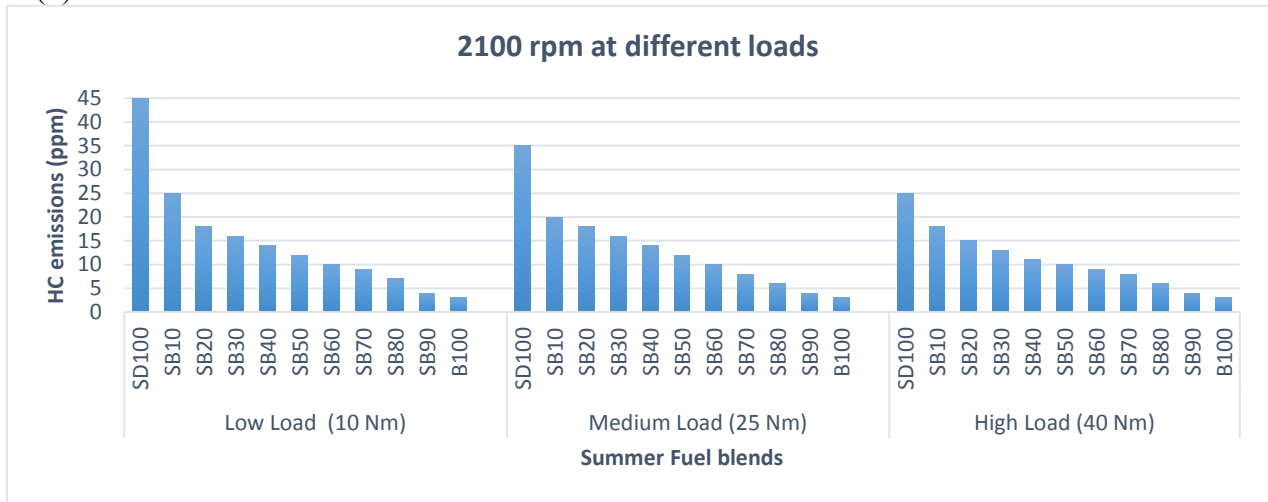
b) HC Emissions

The effect of HC emissions at different engine load and speed for summer diesel-biodiesel blends are shown in Figure 4.21. Unburned hydrocarbon originates from various sources in the cylinder during combustion. Generally in a diesel engine, HC emission is mainly due to fuel trapping in the crevice volumes of the combustion chamber, low temperature bulk quenching of oxidation reactions, locally over lean or over rich mixture, liquid wall films for excessive spray impingement, and incomplete fuel evaporation [92]. Oxygenated compounds in biodiesel reduced the HC emission significantly in all the biodiesel blends. At 3000 rpm, all summer diesel-biodiesel blends and normal biodiesel showed lower HC emissions at high load as compared to different load and speed conditions.

HC emission decreased with increase in engine load due to lean combustion process. At 1000 rpm, average HC emission for pure biodiesel had highest reduction of approximately 94%, 93% and 90% at low, medium and high load respectively, as compared with summer diesel. Moreover, in Figure 4.21 (a) higher HC emission at a lower speed for all the blends was observed. Summer diesel produced maximum amount of HC emissions (50 ppm) compared to other fuel blends. Among the biodiesel blends, SB10 produced the maximum HC emission of 30 ppm. This could be due to increase of lean outer flame zone, which is the envelope of the spray boundary where the fuel is already beyond the flammability limit because of over mixing [93]. At all load and speed condition, SB90 and B100 produced the lowest HC emissions of approximately 3 ppm.



(b)



(c)

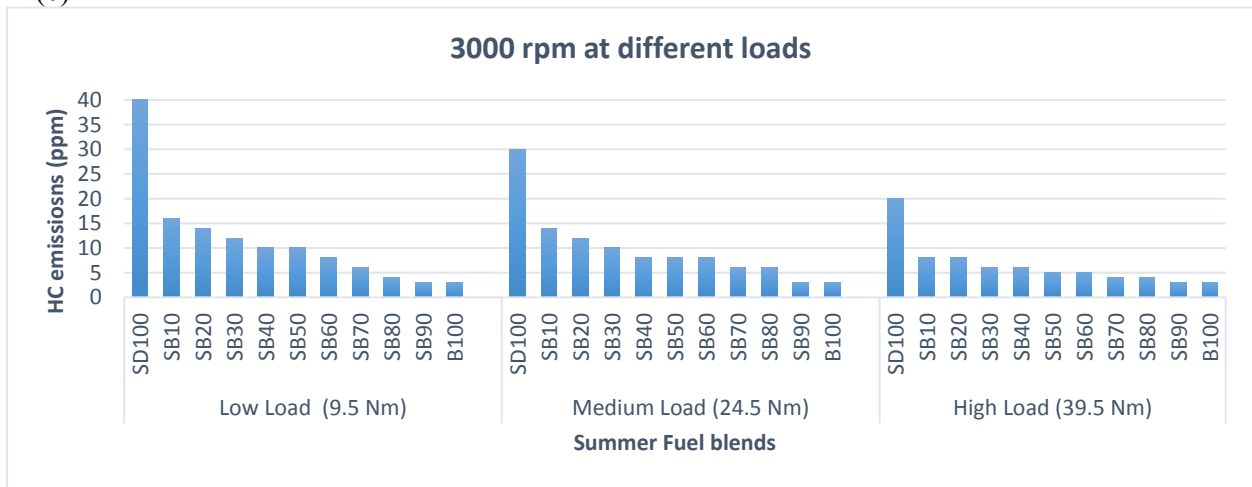


Figure 4.21: HC emission for summer diesel-biodiesel blends under different engine loads at (a) 1000 rpm (b) 2100 rpm (c) 3000 rpm

c) NO_x Emissions

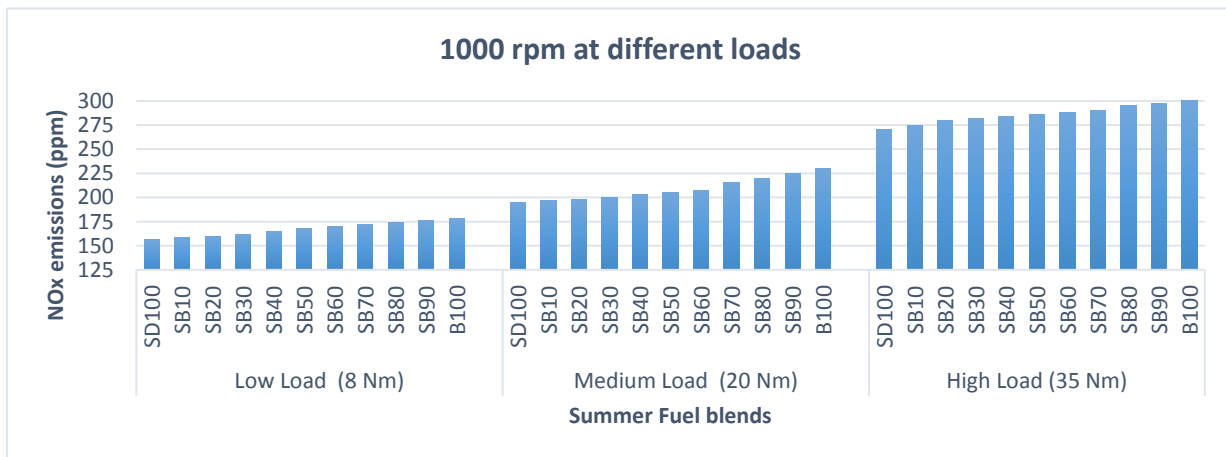
NO (nitric oxide) and NO₂ (nitrogen dioxide) are generally grouped under the NO_x emission. But among the oxides of nitrogen, NO is the predominant oxide produced inside the engine cylinder. Oxidation of atmospheric nitrogen during combustion is the main source of NO_x emission in diesel engines which is known as thermal NO_x. Under high combustion temperature, the strong triple bond of nitrogen molecules breaks down and participate in a series of reaction with oxygen which results in thermal NO_x which is also called as Zeldovich mechanism. However, if the nitrogen content of the fuel is higher, then the nitrogen containing compounds get oxidized and become a potential source of NO_x which is known as fuel NO_x. NO_x formation depends on

numerous factors such as oxygen concentration and in-cylinder temperature. NOx formation occurs both in the flame front as well as in the post flame gases [92].

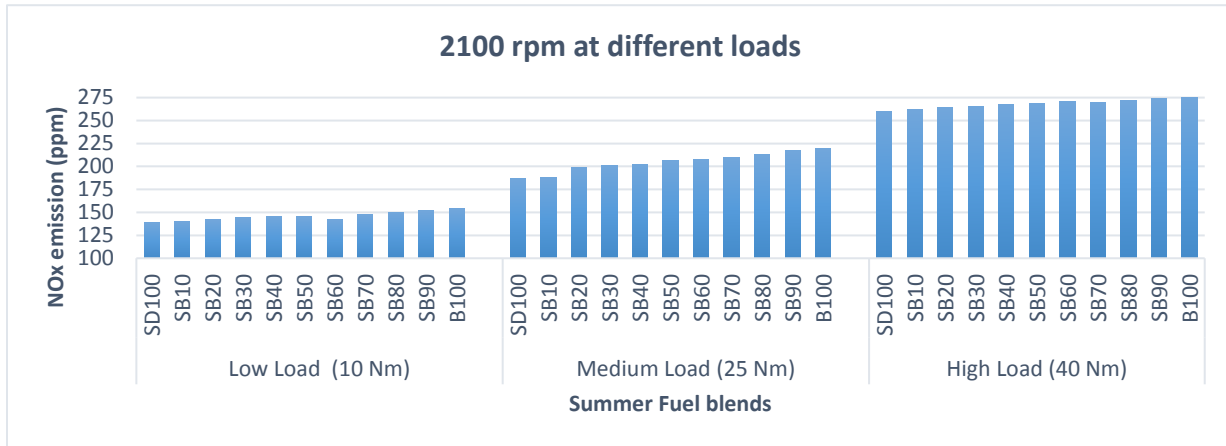
Figure 4.22 shows the NOx emissions for summer diesel-biodiesel fuel at various engine loads and speed. With increasing amount of oxygen content in biodiesel blends, NOx emissions increased considerably. At 1000 rpm, pure biodiesel produced the maximum amount of NOx emission at high load condition measuring almost 301 ppm (11% higher). With increasing load, NOx emissions increased slightly due to high combustion temperature which can be correlated with engine exhaust temperature (Appendix). The average NOx emission at 1000 rpm were 168 ppm, 210 ppm and 287 ppm under low, medium and high loads respectively compared to summer diesel fuel.

As the speed reduced, NOx emission of all the blends increased. This result can be attributed to the higher available combustion time as the speed was reduced. SB50 produced 168 ppm, 205 ppm and 286 ppm of NOx emission at 1000 rpm under low, medium and high loads respectively. At 2100, SB50 produced 145 ppm, 206 ppm and 269 ppm of NOx emission under low, medium and high loads respectively. Similarly at 3000 rpm, SB50 produced 132 ppm, 206 ppm and 258 ppm of NOx emission under low, medium and high loads respectively.

(a)



(b)



(c)

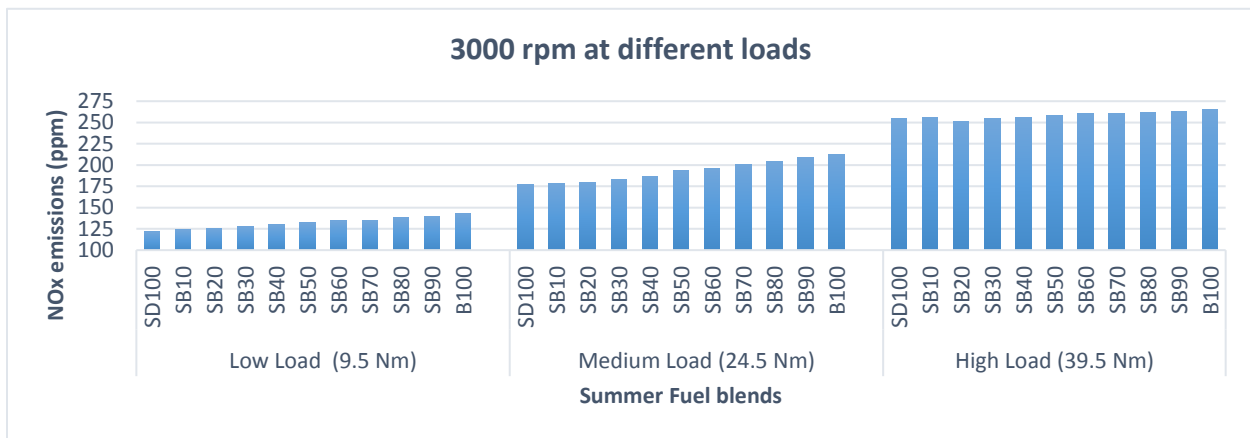


Figure 4.22: NOx emission for summer diesel-biodiesel blends under different engine loads at (a) 1000 rpm (b) 2100 rpm (c) 3000 rpm

d) Smoke Opacity Emissions

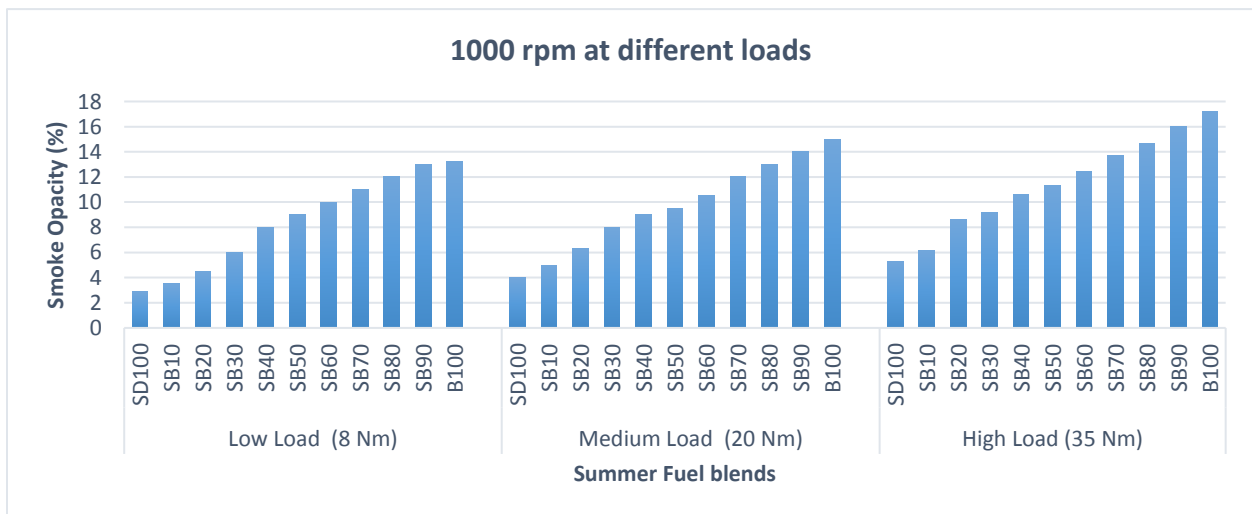
Figure 4.23 show the exhaust smoke opacity for summer diesel-biodiesel blends at different engine loads and speeds. Soot content in the exhaust gas is indicated by the smoke opacity, therefore this parameter can be correlated with fuels tendency to form soot during combustion [94]. Diesel particulates are principally combustion generated carbonaceous material (soot) where some organic compounds remain absorbed and grow via gas to particle conversion process [95]. They are mainly formed due to incomplete combustion of hydrocarbon fuel and the composition of smoke generally depends on engine operating conditions and different fuel properties.

Smoke opacity emissions increased with increase in biodiesel content in biodiesel-diesel blends due to the viscosity effect associated with increase in biodiesel in the blend. The saturated fatty

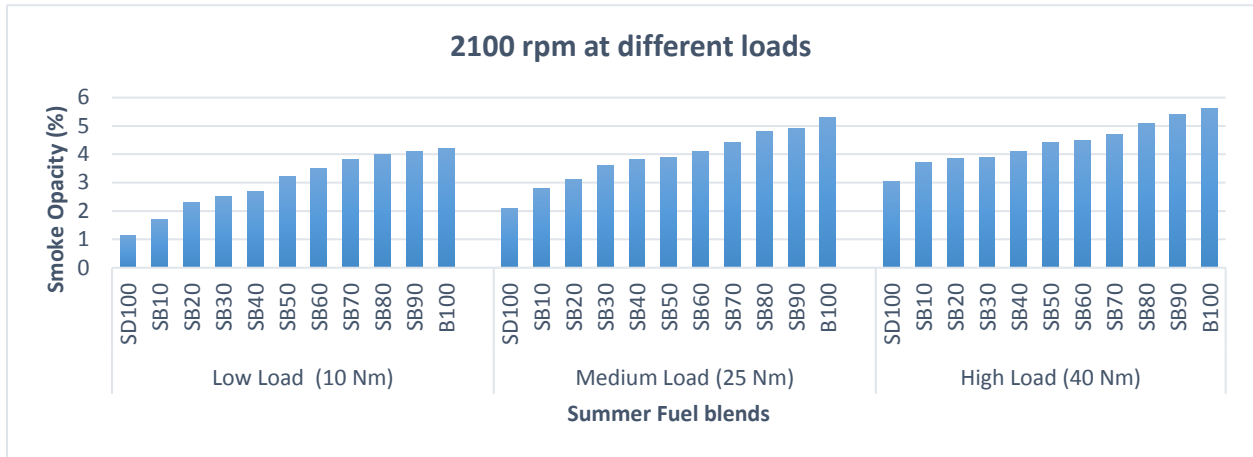
acid compounds present in biodiesel increases the viscosity of the fuel and creates poor atomization which promotes smoke emission due to incomplete combustion. At 2100 rpm under low load, diesel fuel produced only 1.1% of smoke opacity emission. B20 slightly increased the smoke opacity measuring 1.7%. It increased even more with SB50 at 3.2% of smoke opacity emission. Pure biodiesel produced the maximum amount of smoke opacity emission measuring 4.2% at same engine load and speed. With increase in load, smoke opacity increased tremendously. At 1000 rpm, pure biodiesel under low load was 13.2%. Smoke opacity measured 15% under medium load and increased to 17.23% at high load condition. At 2100 rpm, smoke opacity emission for pure biodiesel was 4.2%, 5.3% and 5.6% under low, medium and high load respectively. Similarly at 3000 rpm, smoke opacity for pure biodiesel was 1.7%, 2.2% and 2.8% under low, medium and high load respectively. With higher loads, large amount of fuel is injected inside the combustion chamber creating higher pockets of fuel, which sometimes doesn't involve properly in combustion process, creating higher smoke opacity emissions.

Smoke opacity decreased with increase in speed. At 3000 rpm, pure biodiesel produced the lowest amount of smoke opacity emission of 1.7% compared to other engine speed at low load. Similarly, medium load at 3000 rpm, pure biodiesel produced the lowest amount of smoke opacity of 2.2% compared to other rpm's at medium load. Finally at high load, smoke opacity for pure biodiesel was lower at 3000 rpm with 2.81% of smoke opacity emission compared to other engine speed. Increasing the engine speed, increased the temperature inside the engine which helped in better combustion process emitting lower smoke opacity emissions.

(a)



(b)



(c)

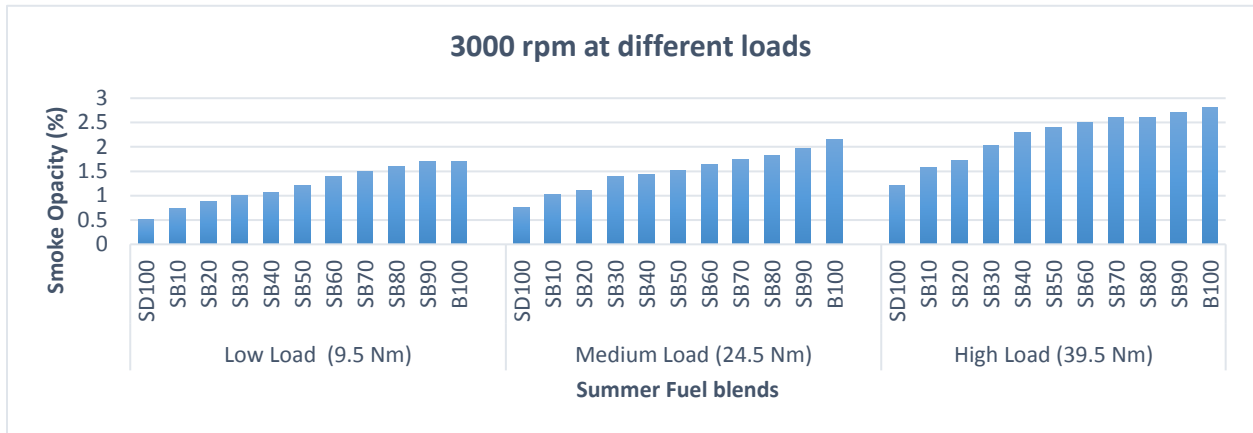


Figure 4.23: Smoke opacity emission for summer diesel-biodiesel blends under different engine loads at (a) 1000 rpm (b) 2100 rpm (c) 3000 rpm

4.5.2 Winter Diesel-Biodiesel Series:

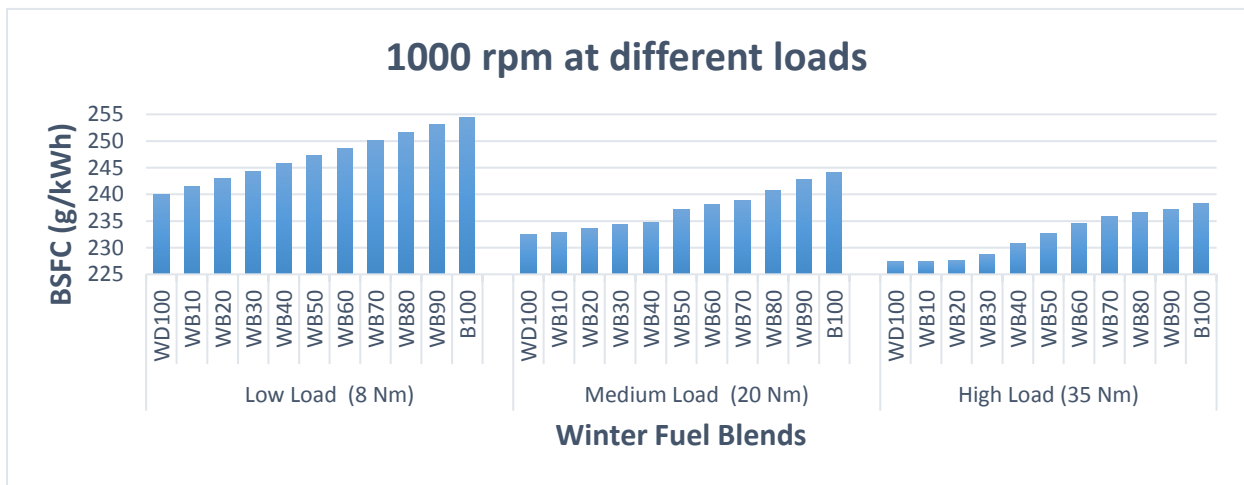
1. Engine Performance:

a) BSFC

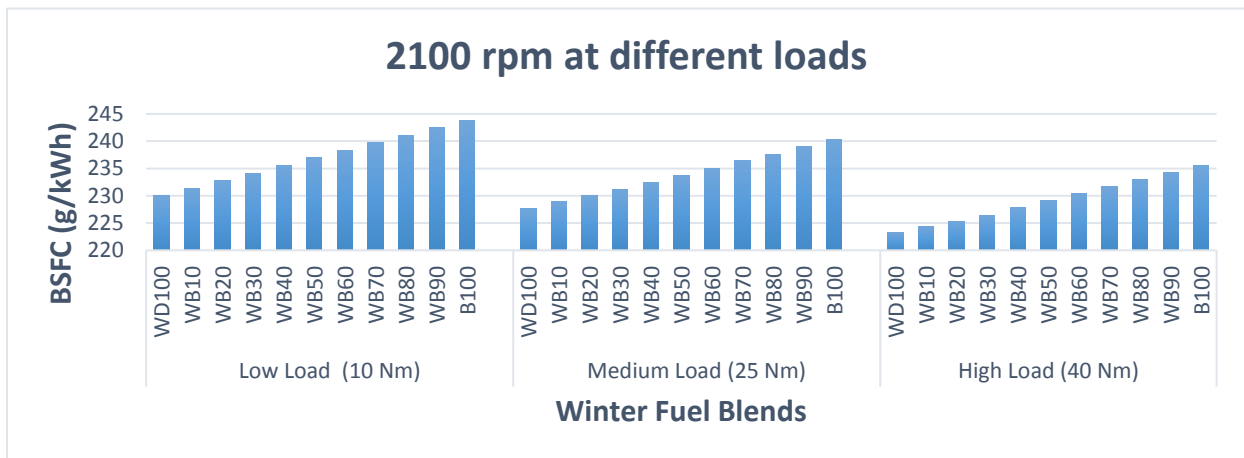
The variation of BSFC for all tested fuels with respect to engine speed and load is depicted in Figure 4.9. BSFC is the ratio between mass fuel consumption and brake power. It was observed that the BSFC of biodiesel was generally higher compared to diesel fuel. Biodiesel normally possesses low higher heating value because of its fuel-borne oxygen. High fuel consumption can be attributed to the volumetric effect of a constant fuel injection rate, along with the high viscosity of biodiesel blends [96] which proved higher BSFC value with increase in biodiesel content.

At 1000 rpm, BSFC value was maximum compared to other rpm condition. BSFC decreased at 2100 rpm and then increased slightly at 3000 rpm. Figure showed decrease in BSFC as the load was increased. At lower loads, very less fuel is injected into the combustion chamber resulting in lowered cylinder pressure and temperatures. With increase in load, more fuel enters the combustion chamber resulting in elevated temperatures which is sufficient for biodiesel to reach its auto-ignition temperature thereby reducing the BSFC gradually. The average brake specific fuel consumption of B20, B50 and B100 are 234 g/kWh, 237 g/kWh and 244 g/kWh at 1000 rpm, 229 g/kWh, 232 g/kWh and 238 g/kWh at 2100 rpm, 231 g/kWh, 235 g/kWh and 241 g/kWh at 3000 rpm respectively.

(a)



(b)



(c)

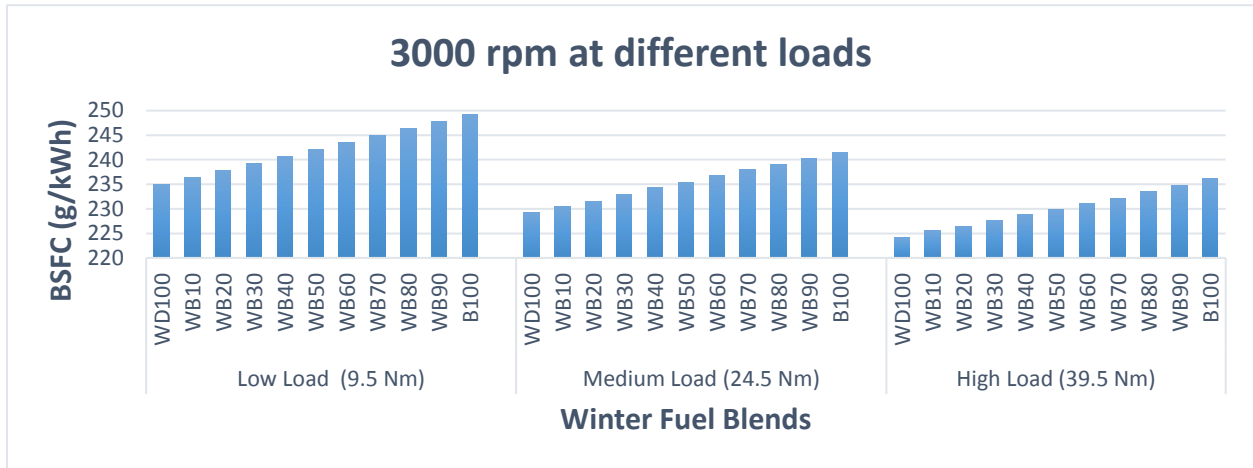


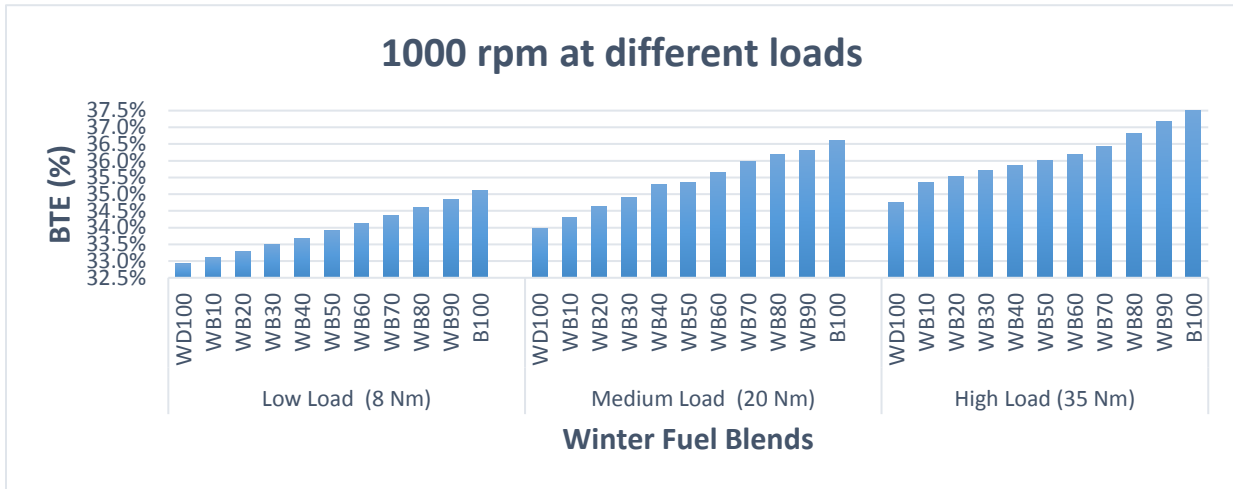
Figure 4.24: BSFC values for winter diesel-biodiesel under different loads at (a) 1000 rpm (b) 2100 rpm (c) 3000 rpm

b) BTE

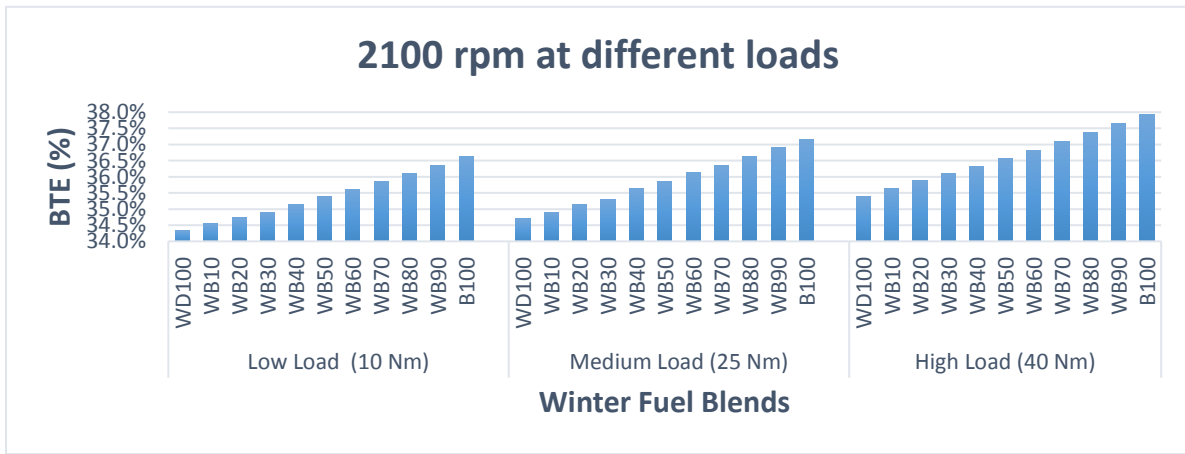
The variation in BTE is shown in Figure 4.25. It is to be noted that brake thermal efficiency is the ratio of brake power and product of fuel consumption and lower calorific value of fuel. The BTE increases with an increase in engine load. This is due to the improvement of the combustion process on account of increased oxygen content in the fuels. It was observed that diesel fuel, despite having lower BSFC, has the lowest BTE in all engine loads.

In a study [97], it was reported that biodiesel combustion had a higher burning rate than normal diesel fuel due to the presence of oxygen in biodiesel, hence increasing the efficiency of combustion with increasing biodiesel percentage in the blend. The average brake thermal efficiency for all the biodiesel fuel blends at 1000 rpm, 2100 rpm and 3000 rpm for different loads are 35.1%, 36.2% and 37% respectively.

(a)



(b)



(c)

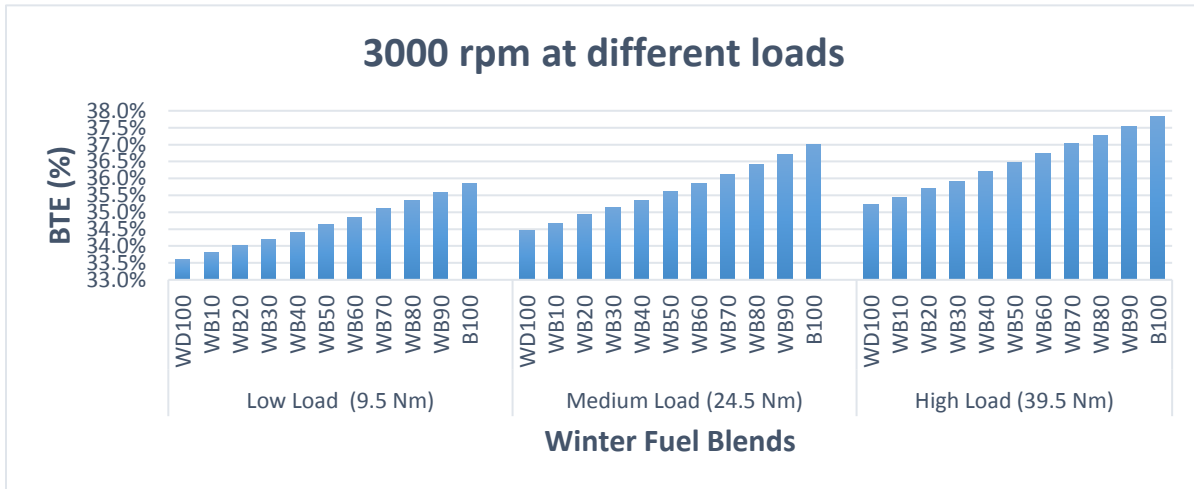


Figure 4.25: BTE values for winter diesel-biodiesel under different loads at (a) 1000 rpm (b) 2100 rpm (c) 3000 rpm

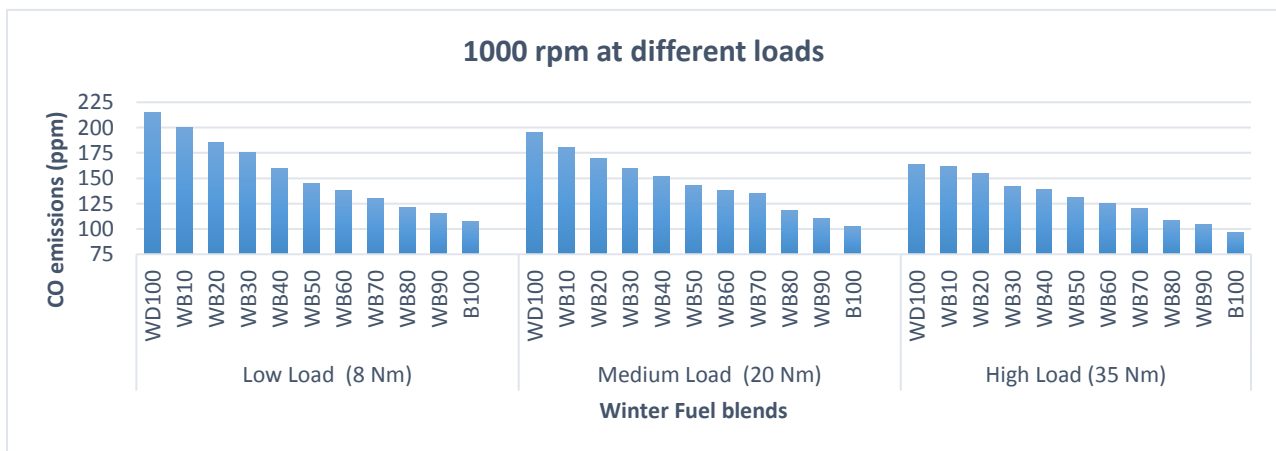
2. Emissions:

a) CO Emissions

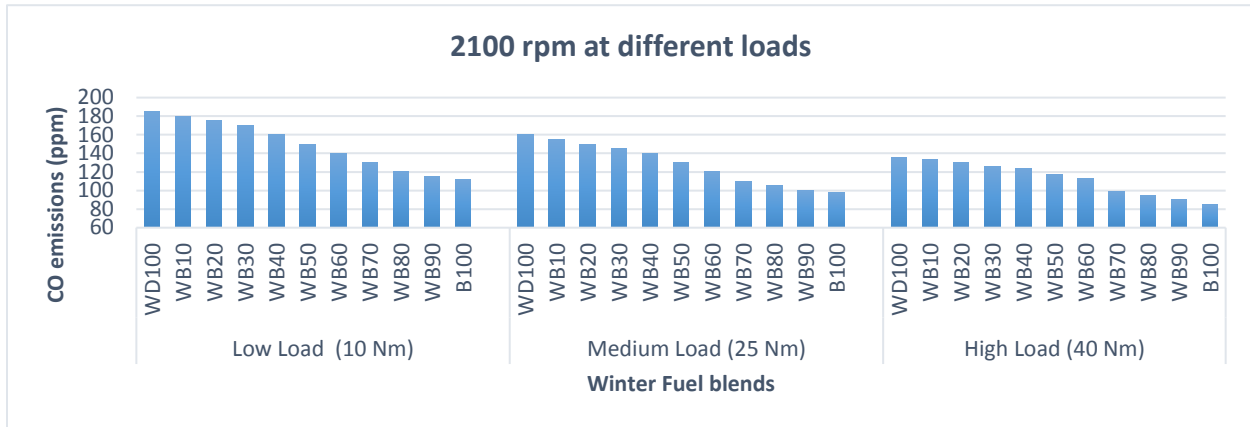
The absence of fuel borne oxygen in the molecular structures of fossil fuel has led incomplete combustion and production of CO emissions [98]. Generally, many factors are responsible which influence CO emissions such as air-fuel ratio, engine speed, engine load and the fuel type. The variation of CO emissions with winter diesel and biodiesel blends is shown in Figure 4.26.

It was found that CO emissions decreased with increasing biodiesel percentage in the blends. This reduction of CO emissions is attributed to the higher oxygen content and cetane number of biodiesel fuel. Biodiesel contains 12% more oxygen than diesel. The higher oxygen content of biodiesel allows more carbon molecules to burn and fuel combustion is complete. At 1000 rpm under low load condition, CO emission emitted by different fuels were 215 ppm from winter diesel, 185 ppm from WB20, 145 ppm from WB50 and 107 ppm from pure biodiesel. With increase in load, CO emissions were reduced. At 1000 rpm, WB50 fuel blends produced 145 ppm, 143 ppm and 131 ppm of CO emissions under low, medium and high load conditions respectively. At 2100 rpm, WB50 produced 150 ppm, 130 ppm and 117 ppm of CO emission under low, medium and high loads respectively. At 3000 rpm, WB50 showed 132 ppm, 121 ppm and 112 ppm of CO emission under low, medium and high loads respectively. Over the entire range of engine speeds, all the fuels reduced CO emissions with increasing speed. The average reduction of CO emissions for all the biodiesel-diesel fuels were 27%, 20% and 16% at 1000 rpm, 2100 rpm and 3000 rpm respectively compared with winter diesel fuel.

(a)



(b)



(c)

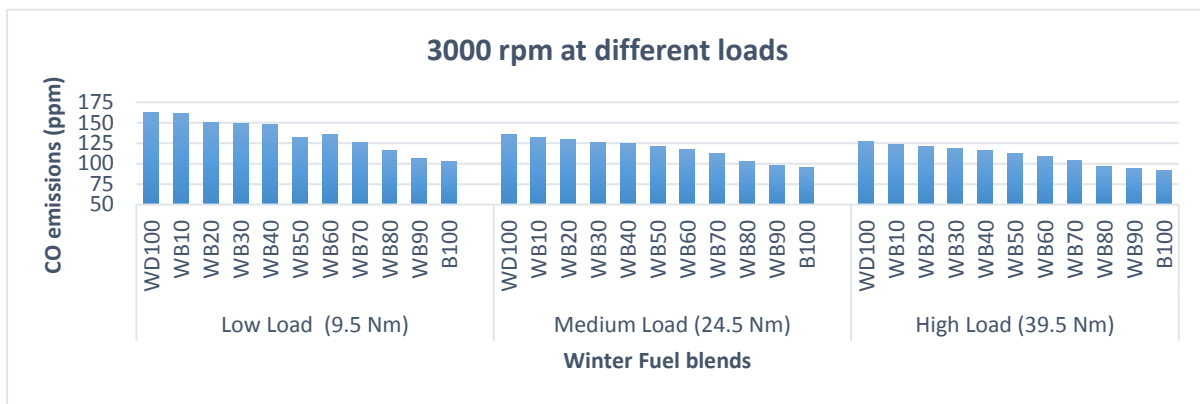


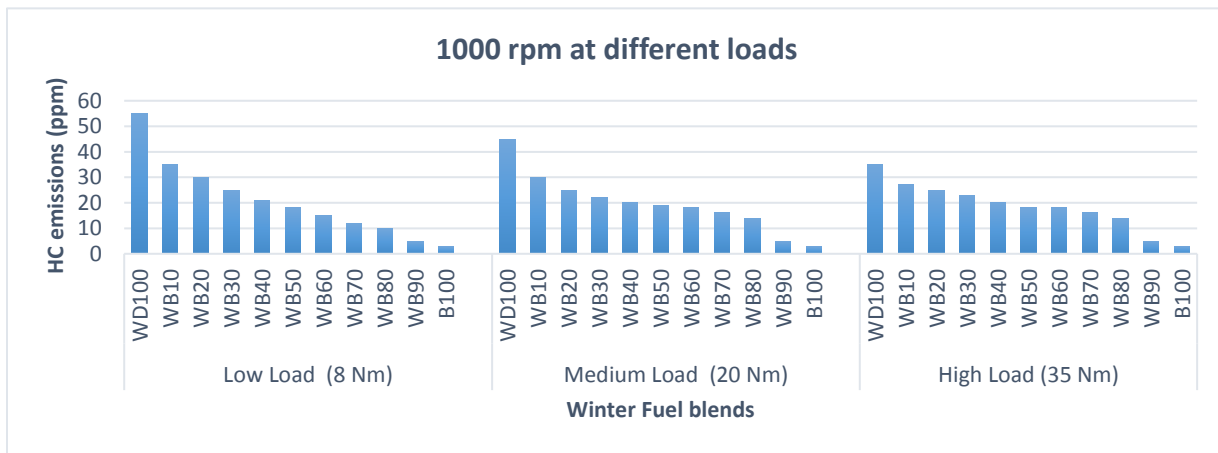
Figure 4.26: CO emission for winter diesel-biodiesel blends under different engine loads at (a) 1000 rpm (b) 2100 rpm (c) 3000 rpm

b) HC Emissions

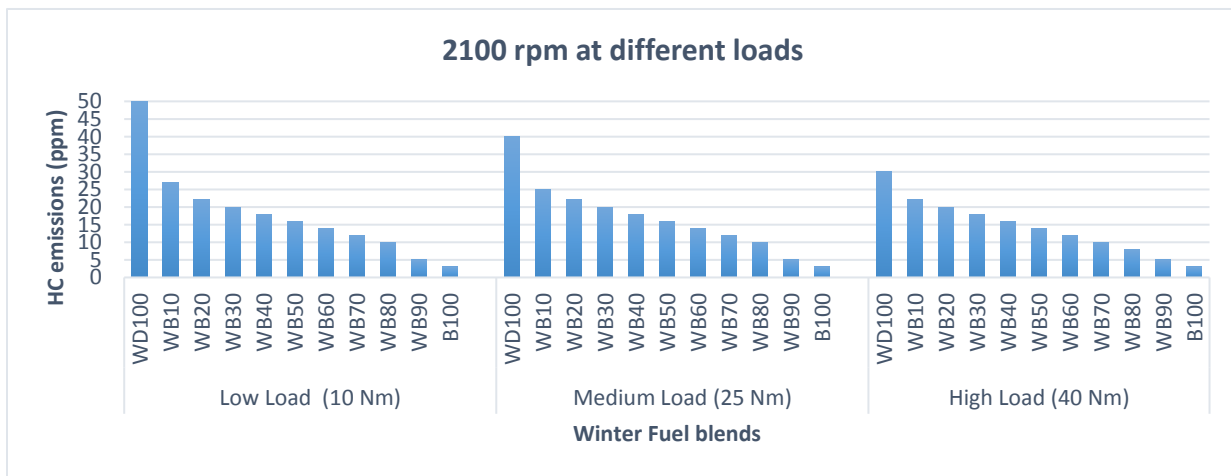
HC emissions for winter diesel and biodiesel blends are shown in Figure 4.27 (a), (b) and (c). HC emissions were decreased with increases in biodiesel percentage in the blend. These results could be attributed to the good HC conversion caused by higher cetane number and oxygen content in fuels. As biodiesel has higher oxygen content, which improves complete combustion and reduce HC emissions [99]. At 1000 rpm under low load condition, HC emissions produced from different fuel blends were 55 ppm from winter diesel, 30 ppm from WB20, 18 ppm from WB50 and 3 ppm emitting lowest from pure biodiesel fuel. Increasing the engine load reduced HC emissions slightly because of lean combustion taking place inside the combustion chamber. At 1000 rpm, HC emissions reduced on an average of 68%, 62% and 52% under low, medium and high load respectively. At 2100 rpm, HC emissions reduced on an average of 71%, 64% and 57% under low,

medium and high load respectively. At 3000 rpm, HC emissions reduced on an average at 76% under low load and 75% under medium and high loads. HC emissions of all fuels were decreased with increases in engine speed due to the lean combustion. When engine speed was at maximum, all fuels showed a lower amount of HC emissions compared to the low engine speed. At 1000 rpm, the average HC emission for WB20 was 27 ppm and decreased to 22 ppm on an average at 2100 rpm. However, HC emissions for WB20 reduced even more at 3000 rpm measuring only 14 ppm.

(a)



(b)



(c)

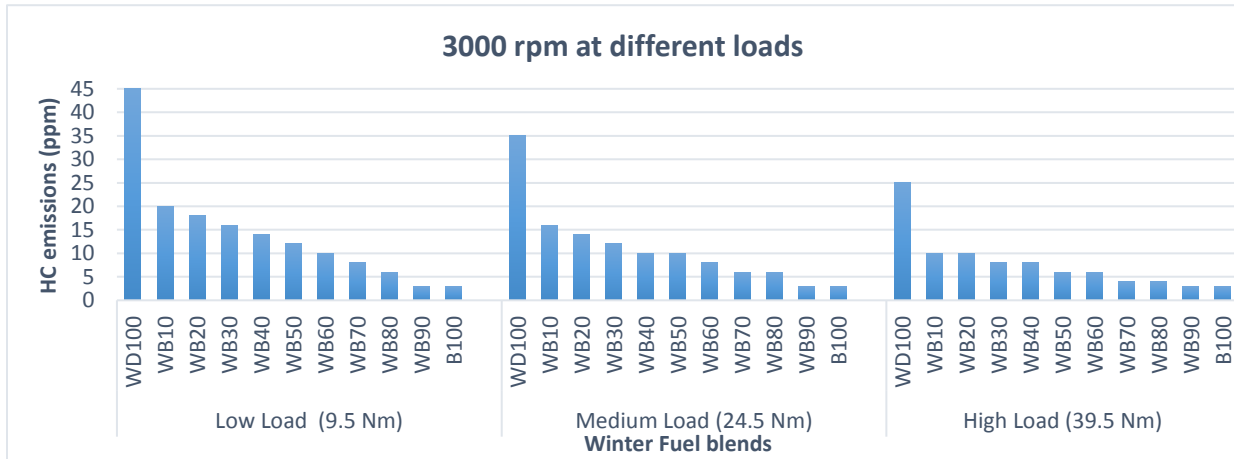


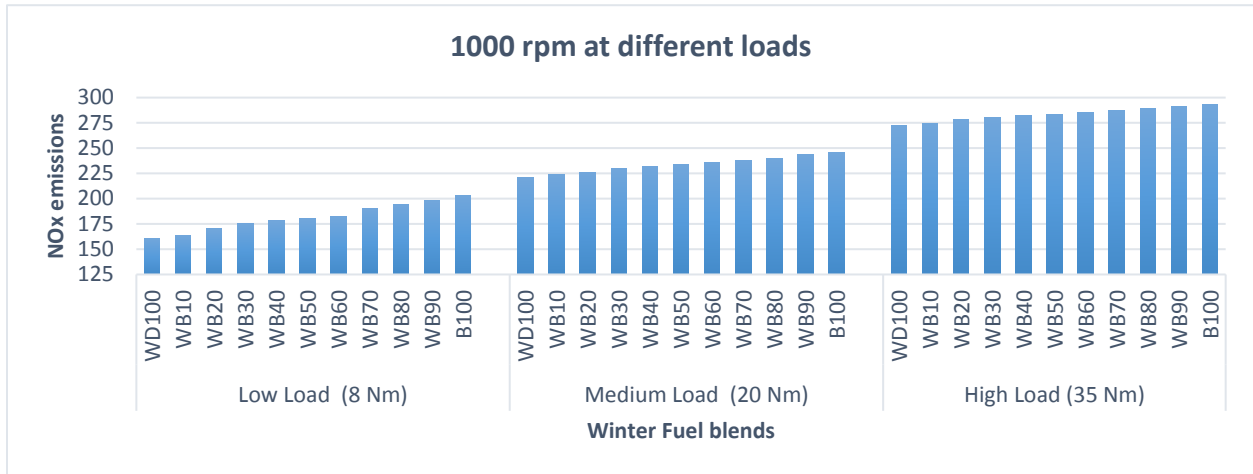
Figure 4.27: HC emission for winter diesel-biodiesel blends under different engine loads at (a) 1000 rpm (b) 2100 rpm (c) 3000 rpm

c) NO_x Emissions

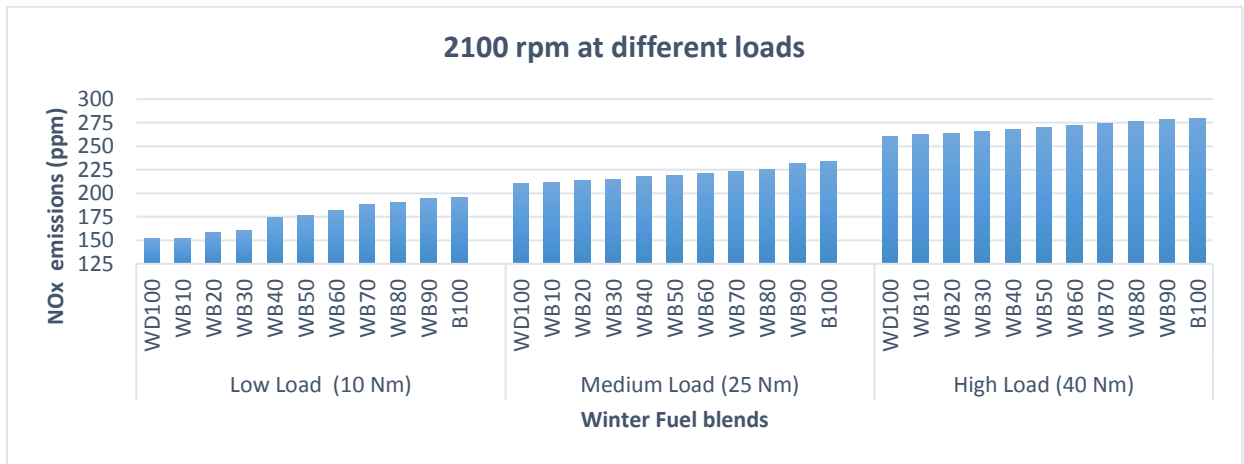
Figure 4.28 illustrates NO_x emissions of different fuel blends for variable engine load and speed. NO_x emissions increased with increasing biodiesel content as was expected due to the oxygen content. Pure biodiesel at 1000 rpm under high load condition showed maximum amount NO_x emission measuring almost 293 ppm. However, winter diesel at same condition showed only 272 ppm of NO_x emission, showing slight increase of NO_x emission with biodiesel compared with diesel fuel.

With increase in load due to the temperature effect, NO_x emissions increased. At 1000 rpm, NO_x increased at 14% on an average under low load but increased slightly at medium and high loads with average emission of 6% and 4% respectively. Similar trend was followed in Figure 4.28 (b) and (c). Speed reduced NO_x emission for all fuel blends because of shorter ignition lag period. At 3000 rpm, winter diesel produced the lowest NO_x emission of 140 ppm compared to winter diesel at 1000 rpm producing 161 ppm of NO_x emission under low load. Similarly for pure biodiesel, NO_x emission was 270 ppm at 3000 rpm compared to pure biodiesel at 1000 rpm measuring 293 ppm under high load condition.

(a)



(b)



(c)

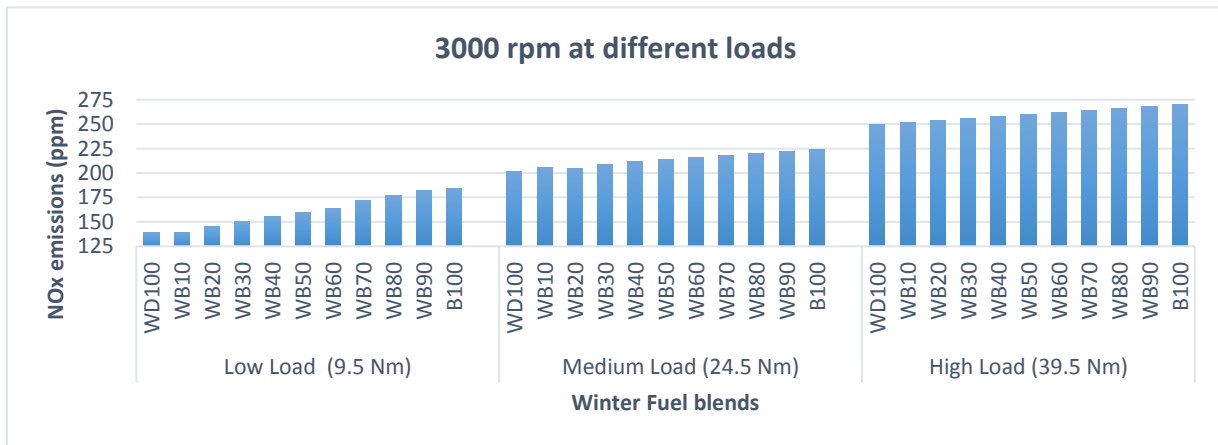


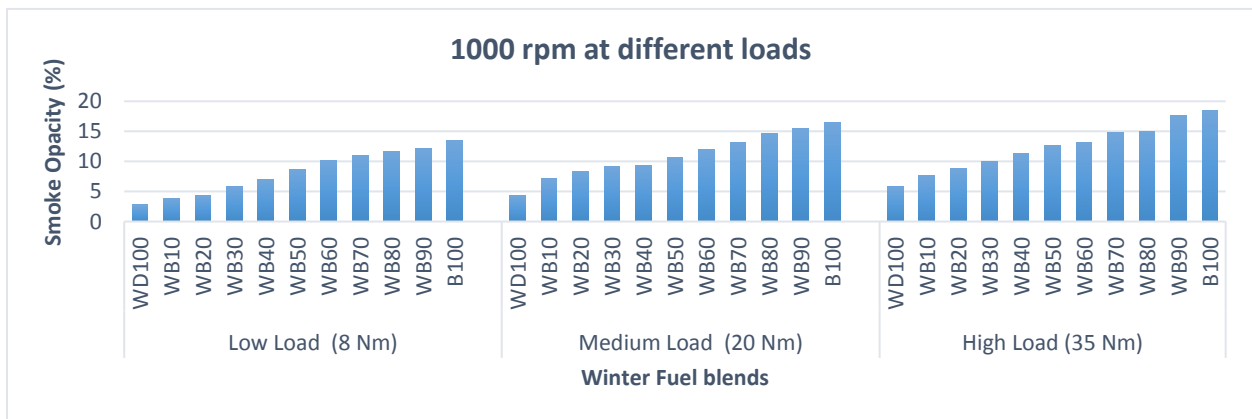
Figure 4.28: NOx emission for winter diesel-biodiesel blends under different engine loads at (a) 1000 rpm (b) 2100 rpm (c) 3000 rpm

d) Smoke Opacity Emissions

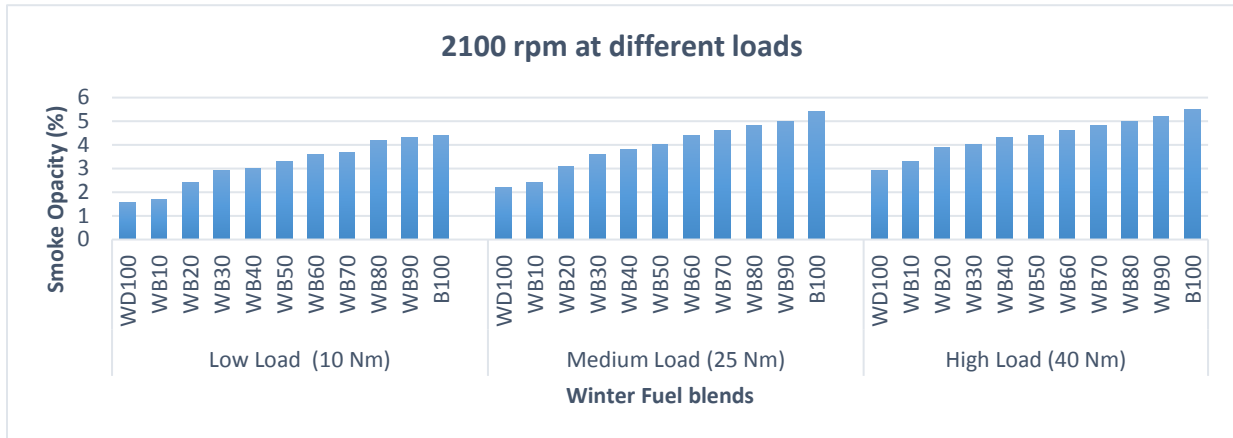
Smoke opacity increased with increasing biodiesel content in the fuel blends due to higher viscosity of the fuels. Pure biodiesel produced the maximum amount of smoke opacity emission of 18.5% at 1000 rpm under high load condition compared to all fuel blends at all engine load and speed. However, winter diesel (5.8%) produced lower smoke emissions at same conditions and smoke opacity emission increased with WB20 (8.8%) and even higher for WB50 (12.6%).

Figure 4.29 show an increase of smoke opacity as the load was increased. This could be due to the fact that in all internal combustion engines, air-fuel ratio decreases with increasing load [100]. Therefore, higher amount of soot formation takes place inside the cylinder. At 1000 rpm, the average smoke emission for biodiesel-diesel blends was 8.8%, 11.7% and 12.9% at low, medium and high loads respectively. At 2100 rpm, the average smoke emission was 3.4%, 4.1% and 4.5% at low, medium and high loads respectively. Similarly at 3000 rpm, the average smoke emission was 1.4%, 1.9% and 2.5% respectively. Increasing the engine speed, lean combustion helped in reducing the smoke opacity emission. The average smoke opacity emission of WB50 at all loads was 10.7%, 3.9% and 1.8% for 1000 rpm, 2100 rpm and 3000 rpm respectively.

(a)



(b)



(c)

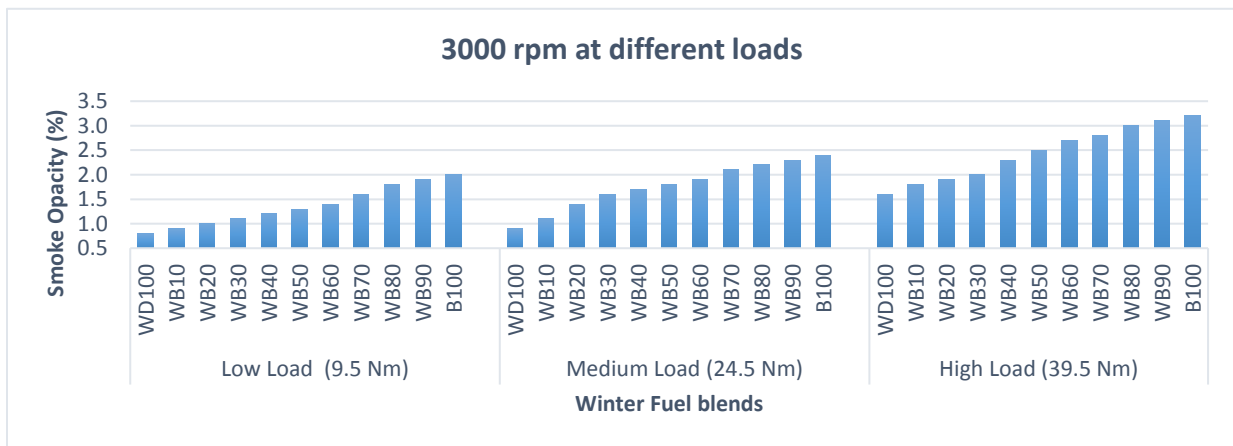


Figure 4.29: Smoke opacity emission for winter diesel-biodiesel blends under different engine loads at (a) 1000 rpm (b) 2100 rpm (c) 3000 rpm

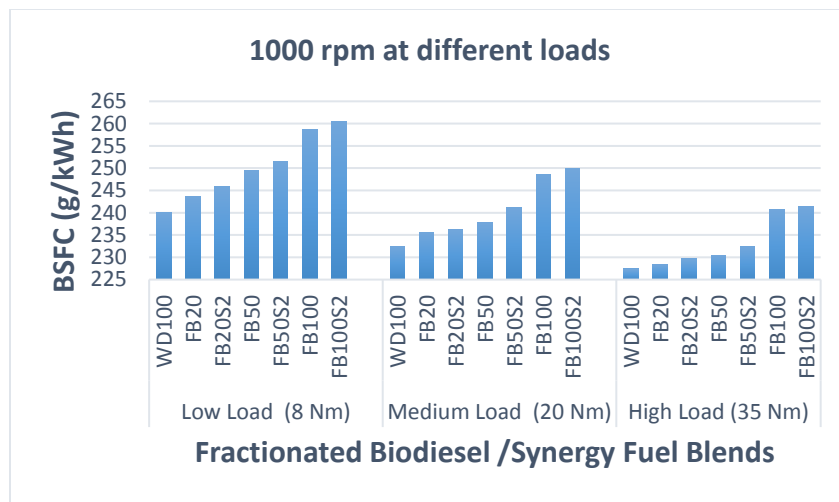
4.5.3 Winter Diesel-Fractionated Biodiesel and 2% Wintron Synergy Additive Series:

1. Engine Performance:

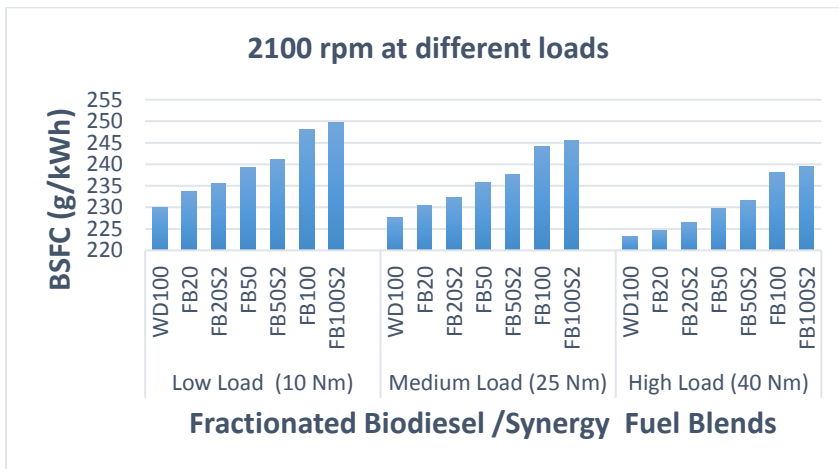
a) BSFC

Figure 4.30 shows the BSFC of the fractionated biodiesel blends and synergy blends at different engine speeds and loads. The higher density of fractionated biodiesel and Wintron Synergy blends compared to conventional diesel indicates that the fuel injection pump is delivering more fuel mass to the engine for the same output power [101]. Higher viscosity resulting in poor mixing of diesel-fractionated biodiesel-synergy blend with air increases BSFC due to weak atomization of fuel. Lower calorific value of higher fractionated biodiesel blends also plays an important role in

increasing the value of BSFC. BSFC decreases as the load increases because more fuel is required to carry a light load, as seen in figure. Overall, FB100 and FB100S2 increases BSFC the most at all loads due to lower heating value compared to other fuel blends. For all test fuels, BSFC decreased with increasing engine speed. Since in-cylinder air turbulence improves with the engine rpm, more homogeneous air-fuel mixture can be achieved. This improvement in the air-fuel mixture formation might be effective in decreasing the BSFC values with increasing engine speed. However, a slight increase in BSFC was noticed at 3000 rpm. The average minimum BSFC value at variable engine speed for the blend with additives (FB20S2) was 240 g/kWh, 234 g/kWh and 228 g/kWh at low, medium and high loads; and without additive (FB20) was 237 g/kWh, 233 g/kWh and 224 g/kWh at low, medium and high loads.



(a)



(b)

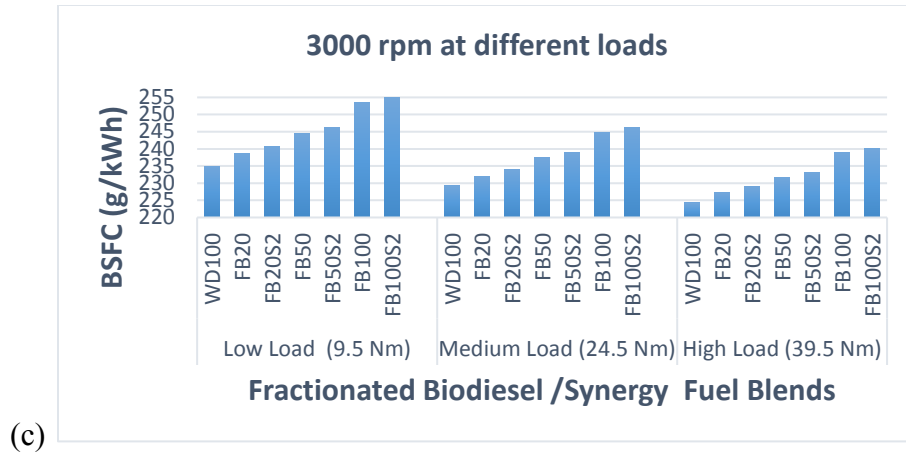


Figure 4.30: BSFC values for winter diesel-fractionated biodiesel under different loads at (a) 1000 rpm (b) 2100 rpm (c) 3000 rpm

b) BTE

Figure 4.31 represents the experimental results of BTE with engine load and speed for various fuel blends. Figure shows that with higher amount of fractionated biodiesel in diesel, BTE was higher due to the oxygen content in fractionated biodiesel that promoted more rapid and complete combustion. The brake thermal efficiency is a function of specific fuel consumption and lower heating value of a fuel. As it is shown in figure, it increased with the engine load. This was due to reduction in heat loss and increase in power developed with increase in load [102].

Results showed that BTE increased with increasing engine speed of the engine from 1000 rpm to 2100 rpm and then reduced slightly for 3000 rpm because of poor spray characteristics of the tested fuel and air-fuel mixing at the engine's high speed [103]. Furthermore, the higher efficiency with fractionated biodiesel-diesel blends than diesel indicates that with blended fuels, combustion is better than diesel fuel combustion. This is attributed to the oxygen content of fractionated biodiesel. Therefore, low emission of CO and HC are expected due to better combustion with fractionated biodiesel. The CO and HC emission results will be discussed in the following subsection. The average increase of BTE with respect to diesel fuel for FB100 for low, medium and high loads are 5%, 6% and 6.4% respectively. Similarly, for FB100S2, the average increase of BTE was 5.8%, 6.6% and 7.3% for low, medium and high loads respectively.

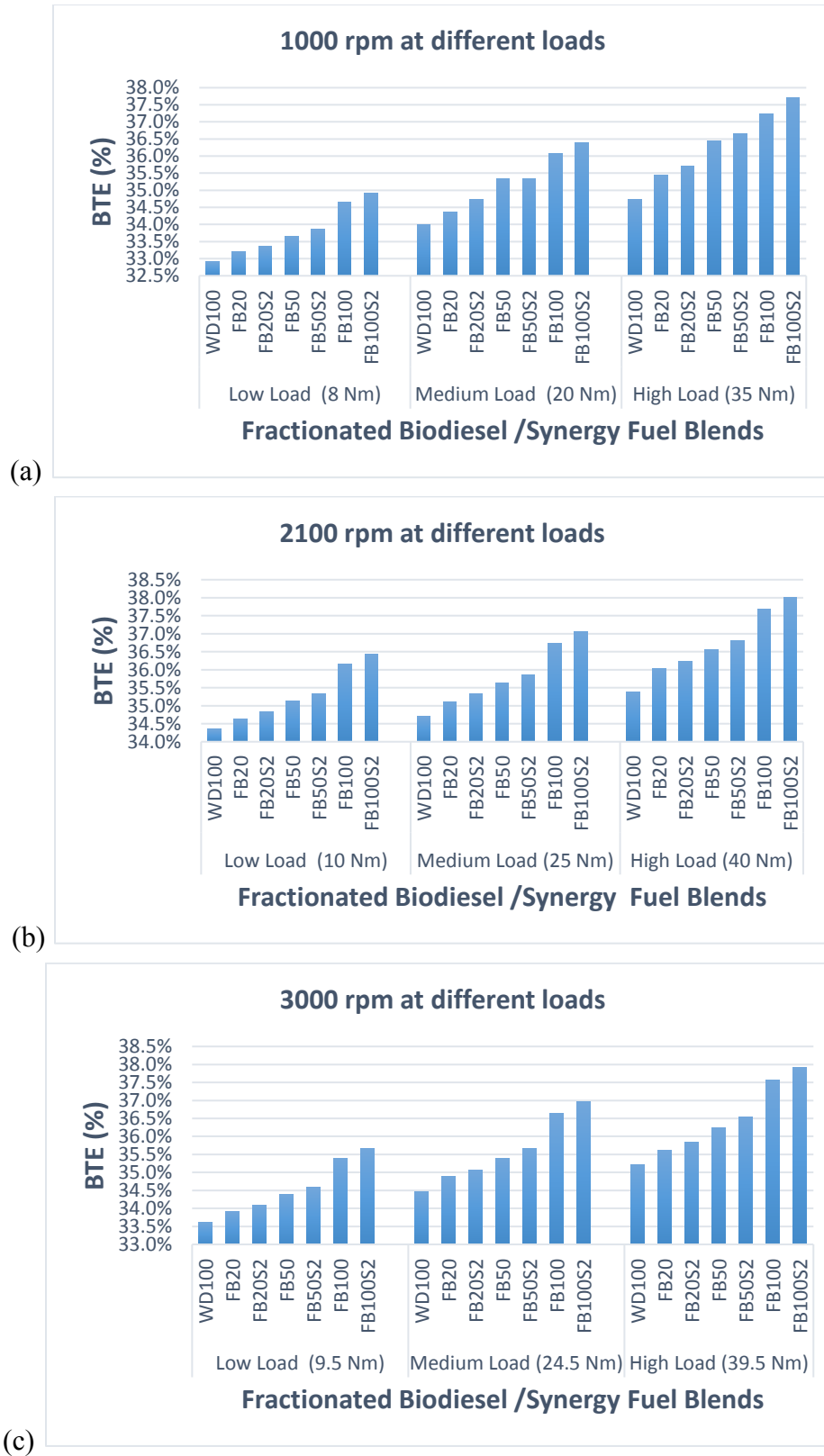


Figure 4.31: BTE values for winter diesel-fractionated biodiesel under different loads at (a) 1000 rpm (b) 2100 rpm (c) 3000 rpm

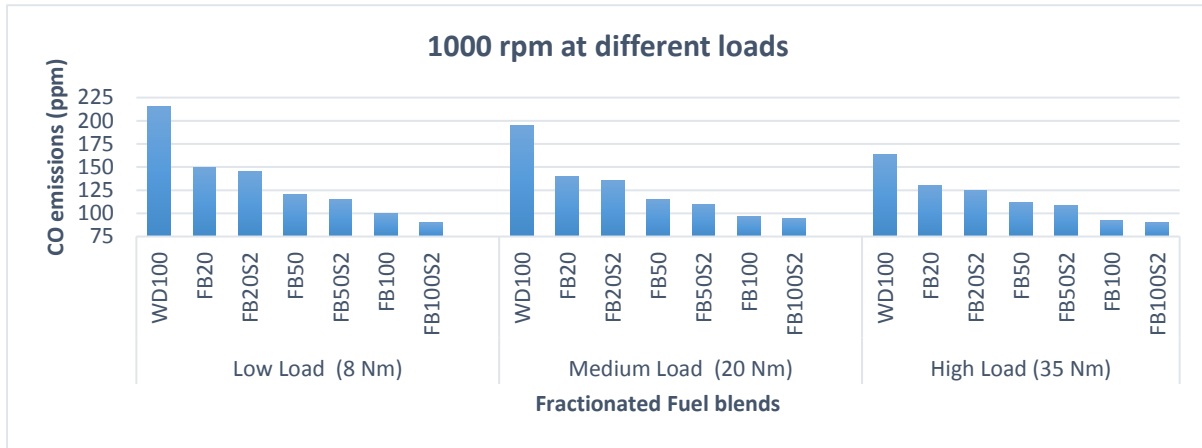
2. Emissions:

a) CO Emissions

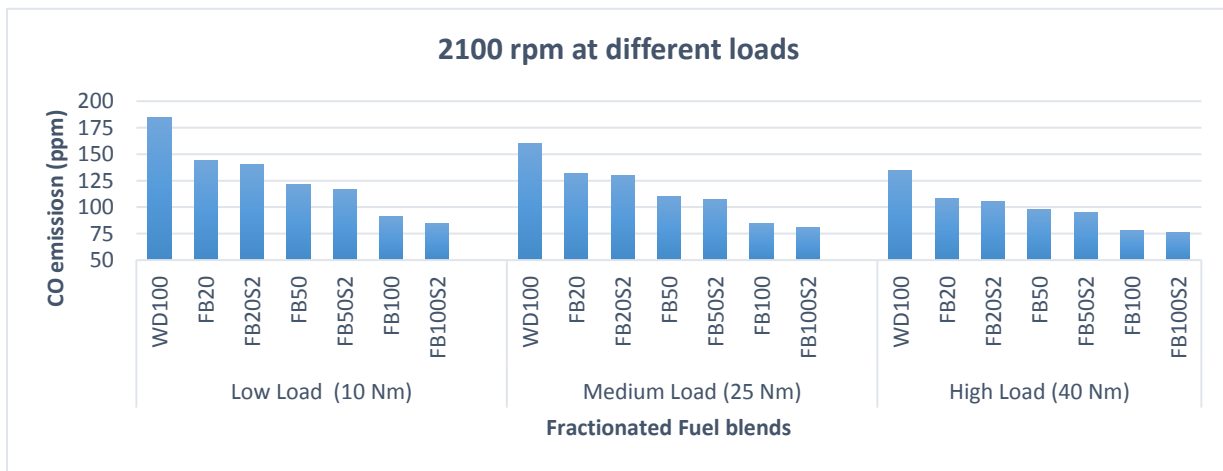
CO results from incomplete combustion of fuel and it is produced mostly from petroleum fuels, which contain no oxygen in their molecular structure. CO emission are usually affected by air-fuel equivalence ratio, fuel type, combustion chamber design, atomization rate, start of injection timing, injection pressure, engine load and speed. CO emission results were presented in Figure 4.32 (a), (b), (c) for different engine load and speed. Similar trend was followed both by fractionated biodiesel-diesel blends and fractionated biodiesel-diesel-synergy blends. Winter diesel has been used as a reference fuel.

With increase in fractionated biodiesel concentration, fractionated biodiesel-diesel fuel blend series decreased at all engine speed and variable engine loads. Similarly with 2% Wintron Synergy in fractionated biodiesel-diesel blend, additional fuel-bound oxygen in the blends ensured CO oxidation even in locally fuel-rich zones, which helped reducing CO emission [104]. FB100S2 produced the lowest CO emissions at all load and speed conditions. All the figures showed decrease of CO emissions as load was increased for all the fuel blends due to temperature condition prevailing inside the cylinder. All the fractionated biodiesel-diesel-synergy blends showed similar CO emission with that of fractionated biodiesel-diesel blends. All fuel blends produced lowest CO emissions at high load levels and gave the lowest emission at 3000 rpm compared to other engine load and speed. FB100 produced 91 ppm, 85 ppm and 78 ppm of CO emissions at low, medium and high loads respectively at 2100 rpm. Higher engine speed reduced the CO emissions for all the fuel blends at different loads because of higher temperature. Average CO emissions for FB100S2 were 92 ppm, 80 ppm and 71 ppm at 1000 rpm, 2100 rpm and 3000 rpm at all engine loads.

(a)



(b)



(c)

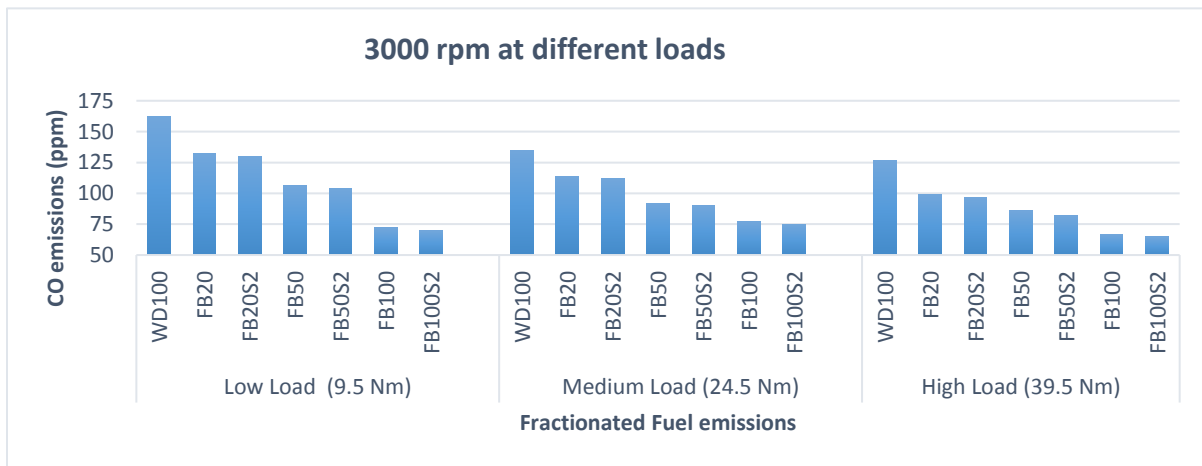


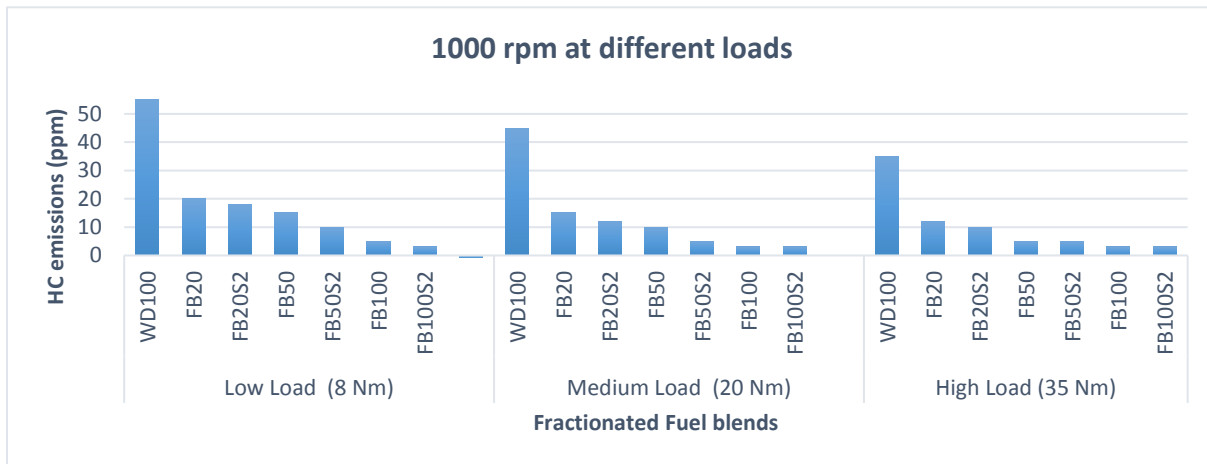
Figure 4.32: CO emission for winter diesel-fractionated biodiesel blends under different engine loads at (a) 1000 rpm (b) 2100 rpm (c) 3000 rpm

b) HC Emission

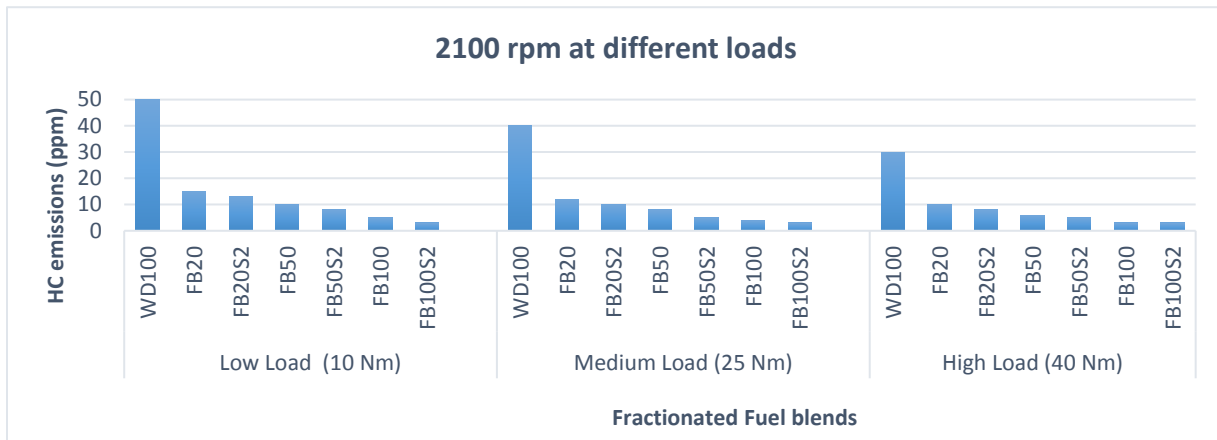
Unburned HC is the result of the incomplete combustion of fuels and flame quenching. The variation of HC emissions for winter diesel with fractionated biodiesel blend and Wintron Synergy blend fuels is shown in Figure 4.33 (a), (b) and (c)

With increasing amount of fractionated biodiesel in fractionated biodiesel-diesel blends and synergy blends, unburned HC emissions were lower than diesel fuel. These reductions can be attributed to the high oxygen contents of fractionated biodiesel and synergy fuel blends and less carbon and hydrogen than diesel fuel, which guarantees more complete combustion. It was noticed that at all engine load and speed, FB100S2 produced the least amount of HC emission as compared with other fuel blends. This was mainly due to temperature effect. FB20S2 produced 18 ppm, 12 ppm and 10 ppm of HC emission at 1000 rpm under low, medium and high load respectively. At 2100 rpm, FB20S2 produced 13 ppm, 10 ppm and 8 ppm of HC emission under low, medium and high load respectively. Similarly at 3000 rpm, FB20S2 produced lower HC emissions measuring an average of 7 ppm under variable loads.

(a)



(b)



(c)

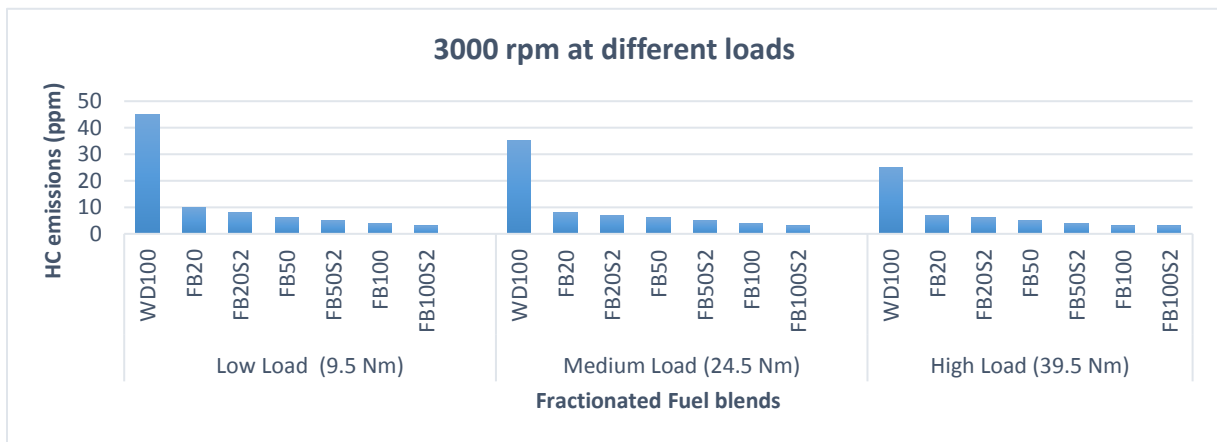


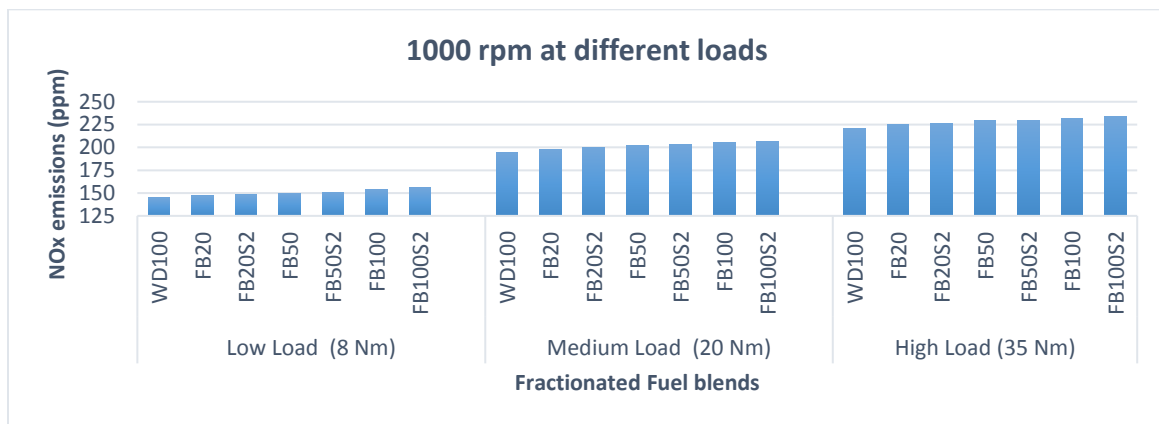
Figure 4.33: HC emission for winter diesel-fractionated biodiesel blends under different engine loads at (a) 1000 rpm (b) 2100 rpm (c) 3000 rpm

c) NO_x Emission

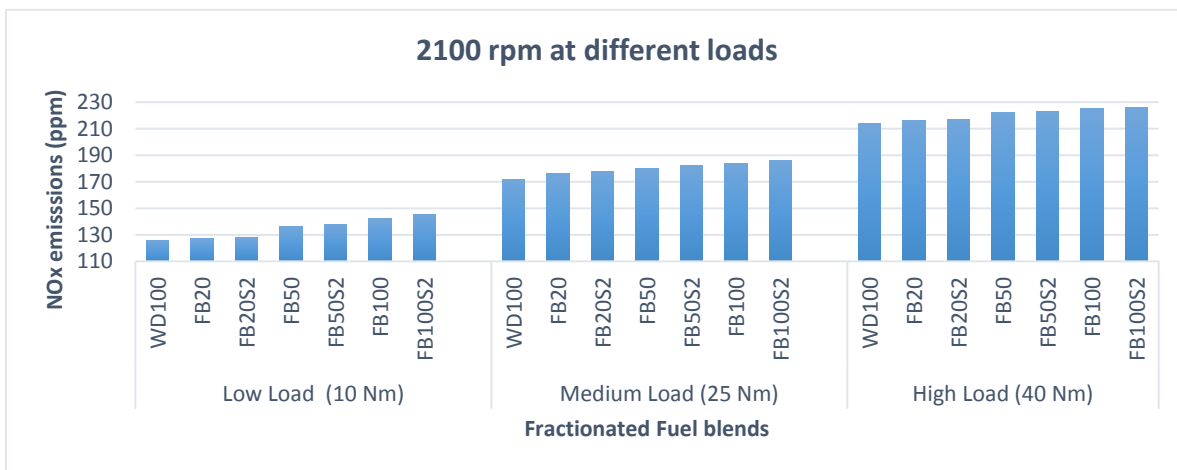
Figure 4.34 shows the NO_x emissions for different winter diesel-fractionated biodiesel blends and winter diesel-fractionated biodiesel-synergy blends with the variations of engine loads and speeds. All fractionated biodiesel blends produce higher amount of NO_x emission than diesel fuel does. The NO_x emissions of diesel-fractionated biodiesel blends and diesel-fractionated biodiesel-synergy blends were gradually increased with the increase in concentration of fractionated biodiesel in both the blends, and increase in engine load. However, NO_x emissions decreased with increase in engine speed. With increase in load, higher amount of exhaust temperature was liberated, however with increase in engine speed, minimal increase of exhaust temperature was recorded.

Fractionated biodiesel has higher oxygen content than diesel fuel [105]. This can be attributed to NO_x formation in the combustion process. In study [106], it was reported that higher oxygen content of fractionated biodiesel blends could raise the temperature and increase the rate of NO_x emission formation. The fractionated biodiesel blends can improve engine combustion because of a higher cetane number similar to normal biodiesel and therefore forming NO_x emission

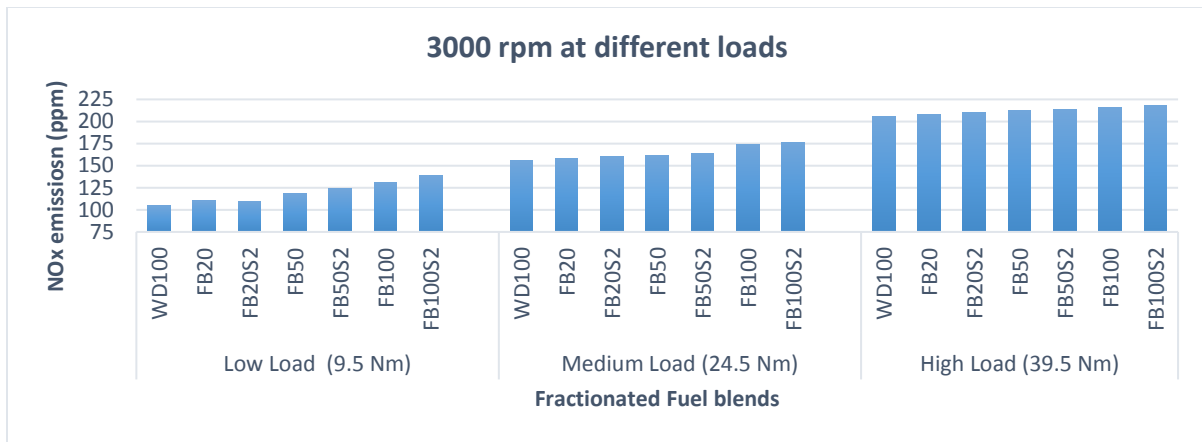
The maximum amount of NO_x emissions was found with fractionated biodiesel with 2% Wintron Synergy additive at approximately 234 ppm at 1000 rpm under high load. Fractionated biodiesel with 2% Wintron Synergy series produced higher NO_x emissions compared with fractionated biodiesel-diesel series because synergy have higher oxygen content in it. At low load conditions, FB20 produced much lower NO_x emissions at all engine speeds compared with other fractionated biodiesel and synergy blends. Winter diesel produced least NO_x emissions at all loads and speed compared to other fuel blends.



(a)



(b)



(c)

Figure 4.34: NOx emission for winter diesel-fractionated biodiesel blends under different engine loads at (a) 1000 rpm (b) 2100 rpm (c) 3000 rpm

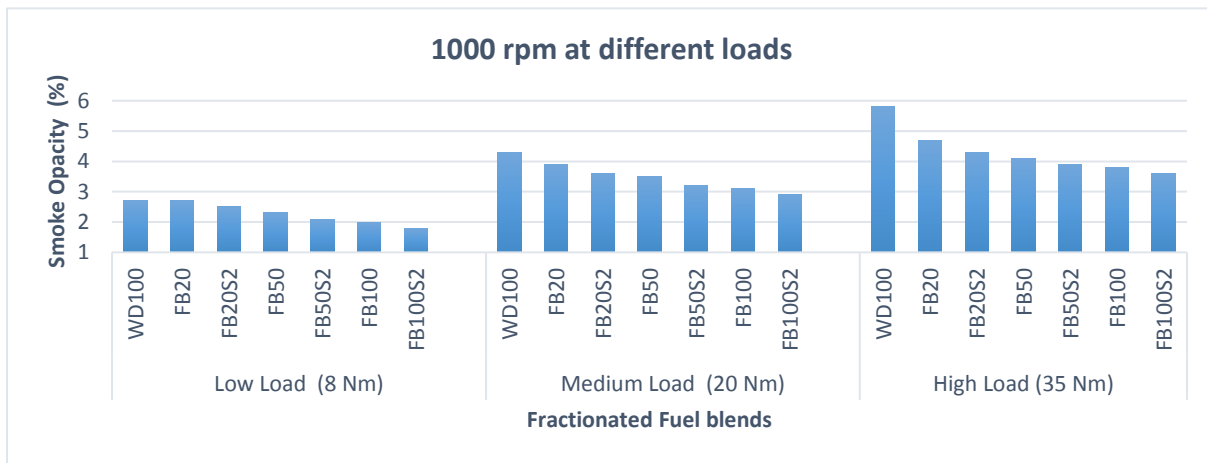
d) Smoke Opacity Emissions

It can be seen that, smoke opacity values were found quite lower for fractionated biodiesel blends than diesel at all rpm. Higher oxygen and lower sulfur content as well as low amount of saturated fatty acid compounds in fractionated biodiesel are responsible for this decrement. Application of oxygenated additives enhanced the decrement even in a better form. In Figure 4.35 (a), (b) and (c), it can be seen that 2% Wintron Synergy additive blends emitted lower soot than corresponding fractionated biodiesel blends. It can be attributed to the extra fuel-bound oxygen of the blends with synergy which assisted the combustion to be leaner even at locally fuel rich zones.

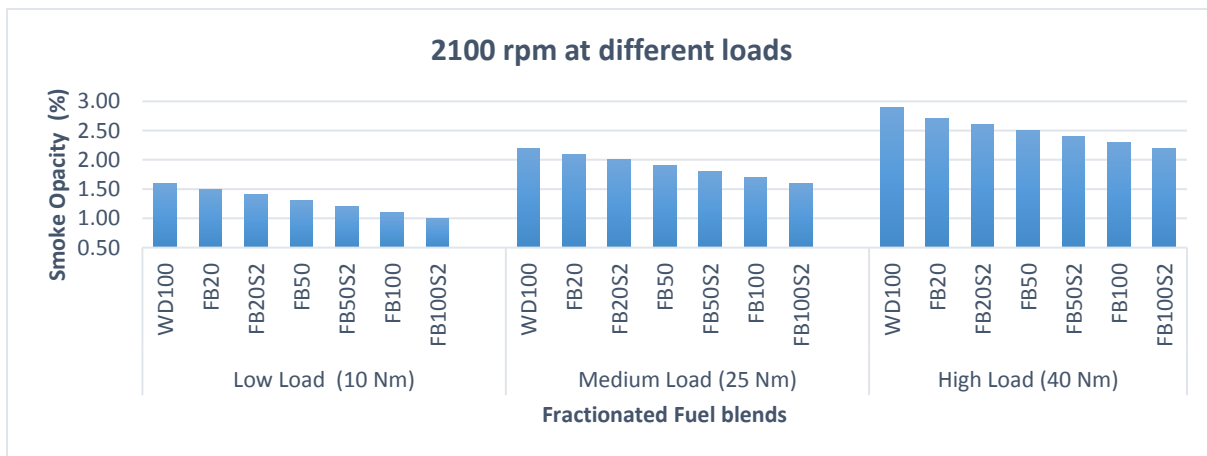
At 1000 rpm, FB100S2 reduced smoke opacity emission by 33% under low and medium load, and 38% reduction at high load compared with winter diesel fuel. At 2100 rpm, FB100S2 reduced by 38%, 28% and 22% under low, medium and high loads respectively. Similarly at 3000 rpm, 25%, 22% and 20% reduction in low, medium and high load respectively. Therefore, it can be figured that addition of 2% Wintron Synergy with use of fractionated biodiesel fuel, smoke opacity could be reduced tremendously. This could be due to removal of long chain fatty acids during fractionation process which acts as smoke forming agent during combustion inside the cylinder. However, with increase in load, smoke opacity emissions were increased slightly at all engine speed. For FB50S2 at 1000 rpm, the smoke opacity emission were 2.1%, 3.2% and 3.9% under low, medium and high loads respectively. Similarly for FB50S2 at 2100 rpm, smoke opacity emissions were 1.2%, 1.8% and 2.4% under low, medium and high loads respectively. Finally at 3000 rpm, smoke opacity emission for FB50S2 were 0.7%, 0.8% and 1.4% under low, medium and high loads respectively.

Fractionated biodiesel blends showed higher reduction against the corresponding normal biodiesel blends, which can be attributed to considerable lower saturated compounds of fractionated biodiesel than normal biodiesel, causing a better atomization of the corresponding blend. Increasing the engine speed helped in reduction of smoke opacity emissions. The average smoke opacity emission for FB20S2 was 3.47%, 2% and 1.1% at 1000 rpm, 2100 rpm and 3000 rpm respectively.

(a)



(b)



(c)

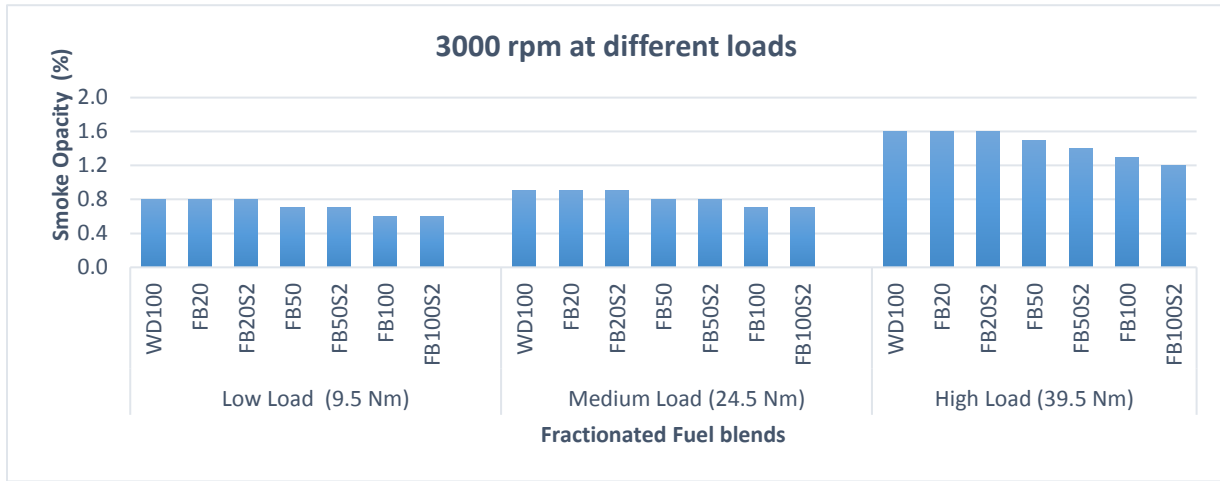


Figure 4.35: Smoke opacity emission for winter diesel-fractionated biodiesel blends under different engine loads at (a) 1000 rpm (b) 2100 rpm (c) 3000 rpm

Chapter 5

Conclusion

In this study, canola biodiesel is produced and their quality and fuel characteristics are investigated. An experimental investigation is conducted to explore the performance and emissions of different normal biodiesel blends and fractionated biodiesel blends on a heavy-duty DI diesel engine and a light-duty DI diesel engine. Also, Wintron Synergy is used with normal biodiesel and fractionated biodiesel to reduce the cloud point of the blends, which could be the first time to study its effect on engine performance and emissions in the literature. Furthermore, there are limited studies on urea fractionated biodiesel as a blending fuel, which is mainly used to reduce the cloud point of the blends. The results obtained suggest the following conclusions:

1. Fuel properties of biodiesel produced from canola oil by transesterification process follows the ASTM standards. The conversion rate is 100% and the collection efficiency is more than 80%. Its heating value is approximately 12% lower than diesel fuel.
2. Viscosity of the fuel blends from normal biodiesel treated with urea fractionation follows the specified limits of ASTM standards. The collection efficiency is about 33%. Its heating value is approximately 13% lower than diesel fuel.
3. The cloud points of fractionated biodiesel blends were lower than the cloud points for normal biodiesel blends. Moreover, cloud points of fractionated biodiesel blends with 2% Wintron Synergy were much lower than normal biodiesel blends with 2% Wintron Synergy additive. Winter diesel has a cloud point of -41°C and FB40S2 has a cloud point of -48.5°C .
4. It was found that fractionated biodiesel-diesel-synergy blend up to 80% fractionated biodiesel in winter diesel is most suited to be used in extreme cold weather conditions.
5. Compared to diesel fuels, all the biodiesel and fractionated fuel blends increased BSFC, however, with increase in engine load, there was reduction in BSFC. At 1000 rpm, all fuel blends showed higher amount of BSFC. At 2100 rpm, BSFC was the lowest and increased slightly at 3000 rpm.
6. Brake thermal efficiency (BTE) was inversely proportional to BSFC in case of load and speed for all fuel series. However, BTE increased with biodiesel content in fuel blend similar to the BSFC trend.

7. CO emissions for all fuel blends are lower at high load condition at each rpm. The higher the biodiesel percentage in biodiesel-diesel blends, the lower the CO emissions at idle to high load conditions. For heavy-duty diesel engine at 800 rpm under idling condition, CO emissions reduced by 30%, 27%, 74%, 53% and 56% for summer diesel-biodiesel blend, winter diesel-biodiesel blend, winter diesel-biodiesel-synergy blend, fractionated biodiesel-diesel blend and fractionated biodiesel-diesel-synergy blend respectively compared to diesel fuel. For light-duty diesel engine at variable engine load and speed, the maximum reduction was achieved by pure biodiesel at low and medium loads at 1000 rpm measuring almost 48% lower emissions than diesel fuel. FB100S2 produced the lowest CO emissions reducing by 56% on an average at low load at all rpm. Furthermore, CO emission reduced with increase in engine speed.
8. HC emissions for all fuels are also lower at high loads when tested on a light duty diesel engine at different engine speed. The HC emissions showed reduction with increase in engine speed. The higher the biodiesel percentage in biodiesel-diesel blends, the lower the HC emissions, a similar trend to that of CO emissions. When pure biodiesel was tested on a heavy duty diesel engine at idling condition, the average HC reduction was 39% lower than diesel fuel. However, when the same engine was tested with fractionated biodiesel, HC emissions reduced even more with 60% lower than diesel fuel. In the case of light duty diesel engine, average HC emission with biodiesel-diesel fuel blends were 14%, 11% and 7% at 1000 rpm, 2100 rpm and 3000 rpm respectively. Furthermore, the average HC emission for fractionated biodiesel and synergy series were 9%, 7% and 5% at 1000 rpm, 2100 rpm and 3000 rpm respectively.
9. The highest NO_x was emitted at high load at 1000 rpm when biodiesel fuel blends were tested with a light-duty diesel engine. NO_x emissions increased with increase in biodiesel content in fuel blends. However, there was reduction in NO_x formation when engine speed was increased. In a heavy-duty diesel engine, all the five fuel blend series showed similar results with slight increase in NO_x emission which was 6% higher than diesel fuel. In case of light duty engine with variable engine load and speed, B100 produced an average NO_x increase of 22%, 13% and 7% with low, medium and high loads at all rpm's respectively. Similarly with FB100S2, average NO_x increase were 18%, 9% and 6% at low, medium and high loads at different engine speeds respectively.

10. Smoke opacity emissions for biodiesel-diesel blends when tested in both the engines were contradictory with the increase in biodiesel percentage in the blends. In heavy-duty diesel engine, B100 reduced smoke opacity emissions up to 96%. Similarly with FB100, smoke opacity reduced up to 89% and blending with 2% Wintron Synergy, 95% reduction was achieved. However, in light-duty engine under variable engine load, smoke opacity increased with increase in biodiesel percentage in the blend. Although, fractionated biodiesel and synergy series were contrary to biodiesel blends and reduced with increasing fractionated biodiesel content in the blend. All the fuel blend series increased with higher engine load and decreased with increase in engine speed. The average smoke opacity emission with biodiesel-diesel blends were 6% and 8% at low and medium load at all rpm. With FB100S2, the overall smoke opacity emissions were 1.1% and 1.7% at low and medium load at all engine speed.

Appendices

Appendix A: Summer Diesel-Biodiesel Blends Data

Heavy-duty Engine-

FUEL	CO	HC	NOx
SD100	172	40	350
SB10	164	38	352
SB20	162	36	354
SB30	164	34	356
SB40	160	33	358
SB50	155	32	360
SB60	150	31	362
SB70	145	30	364
SB80	140	28	366
SB90	130	27	368
B100	120	25	370

Light-duty Engine-

RPM	LOAD	FUEL	CO (PPM)	HC (PPM)	NOx (PPM)	Smoke Opacity (%)	BSFC (g/kwh)	BTE
1000	Low Load (8 Nm)	SD100	209.0	50	156.0	2.9	240.0	33.5%
		SB10	195.0	30	158.0	3.5	241.4	33.6%
		SB20	180	25	160.0	4.5	242.9	33.8%
		SB30	170	21	162.0	6	244.0	34.0%
		SB40	155	18	165.0	8	245.5	34.1%
		SB50	140	15	168.0	9	246.9	34.3%
		SB60	135.0	12	170.0	10	248.4	34.5%
		SB70	129	10	172.0	11	249.8	34.6%
		SB80	127	7	174.0	12	251.0	34.8%
		SB90	115.0	5	176.0	13	252.4	35.0%
B100	112.0	3.0	178.0	13.2	253.8	35.2%		
1000	Medium Load (20 Nm)	SD100	182	40	195.0	4	230.8	34.8%
		SB10	172.0	25	197.0	5	231.6	35.1%
		SB20	168.0	20	198.0	6.3	232.8	35.2%
		SB30	160.0	19	200.0	8	233.6	35.5%
		SB40	150.0	18	203.0	9	234.8	35.7%
		SB50	145.0	16	205.0	9.5	236.1	35.8%
		SB60	135.0	14	207.0	10.5	237.5	36.0%
		SB70	120.0	12	215.0	12	238.8	36.2%
		SB80	112	10	220.0	13	239.6	36.5%
		SB90	105	5	225.0	14	240.0	36.8%
B100	95	3	230.0	15	241.2	37.0%		

1000	High Load (35 Nm)	SD100	160.0	30	270.0	5.25	226.6	35.5%
		SB10	154	22	275.0	6.17	227.2	35.8%
		SB20	145.0	20	280.0	8.64	227.7	36.0%
		SB30	140.0	19	282.0	9.14	228.3	36.3%
		SB40	134.0	18	284.0	10.6	230.2	36.4%
		SB50	126.3	16	286.0	11.31	230.9	36.7%
		SB60	122.0	14	288.0	12.4	230.5	37.1%
		SB70	115	12	290.0	13.74	233.2	37.1%
		SB80	107.3	9	295.0	14.66	233.8	37.4%
		SB90	100	5	297.0	16.03	235.5	37.5%
		B100	92.0	3	301.0	17.23	236.7	37.7%
2100	Low Load (10 Nm)	SD100	180.0	45	138.7	1.1	230.0	35.0%
		SB10	181.3	25	140.0	1.7	231.4	35.1%
		SB20	177.0	18	142.0	2.3	232.8	35.3%
		SB30	170	16	144.0	2.5	233.9	35.4%
		SB40	160.0	14	146.0	2.7	235.3	35.6%
		SB50	150	12	145.0	3.2	236.6	35.8%
		SB60	140.0	10	142.0	3.5	238.0	35.9%
		SB70	130	9	148.0	3.8	239.4	36.1%
		SB80	120.0	7	150.0	4	240.5	36.3%
		SB90	112	4	152.0	4.1	241.9	36.5%
		B100	109	3	154.0	4.2	243.3	36.7%
2100	Medium Load (25 Nm)	SD100	152	35	187.0	2.1	227.4	35.4%
		SB10	150	20	188.0	2.8	228.3	35.6%
		SB20	145.0	18	199.0	3.1	229.7	35.7%
		SB30	140.0	16	201.0	3.6	230.7	35.9%
		SB40	125	14	202.0	3.8	232.2	36.1%
		SB50	122.5	12	206.0	3.9	233.3	36.3%
		SB60	109	10	208.0	4.1	234.5	36.5%
		SB70	108	8	210.0	4.4	235.3	36.7%
		SB80	100	6	213.0	4.8	236.7	36.9%
		SB90	98	4	217.0	4.9	238.1	37.1%
		B100	96	3	220.0	5.3	239.1	37.4%
2100	High Load (40 Nm)	SD100	130	25	260.0	3.04	222.8	36.1%
		SB10	132	18	262.0	3.7	223.8	36.3%
		SB20	128	15	264.0	3.9	225.0	36.5%
		SB30	126.0	13	265.0	3.9	226.0	36.7%
		SB40	122	11	267.0	4.1	227.5	36.8%
		SB50	110	10	269.0	4.4	228.9	37.0%
		SB60	102.0	9	271.0	4.5	230.0	37.2%
		SB70	100	8	270.0	4.7	231.0	37.4%
		SB80	96	6	272.0	5.1	231.1	37.8%
		SB90	94	4	274.0	5.4	232.4	38.0%
		B100	92	3	276.0	5.6	234.2	38.2%
3000	Low Load (9.5 Nm)	SD100	162	40	121.7	0.5	225.0	35.7%
		SB10	160.0	16	124.0	0.74	226.4	35.9%
		SB20	156.0	14	126.0	0.88	227.7	36.0%
		SB30	150.0	12	128.0	1.01	228.8	36.2%
		SB40	145	10	130.0	1.06	230.1	36.4%
		SB50	140	10	132.0	1.2	231.5	36.6%
		SB60	135.0	8	134.7	1.4	232.8	36.7%

		SB70	130	6	135.0	1.5	234.2	36.9%
		SB80	115.0	4	138.0	1.6	235.3	37.1%
		SB90	107.0	3	140.0	1.7	236.6	37.3%
		B100	100.0	3	143.0	1.7	238.0	37.5%
3000	Medium Load (24.5 Nm)	SD100	132	30	177.5	0.75	221.6	36.3%
		SB10	130	14	178.0	1.03	222.6	36.5%
		SB20	129	12	180.0	1.1	223.9	36.6%
		SB30	126	10	181.0	1.4	225.0	36.8%
		SB40	121	8	183.0	1.43	226.3	37.0%
		SB50	114	8	185.0	1.52	227.6	37.2%
		SB60	108	8	184.7	1.64	228.8	37.4%
		SB70	98.0	6	186.0	1.75	230.0	37.6%
		SB80	96	6	187.0	1.82	230.9	37.9%
		SB90	94	3	189.0	1.97	232.1	38.1%
		B100	92	3	192.0	2.16	233.3	38.3%
3000	High Load (39.5 Nm)	SD100	125	20	254.3	1.2	217.7	36.9%
		SB10	122	8	256.0	1.58	218.6	37.2%
		SB20	119	8	251.3	1.72	219.6	37.4%
		SB30	115	6	255.0	2.03	220.3	37.6%
		SB40	112	6	256.0	2.3	221.7	37.8%
		SB50	109	5	250.0	2.4	223.1	37.9%
		SB60	106	5	251.0	2.5	224.3	38.1%
		SB70	96	4	253.0	2.6	225.6	38.3%
		SB80	94.0	4	252.0	2.6	226.8	38.5%
		SB90	92.0	3	253.0	2.7	228.1	38.7%
		B100	90	3	255.0	2.81	229.2	39.0%

Appendix B: Winter Diesel-Biodiesel and Synergy Series Data

Heavy-duty Engine-

FUEL	CO	HC	NOx	Smoke Opacity (%)
WD100	180	45	352	0.38
WB10	178	43	354	0.35
WB20	176	41	356	0.27
WB30	172	39	358	0.24
WB40	168	37	360	0.18
WB50	158	35	362	0.12
WB60	148	33	364	0.09
WB70	144	32	366	0.07
WB80	139	31	368	0.04
WB90	136	29	370	0.02
B100	132	27	372	0.014

Winter Diesel-Biodiesel-Synergy Blends Data

Fuel	CO	HC	NOx
SD100	160	40	320
SB20	152	36	322
WB20S2	125	27	330
SB50	140	33	325
SB50S2	105	20	335
SB100	100	30	330
B100S2	92	14	340

Light-duty Engine-

RPM	LOAD	FUEL	CO (PPM)	HC (PPM)	NOx (PPM)	Smoke Opacity (%)	BSFC (g/kwh)	BTE
1000	Low Load (8 Nm)	WD100	215	55	161.0	2.77	240.0	32.9%
		WB10	200.0	35.0	164.0	3.9	241.4	33.1%
		WB20	185.0	30	170	4.3	242.9	33.3%
		WB30	175	25	175	5.8	244.3	34.2%
		WB40	160	21	178.0	7	245.8	33.7%
		WB50	145	18	180	8.7	247.2	33.9%
		WB60	138	15	182	10.2	248.7	34.1%
		WB70	130.0	12	190	11.0	250.1	34.4%
		WB80	121	10	194.0	11.7	251.6	34.6%
		WB90	115	5	198.0	12.2	253.0	34.8%
		B100	107	3	203	13.4	254.5	35.1%
1000	Medium Load (20 Nm)	WD100	195.0	45	221	4.3	232.4	34.0%
		WB10	180.0	30	224	7.1	232.9	34.3%
		WB20	170.0	25	226	8.4	233.5	34.6%
		WB30	160.0	22	230	9.2	234.3	35.6%

		WB40	152.0	20	232	9.4	234.7	35.3%
		WB50	143	19	234	10.7	237.1	35.4%
		WB60	138.0	18	236	12.0	238.0	35.7%
		WB70	135	16	238	13.2	238.8	36.0%
		WB80	118	14	240	14.7	240.6	36.2%
		WB90	110.0	5	244	15.46	242.8	36.3%
		B100	102	3	246	16.4	244.0	36.6%
1000	High Load (35 Nm)	WD100	164.0	35	272	5.8	227.4	34.7%
		WB10	162.0	27	274	7.68	226.1	35.3%
		WB20	155	25	278	8.88	227.6	35.5%
		WB30	142	23	280	10.0	228.8	36.5%
		WB40	139	20	282	11.4	230.9	35.9%
		WB50	131	18	283	12.6	232.7	36.0%
		WB60	125.0	18	285	13.1	234.6	36.2%
		WB70	120	16	287	14.8	235.9	36.4%
		WB80	108.5	14	289	15	236.5	36.8%
		WB90	104.0	5	291	17.7	237.2	37.2%
		B100	96	3	293	18.5	238.2	37.5%
2100	Low Load (10 Nm)	WD100	185.0	50	151.7	1.6	230.0	34.3%
		WB10	180	27	152.0	1.7	231.4	34.5%
		WB20	175	22	158	2.4	232.8	34.7%
		WB30	170.0	20	160.0	2.91	234.2	35.7%
		WB40	160	18	174	3	235.5	35.2%
		WB50	150	16	176	3.3	236.9	35.4%
		WB60	140	14	182	3.6	238.3	35.6%
		WB70	130	12	188	3.7	239.7	35.9%
		WB80	120.0	10	190.0	4.2	241.1	36.1%
		WB90	115	5	194	4.3	242.5	36.4%
		B100	112.0	3	196.0	4.4	243.9	36.6%
2100	Medium Load (25 Nm)	WD100	160	40	210	2.2	227.6	34.7%
		WB10	155	25	211.0	2.4	228.9	34.9%
		WB20	150	22	214	3.1	230.1	35.1%
		WB30	145	20	215	3.6	231.2	36.1%
		WB40	140	18	218	3.8	232.4	35.6%
		WB50	130	16	219	4	233.8	35.8%
		WB60	120	14	221	4.4	235.0	36.1%
		WB70	110	12	223	4.6	236.4	36.4%
		WB80	105	10	225	4.8	237.7	36.6%
		WB90	100	5	232	5	239.0	36.9%
		B100	98	3	234	5.4	240.4	37.2%
2100	High Load (40 Nm)	WD100	135.0	30	260.0	2.9	223.3	35.4%
		WB10	133	22	262	3.3	224.3	35.6%
		WB20	130	20	264	3.87	225.4	35.9%
		WB30	126.0	18	266	4.0	226.5	36.9%
		WB40	124	16	268	4.3	227.9	36.3%
		WB50	117	14	270	4.4	229.2	36.6%
		WB60	113	12	272	4.6	230.5	36.8%
		WB70	99	10	274	4.8	231.7	37.1%
		WB80	95	8	276	5	232.9	37.4%

		WB90	90	5	278	5.2	234.2	37.6%
		B100	84.5	3	280	5.5	235.5	37.9%
3000	Low Load (9.5 Nm)	WD100	162	45	139.3	0.8	225.0	35.1%
		WB10	161.0	20.0	139.0	0.9	226.4	35.3%
		WB20	150	18	145.0	1	227.7	35.5%
		WB30	149	16	150.0	1.1	229.1	36.5%
		WB40	148	14	155.0	1.2	230.4	35.9%
		WB50	132	12	160.0	1.3	231.8	36.2%
		WB60	136	10	164.0	1.4	233.1	36.4%
		WB70	126	8	172.0	1.6	234.5	36.7%
		WB80	116.0	6	177.0	1.8	235.8	36.9%
		WB90	106	3	182.0	1.9	237.2	37.2%
		B100	102	3	184.0	2	238.6	37.5%
3000	Medium Load (24.5 Nm)	WD100	135	35	202.0	0.9	221.9	35.6%
		WB10	132	16	206.0	1.1	223.2	35.8%
		WB20	129	14	205.0	1.4	224.3	36.0%
		WB30	126	12	209.0	1.6	225.7	37.0%
		WB40	124	10	212.0	1.7	227.0	36.5%
		WB50	121	10	214.0	1.8	228.2	36.7%
		WB60	117	8	216.0	1.9	229.5	37.0%
		WB70	112	6	218.0	2.1	230.8	37.2%
		WB80	102	6	220.0	2.2	231.9	37.5%
		WB90	98	3	222.0	2.3	233.2	37.8%
		B100	95	3	224.0	2.4	234.4	38.1%
3000	High Load (39.5 Nm)	WD100	127	25	250.0	1.6	217.8	36.3%
		WB10	123	10	252.0	1.8	219.1	36.5%
		WB20	121	10	254.0	1.9	220.1	36.7%
		WB30	119	8	256.0	2	221.4	37.7%
		WB40	116	8	258.0	2.3	222.5	37.2%
		WB50	112	6	260.0	2.5	223.5	37.5%
		WB60	109.0	6	262.0	2.7	224.8	37.7%
		WB70	104	4	264.0	2.8	225.9	38.1%
		WB80	96	4	266.0	3	227.3	38.3%
		WB90	94	3	268.0	3.1	228.6	38.6%
		B100	92	3	270.0	3.2	229.8	38.9%

Appendix C: Fractionated Biodiesel and Synergy Series Data

Heavy-duty Engine-

FUEL	CO (ppm)	HC (ppm)	NOx (ppm)	Smoke Opacity (%)
WD100	180	45	352	0.38
FB20	135	34	358	0.21
FB20S2	130	32	360	0.18
FB50	115	25	364	0.11
FB50S2	110	23	366	0.09
FB100	85	17	372	0.04
FB100S2	80	15	374	0.02

Light-duty Engine-

RPM	LOAD	FUEL	CO (PPM)	HC (PPM)	NOx (PPM)	Smoke Opacity (%)	BSFC (g/kwh)	BTE
1000	Low Load (8 Nm)	WD100	215	55	145.0	2.70	240.0	32.9%
		FB20	150.0	20	147.0	2.7	243.8	33.2%
		FB20S2	145.00	18	148	2.50	245.8	33.4%
		FB50	120.0	15	150	2.3	249.5	33.7%
		FB50S2	115.00	10	151.0	2.10	251.6	33.9%
		FB100	100.0	5	154	2	258.8	34.7%
		FB100S2	90.0	3	156	1.8	260.5	34.9%
1000	Medium Load (20 Nm)	WD100	195.0	45	194	4.30	232.4	34.0%
		FB20	140.0	15	198	3.9	235.6	34.4%
		FB20S2	135.0	12	200	3.60	236.2	34.7%
		FB50	115.0	10	202	3.5	237.7	35.3%
		FB50S2	110.00	5.00	203	3.20	241.1	35.3%
		FB100	97.0	3	205	3.1	248.6	36.1%
		FB100S2	95.0	3	206	2.9	250.0	36.4%
1000	High Load (35 Nm)	WD100	164.0	35	221	5.80	227.4	34.7%
		FB20	130	12	225	4.7	228.4	35.4%
		FB20S2	125.00	10	226	4.30	229.7	35.7%
		FB50	112	5	229	4.1	230.5	36.4%
		FB50S2	109.00	5.00	230	3.90	232.3	36.7%
		FB100	92	3	232	3.8	240.8	37.2%
		FB100S2	90.0	3	234	3.6	241.3	37.7%
2100	Low Load (10 Nm)	WD100	185.0	50	126.0	1.60	230.0	34.3%

		FB20	144	15	127.0	1.5	233.6	34.6%
		FB20S2	140.00	13.00	132	1.40	235.5	34.8%
		FB50	121.0	10	135	1.3	239.1	35.1%
		FB50S2	117.00	8.00	138	1.20	241.1	35.3%
		FB100	91.0	5	142.0	1.1	248.0	36.2%
		FB100S2	85.0	3	145	1.0	249.7	36.4%
	Medium Load							
2100	(25 Nm)	WD100	160	40	172	2.20	227.6	34.7%
		FB20	132	12	176	2.1	230.5	35.1%
		FB20S2	130.00	10.00	178	2.00	232.2	35.3%
		FB50	110	8	180	1.9	235.7	35.6%
		FB50S2	107.00	5.00	182.0	1.80	237.6	35.9%
		FB100	85	4	184	1.7	244.1	36.7%
		FB100S2	81.0	3	186	1.6	245.6	37.1%
	High Load (40 Nm)							
2100		WD100	135.0	30	214.0	2.90	223.3	35.4%
		FB20	108	10	216	2.7	224.6	36.0%
		FB20S2	105.00	8.00	217	2.60	226.4	36.2%
		FB50	98	6	222	2.5	229.8	36.6%
		FB50S2	95.00	5.00	223	2.40	231.5	36.8%
		FB100	78	3	225.0	2.3	238.0	37.7%
		FB100S2	76.0	3	226	2.2	239.5	38.0%
	Low Load (9.5 Nm)							
3000		WD100	162	45	105.0	0.8	225.0	35.1%
		FB20	132	10	110.7	0.8	228.5	35.4%
		FB20S2	130.00	8	110.0	0.80	230.4	35.6%
		FB50	106	6	118.3	0.7	233.9	35.9%
		FB50S2	104.00	5	124.0	0.70	235.8	36.1%
		FB100	72	4	131.0	0.6	242.6	37.0%
		FB100S2	70.0	3	139.0	0.60	244.2	37.3%
	Medium Load							
3000	(24.5 Nm)	WD100	135	35	156.0	0.9	221.9	35.6%
		FB20	114	8	158.0	0.9	224.9	36.0%
		FB20S2	112.00	7	160.0	0.90	226.8	36.2%
		FB50	92	6	162.0	0.8	230.2	36.5%
		FB50S2	90.00	5.00	164.0	0.80	231.8	36.7%
		FB100	77	4	174.0	0.7	238.0	37.7%
		FB100S2	75.0	3	176.0	0.70	239.5	38.0%
	High Load (39.5 Nm)							
3000		WD100	127	25	206.0	1.6	217.8	36.3%
		FB20	99	7	208.0	1.6	220.8	36.6%
		FB20S2	97.00	6	210.0	1.60	222.6	36.9%

FB50	86	5	212.7	1.5	225.5	37.2%
FB50S2	82.00	4.00	214.0	1.40	227.0	37.5%
FB100	67	3	216.0	1.3	232.8	38.5%
FB100S2	65.0	3	218.0	1.20	234.1	38.9%

References

- [1] "WMO GREENHOUSE GAS BULLETIN," World Meteorological Organisation, 2016.
- [2] A. S. f. T. a. Materials, Standard specification for biodiesel fuel blend stock (B100) for middle distillate fuels, ASTM International, 2012.
- [3] A. K. Agarwal, "Biofuels (alcohols and biodiesel) applications as fuels for internal combustion engines," *Progress in energy and combustion science*, vol. 33, pp. 233-271, 2007.
- [4] J. P. Szybist and J. Song, "Biodiesel combustion, emissions and emission control," *Fuel processing technology*, vol. 88, pp. 679-691, 2007.
- [5] R. M. Joshi and M. J. Pegg, "Flow properties of biodiesel fuel blends at low temperatures," *Fuel*, vol. 86, pp. 143-151, 2007.
- [6] R. Dunn and M. Shockley, "Improving the low-temperature properties of alternative diesel fuels: vegetable oil-derived methyl esters," *Journal of the American Oil Chemists' Society*, vol. 73, pp. 1719-1728, 1996.
- [7] G. Knothe, "Dependence of biodiesel fuel properties on the structure of fatty acid alkyl esters," *Fuel processing technology*, vol. 86, pp. 1059-1070, 2005.
- [8] P. C. Smith, Y. Ngothai and Q. D. Nguyen, "Improving the low-temperature properties of biodiesel: Methods and consequences," *Renewable Energy*, vol. 35, pp. 1145-1151, 2010.
- [9] L. D. Clements and J. Gerpen, " Biodiesel production technology," *NREL-National Renewable Energy Laboratory. NREL/SR-510-36244*, 2004.
- [10] A. A. Natti, "Standard Test Method for Cloud Point of Petroleum Products," *ASTM International*, 2005.
- [11] F. Anwar and U. Rashid, "Okra (*Hibiscus esculentus*) seed oil for biodiesel production," *Applied Energy*, vol. 87, pp. 779-785, 2010.
- [12] G. Dwivedi and P. Verma, "Impact of Oil and Biodiesel on Engine operation in Cold Climatic condition," *Journal of Materials and Environmental Science*, vol. 12, no. 7, pp. 4540-4555 , 2016.

- [13] M. S. Carvalho and M. A. Mendonça, "Chromatographic analyses of fatty acid methyl esters by HPLC-UV and GC-FID," *Journal of the Brazilian Chemical Society*, vol. 23, pp. 763-769, 2012.
- [14] J. Gallehugh, "Biodiesel Blending Techniques Key to Quality Fuel," July 2008. [Online]. Available: <http://www.biodieselmagazine.com/articles/2476/biodiesel-blending-techniques-key-to-quality-fuel/>. [Accessed December 2016].
- [15] N. R. E. Laboratory, "Biodiesel Handling and Use Guide," December 2009. [Online]. Available: <http://www.nrel.gov/docs/fy09osti/43672.pdf>. [Accessed December 2016].
- [16] S. Kerschbaum and G. Rinke, "Winterization of biodiesel by micro process engineering," *Fuel*, vol. 87, pp. 2590-2597, 2008.
- [17] G. Dwivedi and M. Sharma, "Investigation and improvement in cold flow properties of Pongamia biodiesel," *Waste and Biomass Valorization*, vol. 6, pp. 73-79, 2015.
- [18] K. Addison, "The Biodiesel Bible," *Journey to Forever: Handmade Products*, 2013.
- [19] Biofuel Systems Group Limited, "Wintron Synergy- Cold Flow Additive for Biodiesel," [Online]. Available: http://www.biofuelsystems.com/other/wintron_synergy.pdf. [Accessed November 2016].
- [20] P. F. Holmes and M. Bohrer, "Exploration of polymethacrylate structure–property correlations: Advances towards combinatorial and high-throughput methods for biomaterials discovery," *Progress in polymer science*, vol. 33, pp. 787-796, 2008.
- [21] J. Wang and L. Cao, "Effect of polymeric cold flow improvers on flow properties of biodiesel from waste cooking oil," *Fuel*, vol. 117, pp. 876-881, 2014.
- [22] L. R. Rudnick and B. G. Kinker, "Polymethacrylate Viscosity Modifiers," in *Lubricant additives: chemistry and applications*, Pennsylvania, USA, CRC press, 2009, pp. 329-353.
- [23] A. Nealen, "Decreasing the Gel Temperature of Biodiesel," December 2009. [Online]. Available: my.umbc.edu/groups/biodieselclub/files/239. [Accessed December 2016].
- [24] G. Dwivedi and M. Sharma, "Impact of cold flow properties of biodiesel on engine performance," *Renewable and Sustainable Energy Reviews*, vol. 31, pp. 650-656, 2014.

- [25] P. Verma and V. M. Singh, "Assessment of diesel engine performance using cotton seed biodiesel," *Integrated Research Advances*, 2014.
- [26] M. M. Roy, M. Alawi and W. Wang, "Effects of canola biodiesel on a DI diesel engine performance and emissions," *International Journal of Mechatronics Engineering*, vol. 13, pp. 46-53, 2013.
- [27] M. M. Roy, W. Wang and J. Bujold, "Biodiesel production and comparison of emissions of a DI diesel engine fueled by biodiesel–diesel and canola oil–diesel blends at high idling operations," *Applied Energy*, vol. 106, pp. 198-208, 2013.
- [28] A. Dhar and A. K. Agarwal, "Performance, emissions and combustion characteristics of Karanja biodiesel in a transportation engine," *Fuel*, vol. 119, pp. 70-80, 2014.
- [29] A. N. Ozsezen and M. Canakci, "Determination of performance and combustion characteristics of a diesel engine fueled with canola and waste palm oil methyl esters," *Energy Conversion and Management*, vol. 52, pp. 108-116, 2011.
- [30] O. Özener and L. Yüksek, "Effects of soybean biodiesel on a DI diesel engine performance, emission and combustion characteristics," *Fuel*, vol. 115, pp. 875-883, 2014.
- [31] A. Liaquat and H. Masjuki, "Effect of coconut biodiesel blended fuels on engine performance and emission characteristics," *Procedia Engineering*, vol. 56, pp. 583-590, 2013.
- [32] A. Liaquat and H. Masjuki, "Impact of palm biodiesel blend on injector deposit formation," *Applied energy*, vol. 111, pp. 882-893, 2013.
- [33] M. Habibullah and H. Masjuki, "Biodiesel production and performance evaluation of coconut, palm and their combined blend with diesel in a single-cylinder diesel engine," *Energy Conversion and Management*, vol. 87, pp. 250-257, 2014.
- [34] I. R. Fattah and H. Masjuki, "Performance and emission characteristics of a CI engine fueled with *Cocos nucifera* and *Jatropha curcas* B20 blends accompanying antioxidants," *Industrial Crops and Products*, vol. 57, pp. 132-140, 2014.

- [35] G. Dwivedi, "Performance evaluation of diesel engine using biodiesel from Pongamia oil," *International Journal of Renewable Energy Research (IJRER)*, vol. 3, pp. 325-330, 2013.
- [36] G. Dwivedi and S. Jain, "Impact of biodiesel and its blends with diesel and methanol on engine performance," *International Journal of Energy Science*, vol. 1, pp. 2304-3679, 2011.
- [37] M. Bhuiya and M. Rasul, "Prospects of 2nd generation biodiesel as a sustainable fuel— Part 2: Properties, performance and emission characteristics," *Renewable and Sustainable Energy Reviews*, vol. 55, pp. 1129-1146, 2016.
- [38] O. Armas and R. García-Contreras, "Impact of alternative fuels on performance and pollutant emissions of a light duty engine tested under the new European driving cycle," *Applied energy*, vol. 107, pp. 183-190, 2013.
- [39] D. Singh and K. Subramanian, "Emissions and fuel consumption characteristics of a heavy duty diesel engine fueled with hydroprocessed renewable diesel and biodiesel," *Applied Energy*, vol. 155, pp. 440-446, 2015.
- [40] H. An and W. Yang, "Performance, combustion and emission characteristics of biodiesel derived from waste cooking oils," *Applied energy*, vol. 112, pp. 493-499, 2013.
- [41] H. An and W. Yang, "Combustion and emissions characteristics of diesel engine fueled by biodiesel at partial load conditions," *Applied Energy*, vol. 99, pp. 363-371, 2012.
- [42] K. Cheikh and A. Sary, "Experimental assessment of performance and emissions maps for biodiesel fueled compression ignition engine," *Applied Energy*, vol. 161, pp. 320-329, 2016.
- [43] S. A. Rahman and H. Masjuki, "Effect of idling on fuel consumption and emissions of a diesel engine fueled by Jatropha biodiesel blends," *Journal of cleaner production*, vol. 69, pp. 208-215, 2014.
- [44] W. Yang and H. An, "Combustion and emissions characteristics of diesel engine fueled by biodiesel at partial load conditions," *Applied Energy*, vol. 99, pp. 363-371, 2012.
- [45] W. Yang and H. An, "Performance, combustion and emission characteristics of biodiesel derived from waste cooking oils," *Applied energy*, vol. 112, pp. 493-499, 2013.

- [46] M. Habibullah and I. Rizwanul Fattah, "Effects of palm–coconut biodiesel blends on the performance and emission of a single-cylinder diesel engine," *Energy & Fuels*, vol. 29, pp. 734-743, 2015.
- [47] H. How and H. Masjuki, "An investigation of the engine performance, emissions and combustion characteristics of coconut biodiesel in a high-pressure common-rail diesel engine," *Energy*, vol. 69, pp. 749-759, 2014.
- [48] M. M. Rahman and M. H. Hassan, "Comparative evaluation of performance and emission characteristics of Moringa oleifera and Palm oil based biodiesel in a diesel engine," *Industrial Crops and Products*, vol. 53, pp. 78-84, 2014.
- [49] M. M. Rahman and M. Hassan, "Performance and emission analysis of Jatropha curcas and Moringa oleifera methyl ester fuel blends in a multi-cylinder diesel engine," *Journal of Cleaner Production*, vol. 65, pp. 304-310, 2014.
- [50] L. Zhu and C. Cheung, "Emissions characteristics of a diesel engine operating on biodiesel and biodiesel blended with ethanol and methanol," *Science of the Total Environment*, vol. 408, pp. 914-921, 2010.
- [51] N. Yilmaz and F. M. Vigil, "Investigation of CI engine emissions in biodiesel–ethanol–diesel blends as a function of ethanol concentration," *Fuel*, vol. 115, pp. 790-793, 2014.
- [52] D. Selvam and K. Vadivel, "The effects of ethanol addition with waste pork lard methyl ester on performance, emission, and combustion characteristics of a diesel engine," *Thermal Science*, vol. 18, pp. 217-228, 2014.
- [53] D. Jagadish and P. R. Kumar, "The Effect of Supercharging on Performance and Emission Characteristics of Compression Ignition Engine with Diesel-Ethanol-Ester Blends," *Thermal Science*, vol. 15, pp. 1165-1174, 2011.
- [54] L. Pidol and B. Lecoite, "Ethanol–biodiesel–diesel fuel blends: performances and emissions in conventional diesel and advanced low temperature combustions," *Fuel*, vol. 93, pp. 329-338, 2012.
- [55] Z.-H. Zhang and R. Balasubramanian, "Investigation of particulate emission characteristics of a diesel engine fueled with higher alcohols/biodiesel blends," *Applied Energy*, vol. 163, pp. 71-80, 2016.

- [56] S. H. Park and J. Cha, "Impact of biodiesel in bioethanol blended diesel on the engine performance and emissions characteristics in compression ignition engine," *Applied Energy*, vol. 99, pp. 334-343, 2012.
- [57] D. C. Rakopoulos, "Comparison of combustion, performance, and emissions of HSDI diesel engine operating on blends of diesel fuel with ethanol, n-butanol, or butanol isomer ether DEE," *Journal of Energy Engineering*, vol. 141, 2014.
- [58] R. Lanjekar and D. Deshmukh, "A review of the effect of the composition of biodiesel on NO_x emission, oxidative stability and cold flow properties," *Renewable and Sustainable Energy Reviews*, vol. 54, pp. 1401-1411, 2016.
- [59] L. M. da Silva Freire and I. M. G. dos Santos, "Influence of the synthesis process on the properties of flow and oxidative stability of biodiesel from *Jatropha curcas* biodiesel," *Fuel*, vol. 94, pp. 313-316, 2012.
- [60] A. K. Agarwal and D. Khurana, "Long-term storage oxidation stability of Karanja biodiesel with the use of antioxidants," *Fuel processing technology*, vol. 106, pp. 447-452, 2013.
- [61] M. M. Rahman and M. H. Hassan, "Effect of biodiesel-diesel blending on physico-chemical properties of biodiesel produced from *Moringa oleifera*," *Procedia Engineering*, vol. 105, pp. 665-669, 2015.
- [62] P. Kwanchareon and A. Luengnaruemitchai, "Solubility of a diesel–biodiesel–ethanol blend, its fuel properties, and its emission characteristics from diesel engine," *Fuel*, vol. 86, pp. 1053-1061, 2007.
- [63] P. Verma and M. Sharma, "Evaluation and enhancement of cold flow properties of palm oil and its biodiesel," *Energy Reports*, vol. 2, pp. 2352-4847, 2016.
- [64] P. Bhale and N. V. Deshpande, "Improving the low temperature properties of biodiesel fuel," *Renewable Energy*, vol. 34, pp. 794-800, 2009.
- [65] M. Altaie and R. Janius, "Cold flow and fuel properties of methyl oleate and palm-oil methyl ester blends," *Fuel*, vol. 160, pp. 238-244, 2015.

- [66] L. Cao, J. Wang and S. Han, "Ethyl acetoacetate: A potential bio-based diluent for improving the cold flow properties of biodiesel from waste cooking oil," *Applied Energy*, vol. 114, pp. 18-21, 2014.
- [67] L. Cao and J. Wang, "Ethylene vinyl acetate copolymer: A bio-based cold flow improver for waste cooking oil derived biodiesel blends," *Applied Energy*, vol. 132, pp. 163-167, 2014.
- [68] R. O. Dunn, H. L. Ngo and M. J. Haas, "Branched-chain fatty acid methyl esters as cold flow improvers for biodiesel," *Journal of the American Oil Chemists' Society*, vol. 92, pp. 853-869, 2015.
- [69] M. Abe and S. Hirata, "Thermodynamic selection of effective additives to improve the cloud point of biodiesel fuels," *Fuel*, vol. 171, pp. 94-100, 2016.
- [70] C. Boshui and S. Yuqiu, "Effect of cold flow improvers on flow properties of soybean biodiesel," *Biomass and bioenergy*, vol. 34, pp. 1309-1313, 2010.
- [71] M. Tesfaye and V. Katiyar, "Microwave assisted synthesis of biodiesel from soybean oil: Effect of poly (lactic acid)-oligomer on cold flow properties, IC engine performance and emission characteristics," *Fuel*, vol. 170, pp. 107-114, 2016.
- [72] W. Zhao and Y. Xue, "Improving the cold flow properties of high-proportional waste cooking oil biodiesel blends with mixed cold flow improvers," *RSC Advances*, vol. 6, pp. 13365-13370, 2016.
- [73] S. Y. Giraldo and L. A. Rios, "Comparison of glycerol ketals, glycerol acetates and branched alcohol-derived fatty esters as cold-flow improvers for palm biodiesel," *Fuel*, vol. 108, pp. 709-714, 2013.
- [74] H. Joshi and B. R. Moser, "Ethyl levulinate: A potential bio-based diluent for biodiesel which improves cold flow properties," *Biomass and bioenergy*, vol. 35, pp. 3262-3266, 2011.
- [75] T. Q. Chastek, "Improving cold flow properties of canola-based biodiesel," *biomass and bioenergy*, vol. 35, pp. 600-607, 2011.
- [76] H. Joshi and B. R. Moser, "Effects of blending alcohols with poultry fat methyl esters on cold flow properties," *Renewable Energy*, vol. 35, pp. 2207-2210, 2010.

- [77] V. Makarevičienė and K. Kazancev, "Possibilities for improving the cold flow properties of biodiesel fuel by blending with butanol," *Renewable Energy*, vol. 75, pp. 805-807, 2015.
- [78] C.-W. Chiu and L. G. Schumacher, "Impact of cold flow improvers on soybean biodiesel blend," *Biomass and Bioenergy*, vol. 27, pp. 485-491, 2004.
- [79] O. Edith and R. B. Janius, "Factors affecting the cold flow behaviour of biodiesel and methods for improvement—a review," *Pertanika Journal of Science & Technology*, vol. 20, pp. 1-14, 2012.
- [80] G. Knothe, J. Krahl and J. Van Gerpen, *The biodiesel handbook*, Elsevier, 2015.
- [81] H. Kreulen, "Fractionation and winterization of edible fats and oils," *Journal of the American Oil Chemists' Society*, vol. 53, pp. 393-396, 1976.
- [82] Á. Pérez and A. Casas, "Winterization of peanut biodiesel to improve the cold flow properties," *Bioresource technology*, vol. 101, pp. 7375-7381, 2010.
- [83] R. Sedgwick and C. Hoerr, "Solubilities of saturated fatty acid esters," *The Journal of Organic Chemistry*, vol. 17, pp. 327-337, 1952.
- [84] T. H. Doğan and H. Temur, "Effect of fractional winterization of beef tallow biodiesel on the cold flow properties and viscosity," *Fuel*, vol. 108, pp. 793-796, 2013.
- [85] Y. Wang and S. Ma, "Improving the cold flow properties of biodiesel from waste cooking oil by surfactants and detergent fractionation," *Fuel*, vol. 90, pp. 1036-1040, 2011.
- [86] C. M. Fernández and L. Fiori, "Supercritical extraction and fractionation of *Jatropha curcas* L. oil for biodiesel production," *The Journal of Supercritical Fluids*, vol. 97, pp. 100-106, 2015.
- [87] S. C. Johnson, "Low Cloud Point Biodiesel - Oregon State University," September 2014. [Online]. Available: <https://ir.library.oregonstate.edu/xmlui/bitstream/handle/1957/54822/Shanti%20Johnson%20thesis%20document%209.2014.pdf?sequence=1>. [Accessed December 2016].
- [88] N. B. Board, "Biodiesel Beats the Cold- Hot Tips for Using Biodiesel in Cold Weather," 2008. [Online]. Available: <http://biodiesel.org/docs/default-source/ffs->

performace_usage/hot-tips-for-using-biodiesel-in-cold-weather-(general).pdf?sfvrsn=6.
[Accessed December 2016].

- [89] G. o. Canada, "Historical Climate Data," [Online]. Available: http://climate.weather.gc.ca/prods_servs/cdn_climate_summary_e.html. [Accessed October 2016].
- [90] D. Qi and C. Lee, "Experimental investigations of combustion and emission characteristics of rapeseed oil–diesel blends in a two cylinder agricultural diesel engine," *Energy Conversion and Management*, vol. 77, pp. 227-232, 2014.
- [91] A. N. Ozsezen and M. Canakci, "Performance and combustion characteristics of a DI diesel engine fueled with waste palm oil and canola oil methyl esters," *Fuel*, vol. 88, pp. 629-636, 2009.
- [92] J. B. Heywood, *Internal combustion engine fundamentals*, New York: Mcgraw-hill, 1988.
- [93] D. Rakopoulos, "Combustion and emissions of cottonseed oil and its bio-diesel in blends with either n-butanol or diethyl ether in HSDI diesel engine," *Fuel*, vol. 105, pp. 603-613, 2013.
- [94] S. Imtenan and M. Varman, "Impact of low temperature combustion attaining strategies on diesel engine emissions for diesel and biodiesels: a review," *Energy Conversion and Management*, vol. 80, pp. 329-356, 2014.
- [95] C. Rakopoulos and K. Antonopoulos, "Development and application of multi-zone model for combustion and pollutants formation in direct injection diesel engine running with vegetable oil or its bio-diesel," *Energy conversion and management*, vol. 48, pp. 1881-1901, 2007.
- [96] I. R. Fattah and M. Kalam, "Biodiesel production, characterization, engine performance, and emission characteristics of Malaysian Alexandrian laurel oil," *Rsc Advances*, vol. 4, pp. 17787-17796, 2014.
- [97] D. Y. Chang and J. H. Van Gerpen, "Fuel properties and engine performance for biodiesel prepared from modified feedstocks," SAE Technical Paper, 1997.

- [98] M. Gumus and C. Sayin, "The impact of fuel injection pressure on the exhaust emissions of a direct injection diesel engine fueled with biodiesel–diesel fuel blends," *Fuel*, vol. 95, pp. 486-494, 2012.
- [99] H. C. Ong and H. Masjuki, "Engine performance and emissions using *Jatropha curcas*, *Ceiba pentandra* and *Calophyllum inophyllum* biodiesel in a CI diesel engine," *Energy*, vol. 69, pp. 427-445, 2014.
- [100] A. Ramadhas and C. Muraleedharan, "Performance and emission evaluation of a diesel engine fueled with methyl esters of rubber seed oil," *Renewable energy*, vol. 30, pp. 1789-1800, 2005.
- [101] A. N. Ozsezen and M. Canakci, "Determination of performance and combustion characteristics of a diesel engine fueled with canola and waste palm oil methyl esters," *Energy Conversion and Management*, vol. 52, pp. 108-116, 2011.
- [102] N. Panwar and H. Y. Shrirame, "Performance evaluation of a diesel engine fueled with methyl ester of castor seed oil," *Applied Thermal Engineering*, vol. 30, pp. 245-249, 2010.
- [103] M. N. Nabi and M. M. Rahman, "Biodiesel from cotton seed oil and its effect on engine performance and exhaust emissions," *Applied Thermal Engineering*, vol. 29, pp. 2265-2270, 2009.
- [104] Z. Xiao, "The effect of aromatic hydrocarbons and oxygenates on diesel engine emissions," *Proceedings of the Institution of Mechanical Engineers, Part D: Journal of Automobile Engineering*, vol. 214, pp. 307-332, 2000.
- [105] P. Devan and N. Mahalakshmi, "A study of the performance, emission and combustion characteristics of a compression ignition engine using methyl ester of paradise oil–eucalyptus oil blends," *Applied Energy*, vol. 86, pp. 675-680, 2009.
- [106] C. İlkılıç and H. Aydın, "Determination of performance and exhaust emissions properties of B75 in a CI engine application," *Fuel processing technology*, vol. 92, pp. 1790-1795, 2011.
- [107] J. E. Chandler and F. G. Horneck, "The effect of cold flow additives on low temperature operability of diesel fuels," SAE Technical Paper, 1992.